

AD-A266 006



DTIC
S ELECTE D
C JUN 22 1993

2

Limitations to the Quality of Optical Phase
Conjugation by Stimulated Brillouin Scattering

2

by
Thomas Richard Moore

Submitted in Partial Fulfillment
of the
Requirements for the Degree
DOCTOR OF PHILOSOPHY

Supervised by
Professor Robert W. Boyd

DISTRIBUTION STATEMENT A
Approved for public release
Distribution Unlimited

The Institute of Optics
University of Rochester
Rochester, New York

1993

93 6 21 005

93-13904
Barcode

REPORT DOCUMENTATION PAGE

Form Approved
OMB No. 0704-0188

Public reporting burden for this collection of information is estimated to average 1 hour per response, including the time for reviewing instructions, searching existing data sources, gathering and maintaining the data needed, and completing and reviewing the collection of information. Send comments regarding this burden estimate or any other aspect of this collection of information, including suggestions for reducing this burden to Washington Headquarters Service, Directorate for Information Operations and Reports, 1215 Jefferson Davis Highway, Suite 1204, Arlington, VA 22202-4302, and to the Office of Management and Budget, Paperwork Reduction Project (0704-0188), Washington, DC 20503.

1. AGENCY USE ONLY (Leave blank)	2. REPORT DATE	3. REPORT TYPE AND DATES COVERED	
4. TITLE AND SUBTITLE Limitations to the Quality of Optical Phase Conjugation by Stimulated Brillouin Scattering		5. FUNDING NUMBERS	
6. AUTHOR(S) Thomas R. Moore			
7. PERFORMING ORGANIZATION NAME(S) AND ADDRESS(ES) Institute of Optics University of Rochester Rochester, NY 14627		8. PERFORMING ORGANIZATION REPORT NUMBER	
9. SPONSORING/MONITORING AGENCY NAME(S) AND ADDRESS(ES) Commander U.S. Army Student Detachment Fort Benjamine Harrison, IN		10. SPONSORING/MONITORING AGENCY REPORT NUMBER	
11. SUPPLEMENTARY NOTES PhD Dissertation			
12a. DISTRIBUTION/AVAILABILITY STATEMENT ulimited distribution		12b. DISTRIBUTION CODE	
13. ABSTRACT (Maximum 200 words) <p style="text-align: center;">The process of optical phase conjugation by stimulated Brillouin scattering is studied both theoretically and experimentally, with emphasis on aspects that apply to phase-conjugate lasers. A theoretical formalism based on decomposing the optical field into a set of orthogonal modes is presented; this formalism is then used as the basis for numerical modeling.</p> <p>Many of the steady-state aspects of stimulated Brillouin scattering are investigated including: the distribution of energy in the interaction region, the spatial effects of distributed noise, phase pulling of the Stokes wave and the affects of adding smooth aberrations to the pump beam. A new design for a robust, inexpensive, solid-state, phase-conjugate laser is also presented.</p>			
14. SUBJECT TERMS optics, phase conjugation, stimulated Brillouin scattering, lasers, nonlinear optics, phase-conjugate lasers		15. NUMBER OF PAGES	
		16. PRICE CODE	
17. SECURITY CLASSIFICATION OF REPORT UNCLASSIFIED	18. SECURITY CLASSIFICATION OF THIS PAGE UNCLASSIFIED	19. SECURITY CLASSIFICATION OF ABSTRACT UNCLASSIFIED	20. LIMITATION OF ABSTRACT UL

Limitations to the Quality of Optical Phase Conjugation by Stimulated Brillouin Scattering

by
Thomas Richard Moore

Submitted in Partial Fulfillment
of the
Requirements for the Degree

DOCTOR OF PHILOSOPHY

Supervised by
Professor Robert W. Boyd

The Institute of Optics
University of Rochester
Rochester, New York

1993

Accession For	
NTIS CRA&I	<input checked="" type="checkbox"/>
DTIC TAB	<input type="checkbox"/>
Unannounced	<input type="checkbox"/>
Justification	
By _____	
Distribution /	
Availability Codes	
Dist	Avail and/or Special
A-1	

*for
Cathy, Sarah and Robert
on whose love and sacrifice this work is built*

Curriculum Vitae

Major Thomas R. Moore was born in Panama City, Florida on December 31, 1956. He entered Stetson University in 1975 and in 1978 was awarded the Bachelor of Science Degree in Physics. That same year he was commissioned a Second Lieutenant in the United States Army. He attended the United States Naval Postgraduate School from 1985 to 1987 where he received his Master of Science Degree (with distinction) in Nuclear Physics. In the fall of 1989 he came to the University of Rochester and began graduate studies at the Institute of Optics. He pursued his research in nonlinear optics under the direction of Professor Robert W. Boyd.

Major Moore has served in various positions throughout the world, including as a company-level commander in Europe and as a Military Research Associate at the Lawrence Livermore National Laboratory. His awards and decorations include the Army Commendation Medal and the Meritorious Service Medal (with Oak Leaf Cluster). He is married to the former Miss Cathy Perry of Fernandina Beach, Florida and has two children.

Publications

Thomas R. Moore and Donald L. Walters, "Observations on centrosymmetric and asymmetric scattering in barium titanate," *J. Opt. Soc. Am. B* **5**, 1806 (1988).

Andrew V. Nowak, Thomas R. Moore and Robert A. Fisher, "Observations of internal beam production in barium titanate phase conjugators," *J. Opt. Soc. Am. B* **5**, 1864 (1988).

G. F. Albrecht, H. F. Robey and T. R. Moore, "Optical technique for the measurement of turbulent spectra using the photorefractive properties of BaTiO_3 ," *Appl. Phys. Lett.* **57**, 864 (1990).

O. Kulagin, G. A. Pasmanik, Alexander L. Gaeta, Thomas R. Moore, Glenn J. Benecke and Robert W. Boyd, "Observation of Brillouin chaos with counterpropagating laser beams," *J. Opt. Soc. Am. B* **8**, 2155 (1991).

Thomas R. Moore and Robert W. Boyd, "Improvement of the photorefractive efficiency of BaTiO_3 by γ irradiation," *Appl. Phys. Lett.* **61**, 2015 (1992).

H-J. Zhang, Z-S. Tang, Thomas R. Moore and Robert W. Boyd, "High-Order diffraction in photorefractive SBN:Ce due to non-sinusoidal gratings formed by beams of comparable intensity," *Int. J. Nonlinear Optical Physics* **2**, to be published (1993).

Thomas R. Moore, Alexander L. Gaeta and Robert W. Boyd, "Amplitude and phase fluctuations in stimulated Brillouin scattering," in review.

Patents

Optical Monitor for Observing Turbulent Flow, George F. Albrecht and Thomas R. Moore, #5,121,985, June 16, 1992.

Acknowledgments

I wish to acknowledge the support and guidance of R. W. Boyd, the assistance of A. L. Gaeta in many aspects of the work presented in Chapter 5, and the assistance of G. L. Fischer in obtaining some of the experimental results presented in Chapters 3 and 4. I am indebted to G. R. Gray for the generous donation of computer time, and I would like to thank R. T. Moore for many helpful discussions. Support for this work was provided by the United States Army through the Advanced Civil Schooling Program.

Abstract

The process of optical phase conjugation by stimulated Brillouin scattering is studied both theoretically and experimentally, with emphasis on aspects that apply to phase-conjugate lasers. A theoretical formalism based on decomposing the optical field into a set of orthogonal modes is presented; this formalism is then used as the basis for a numerical modeling effort.

Many of the steady-state aspects of stimulated Brillouin scattering are investigated including: the distribution of energy in the interaction region, the spatial effects of distributed noise, phase-pulling of the Stokes wave and the effects of adding smooth aberrations to the pump beam. Among other things, it is shown that for focused Gaussian beams the distance from the focal point of the lens to the front of the Brillouin medium defines the pump depletion region.

The study of SBS with pump beams that include smooth aberrations is used to investigate the limitations of optical phase conjugation by stimulated Brillouin scattering. It is shown that the presence of intensity maxima that do not coincide with a region in which the phase is varying rapidly in space can lead to poor phase conjugation; this situation can occur when the pump beam contains a significant amount of a smooth aberration such as astigmatism. It is determined that the limitations imposed by the presence of smooth aberrations on the pump beam may be avoided by ensuring that the SBS process occurs in the regime where the pump beam is virtually undepleted.

Dynamic effects caused by the stochastic initiation of the stimulated Brillouin scattering process are also investigated. It is shown that both the amplitude and phase fluctuations, which are the signature of the initiating noise, may be suppressed by a judicious choice of pump geometry. In particular, by insisting that the product of the Brillouin linewidth and the transit time of light through the medium be less than unity, almost all phase and amplitude noise on the Stokes beam can be suppressed.

In concluding the work, the design and construction of an efficient, inexpensive and robust Q-switched phase-conjugate laser is presented. The effects of feedback into the laser are eliminated by utilizing an entirely solid-state ring oscillator with a color-center Q-switch. The laser has been shown to produce transform-limited

pulses from 40 to 400 ns long with energy up to one Joule per pulse and near diffraction-limited beam quality.

Table of Contents

Curriculum Vitae	v
Publications	vi
Patents	vii
Acknowledgments	viii
Abstract	ix
Table of Contents	xi
List of Tables	xiii
List of Figures	xiv
Chapter 1 Introduction.....	1
1.1 Optical phase conjugation	2
1.2 Phase conjugation for laser applications	4
1.3 Optical phase conjugation by SBS in the literature.....	7
1.4 Overview of research	9
Chapter 2 Theory and Modeling of SBS Phase Conjugation.....	11
2.1 SBS theory.....	12
2.2 SBS phase conjugation.....	16
2.3 An alternative theoretical formalism for SBS	18
2.4 Modeling of the SBS process	24
2.5 Initial results of the modeling effort.....	28
2.6 Noise initiation of SBS.....	30
2.7 Phase pulling of the Stokes modes.....	33
2.8 The Brillouin gain parameter	38
2.9 Conclusions	43
Chapter 3 Energy Distribution in the Interaction region.....	44
3.1 Intuition and experience	45
3.2 Simulations of SBS using focused beams	46
3.3 Experimental investigation of the energy distribution	50
3.4 Conclusions	51
Chapter 4 SBS Phase Conjugation of Beams with Smooth Aberrations.....	54

4.1 Smooth aberrations and phase conjugation.....	54
4.2 Characterization of astigmatic beams	56
4.3 Measuring the quality of phase-conjugate mirrors.....	58
4.4 Experimental investigation of SBS with astigmatic beams	63
4.5 Modeling of SBS with astigmatic pump beams	67
4.6 The etiology of poor phase conjugation with astigmatic pump beams.....	70
4.7 The effects of the Guoy phase shift and n_2	76
4.8 Discussion	81
4.9 Conclusions	83
Chapter 5 Amplitude and Phase Fluctuations in Stimulated Brillouin Scattering	85
5.1 Effects of amplitude fluctuations of the initiating radiation	85
5.2 Effects of phase fluctuations of the initiating radiation	88
5.3 Experimental verification.....	91
5.4 Conclusions	97
Chapter 6 Design and Construction of a Solid-State Phase-Conjugate Laser	98
6.1 Issues in the design of solid-state phase-conjugate lasers.....	98
6.2 Design for a phase-conjugate laser.....	101
6.3 Conclusions	103
Chapter 7 Conclusions.....	105
Appendix A Derivation of the Dependence of Beam Parameters on SBS Threshold for Focused Gaussian Beams.....	108
Appendix B Derivation of the Relationship Between Astigmatism on a Laser Beam and the Separation of Foci	110
Appendix C Overlap Integrals for the First Three Hermite-Gaussian Modes	112
Bibliography.....	113

List of Tables

Table 4.1. The ratio $\chi_{SBS}^{(3)} / \chi_{Kerr}^{(3)}$ for some common Brillouin media.....	79
Table c.1. Values of the overlap integrals for the first three Hermite-Gaussian modes.	112

List of Figures

1.1	A schematic of a plane wave passing through a distorting medium and its counter-propagating phase conjugate wave demonstrates aberration correction by phase conjugation.....	3
1.2	Conventional arrangement for a Q-switched phase-conjugate laser.....	6
2.1	The physical geometry and the coordinate system assumed in the model.....	27
2.2	Power in the (0,0) mode of the pump beam and the (0,0) and (0,2) modes of the Stokes beam as a function of distance within the Brillouin medium during SBS.....	28
2.3	Plot of the log of the power in the first three even modes of the Stokes wave showing the amplification of noise and discrimination against nonconjugate modes.....	30
2.4	The phase of the lowest order mode of the Stokes radiation far below SBS threshold and ten times above SBS threshold.....	32
2.5	Demonstration of the effects of noise modes on the phase of the Stokes mode that is conjugate to the pump.....	34
2.6	Evolution of the Brillouin gain parameter $\eta(z)$ as a function of distance within the medium.....	39
2.7	Power in the pump beam at different points in the Brillouin medium plotted as a function of the input pump power.....	40
2.8	The saturation parameter plotted as a function of position in the Brillouin medium.....	41
2.9	Power in the Stokes beam at different points in the Brillouin medium plotted as a function of the input pump power.....	42
3.1	The power in the Stokes wave plotted as a function of position in the medium for four different pump powers.....	47
3.2	The normalized power in the Stokes wave plotted as a function of position fc a short medium.....	48

3.3	Intensity of a focused pump beam as a function of position in the Brillouin medium.	50
3.4	Experimental arrangement for determining the energy in the Brillouin interaction region for focused beams.	51
3.5	Dependence of the energy in the Stokes beam as a function of position in the medium.	52
4.1	Experimental arrangement for investigating the near-field beam quality of an SBS Stokes beam.	60
4.2	Apparatus for phase-conjugate beam quality measurement in the far-field of the aberrant optic.	61
4.3	Intensity profiles of the Stokes beam with and without astigmatism present.	62
4.4	Photograph of Stokes beam when the pump beam is astigmatic and high above threshold.	63
4.5	Stokes beam quality as a function of pump energy for the case of pump beam with no astigmatism.	63
4.6	Stokes beam quality as a function of pump energy for an astigmatic pump beam.	64
4.7	Normalized on-axis intensity for focused beams with different amounts of astigmatism.	66
4.8	Evolution of the first two Hermite-Gaussian modes of the Stokes wave for the case of an astigmatic pump 55 times the SBS threshold.	68
4.9.	Stokes beam quality as a function of pump power for a pump beam containing 3λ astigmatism.	69
4.10	The phase evolution of the Stokes modes at the sagittal focus under the undepleted pump approximation.	72
4.11	The phase evolution of the Stokes modes at the sagittal focus with pump depletion.	74
4.12	Theoretical beam quality of the Stokes beam as a function of pump power.	75
4.13	Effect of adding a Kerr-type nonlinearity to the simulation of SBS for beams without astigmatism.	80
4.14	Theoretically predicted Stokes beam profiles for a pump beam with no astigmatism and a beam with astigmatism at a pump power near the onset of spatial instability.	81

5.1	Typical Stokes pulse profiles for varying interaction lengths.....	92
5.2	Experimental verification of the dependence of intensity fluctuations of the Stokes beam on the length of the SBS interaction region.....	93
5.3	Experimental arrangement for the investigation of phase fluctuations.....	94
5.4	Interference pattern produced by two Stokes beams, each having a duration in excess of 100 phonon lifetimes.....	95
5.5	Variation of the linewidth of the Stokes emission with increasing interaction length.....	96
6.1	Block diagram of a phase-conjugate laser.....	99
6.2	Method for passive extraction of phase-conjugate radiation.	100
6.3	High pressure nitrogen cell in a folded oscillator/amplifier design.	102
6.4	Detailed schematic of the phase-conjugate laser.....	104

Chapter 1

Introduction

The scattering of light from pressure fluctuations (sound waves) within a medium is termed Brillouin scattering.¹ When the intensity of the light is low, such that the presence of the light has a negligible effect on the sound wave, the scattering is due entirely to the presence of thermal fluctuations in the medium. Typically the magnitude of these fluctuations is such that the scattered intensity is on the order of 10^{-12} of the input intensity.^{2,3} If the intensity of the incident light is such that the presence of the light significantly affects the medium response, causing the light to couple to the pressure waves present in the medium, then stimulated Brillouin scattering (SBS) can result and near total scattering of the incident light is possible.

The study of stimulated Brillouin scattering was made possible by the invention of the laser, and by the end of the 1960's the physical process of SBS was well characterized.^{1,4} It was well known that the scattered light, termed the Stokes light, is scattered predominately in the direction counter-propagating to the incident light, due to the increased interaction length over that experienced at other angles. However in 1972 Ragul'skii and coworkers discovered experimentally that the phase of the scattered light from the process of SBS had the characteristics of the reverse of the phase of the incident light. The theoretical explanation for this effect was provided by Zel'dovich and the study of optical phase conjugation by SBS began.^{5,6}

Since 1972 literally thousands of articles have been published on the phenomenon of optical phase conjugation by SBS. Much of the interest in the field is attributable to the continuing anticipation that optical phase conjugation by SBS can help produce high energy, diffraction-limited lasers. Indeed, there is ample evidence that a significant improvement in the beam quality of solid state lasers can be achieved through the use of SBS;⁷⁻³⁵ however, there is also ample evidence that much of the early enthusiasm was misguided.³⁶⁻³⁹ Additionally there is some anecdotal evidence that suggests that investigations indicating some limitations to optical phase conjugation by SBS were not widely promulgated.

Many of the issues important in the formation and use of a phase-conjugate wave created via SBS will be discussed in detail in the following chapters. The remainder of this chapter will be devoted to establishing the background for the research presented later. In section 1.1 a review of the theory of optical phase conjugation and its ability to correct for aberrations is presented. Section 1.2 provides a general overview of the current and proposed uses of SBS phase conjugation, concentrating on its use in the development of Q-switched laser systems. Section 1.3 is a brief review of some of the problems encountered when attempting to perform phase conjugation by SBS, followed by a brief overview of the following chapters in section 1.4.

1.1 Optical phase conjugation

In considering the process of optical phase conjugation and its importance to the field of optics I will follow the derivation that may be found in several places in the literature.^{3,40} Consider a wave propagating through an inhomogeneous, nonabsorbing, linear and time-independent medium with a (real) index of refraction given by $n(\mathbf{r}) = \sqrt{\epsilon(\mathbf{r})}$. We will consider a plane wave that is incident on the medium but becomes distorted by the variation in ϵ as it propagates through the medium. This situation is shown schematically by the thin lines in Figure 1.1. We assume that the variation in $\epsilon(\mathbf{r})$ occurs on a spatial scale significantly larger than an optical wavelength. We will consider a wave whose wave vector is predominately in the z direction and write the electric field of the light as

$$\vec{E}(\mathbf{r}, t) = E(\mathbf{r})e^{i(kz - \omega t)} + c.c., \quad (1.1)$$

where $E(\mathbf{r})$ is the slowly varying amplitude of the electric field and k and ω have their usual meaning of the wave number and frequency of the light.

Since the wave vector is considered to be predominately in the z direction, it is useful to separate the Laplacian operator in the wave equation into two terms, one operating in the longitudinal dimension ($\partial^2 / \partial z^2$) and one only for the transverse dimensions ($\nabla_{\perp}^2 = \partial^2 / \partial x^2 + \partial^2 / \partial y^2$). The homogeneous wave equation for the field described by equation (1.1) may then be written as

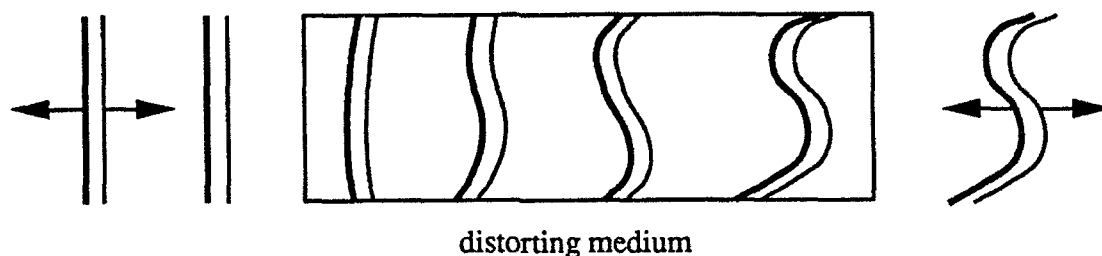


Figure 1.1. A schematic of a plane wave passing through a distorting medium (thin lines) and its counter-propagating phase conjugate wave (thick lines) demonstrates aberration correction by phase conjugation.

$$\nabla_{\text{T}}^2 E + \left[\frac{\omega^2 \epsilon(\mathbf{r})}{c^2} - k^2 \right] E + 2ik \frac{\partial E}{\partial z} = 0. \quad (1.2)$$

We now take the purely mathematical step of taking the complex conjugate of equation (1.2). This operation produces the equation

$$\nabla_{\text{T}}^2 E^* + \left[\frac{\omega^2 \epsilon(\mathbf{r})}{c^2} - k^2 \right] E^* - 2ik \frac{\partial E^*}{\partial z} = 0. \quad (1.3)$$

Equation (1.3) is the wave equation for a wave traveling through the medium, with amplitude equal to the complex conjugate of the wave described by equation (1.1) and traveling in the opposite direction. We call this field the conjugate field, \tilde{E}_{c} , and note that it may be written as

$$\tilde{E}_{\text{c}}(\mathbf{r}) = a E^*(\mathbf{r}) e^{-i(kz + \omega t)} + c.c., \quad (1.4)$$

where a is any complex constant.

It is important to note that equation (1.3) is valid at all points, so that no matter how the incident beam is modified by the presence of the medium, the wave

described by equation (1.4) will emerge from the medium with an amplitude characterized completely by the complex conjugate of the incident wavefront. This phase-conjugate wave is shown schematically by the thick lines in Figure 1.1.

As shown in Figure 1.1, correction for distortions can be achieved by double passing an aberrating medium, if the wave during the second pass of the medium is the phase-conjugate of the wave during the first pass. Generically, any device or process that produces an electric field whose amplitude is characterized by the complex conjugate of some incident field (to within a complex constant) is termed a phase-conjugate mirror or PCM. While a true phase-conjugate mirror must conjugate all aspects of the incident beam including the polarization, in practice the reversal of direction of the wave vector and the conjugation of the amplitude and phase of the electric field are sufficient conditions to apply the term phase-conjugate mirror. Generally, a true phase-conjugate mirror (i.e. one that also conjugates the polarization of the incident wave) is termed a *vector* phase-conjugate mirror. Vector phase conjugation will not be addressed here, and in the remainder of this work the term phase-conjugate mirror will refer to one that does not necessarily produce a conjugate polarization vector.

There are several methods of producing the phase-conjugate of an incident wave;^{3,40} among the more widely used are four-wave mixing (using various nonlinear processes) and many types of stimulated scattering including Brillouin, Raman, Rayleigh and photorefractive. Other more exotic and complicated ways include photon echoes,⁴¹⁻⁴⁴ mutually pumped phase conjugation⁴⁵⁻⁴⁷ and rubber mirror technology.⁴⁸ If one may judge the popularity of a given method from the number of journal articles published on the subject, the most widely used of the available methods of phase conjugation are photorefractivity and stimulated Brillouin scattering. Photorefractive methods are predominately applied to low power cw situations and SBS is generally applied to high power pulsed situations.

1.2 Phase conjugation for laser applications

Within the past two decades the allure of phase conjugation has been the anticipation that many (if not all) of the problems due to distortion of optical beams by imperfect optical elements could be eliminated. Additionally, phase conjugation has been proposed to solve problems as diverse as fast and accurate pointing of lasers, automatic tracking of small moving objects and elimination of the errors in

lithography due to diffraction off of the edges of the masks.^{49,50,51} Of particular interest in both science and industrial applications is the anticipation that phase conjugation can be used to correct distortions induced by the elements within state-of-the-art lasers. Indeed a significant amount of research has been undertaken toward the goal of the "perfect" laser wavefront, and there are several examples of lasers in use in research laboratories that utilize phase conjugation.^{20,27,32-35}

In general the use of phase conjugation in laser development can be grouped into two classes: phase-conjugate oscillator arrangements and phase-conjugate amplifier arrangements. In the phase-conjugate oscillator the advantages of self-alignment and aberration correction by the phase-conjugate mirror are exploited to produce a high quality output from an oscillator with imperfect elements. Although there have been some attempts to exploit the phase-conjugate geometry for pulsed oscillators,^{21,28,52,53} it is more common to see this type of arrangement used in cw oscillators with phase-conjugate mirrors of the photorefractive type.⁵⁴⁻⁵⁸

Of more general interest in the high power and pulsed laser community is the use of phase conjugation to correct for distortions induced by amplifying media. Since high quality, low energy beams are easily produced with current solid-state technology, most of the distortions in high-energy solid-state lasers are attributable to the amplifying media. Therefore, to take advantage of a phase-conjugate mirror, an arrangement similar to that shown in Figure 1.2 is used, where the aberrations that are induced on the beam in one pass through the amplifier are removed on the second pass after phase conjugation.⁷⁻³⁵ Often this type of system uses a phase-conjugate wave produced by stimulated Brillouin scattering. Variations on the design include the use of multiple phase-conjugate mirrors to produce a vector phase conjugator,⁵⁹ and schemes that involve multiple passes of the amplifier either by a regenerative scheme⁶⁰ or by off-axis propagation through the amplifying medium.²³

From this point forward only Q-switched solid-state laser systems will be considered. This limitation is necessary due to the disparate issues applied to phase conjugation within the various laser architectures. Although some of the issues are broad-based and apply to many different laser types, in general the Q-switched solid-state laser system shows the most potential (i.e. fewest problems) for the efficient application of optical phase conjugation. Specifically, the ability to use stimulated Brillouin scattering as the method of phase conjugation is the factor that distinguishes pulsed lasers from other types when considering the use of a phase-conjugate mirror.

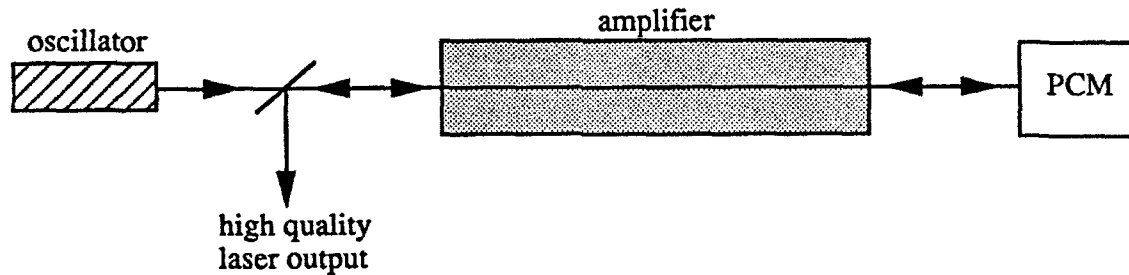


Figure 1.2. Conventional arrangement for a Q-switched phase-conjugate laser. Distortions imposed on the beam by the high power amplifier are phase-conjugated by the PCM and removed upon the second pass.

Therefore the focus of this work has been narrowed to optical phase conjugation via stimulated Brillouin scattering for Q-switched lasers. Additionally, while there are several types of pulsed lasers, we will be concerned here only with solid-state laser technology; naturally some of the issues are similar for other types of pulsed lasers.

While there is ample evidence that optical phase conjugation can be used to enhance the quality of the wavefront of a solid-state Q-switched laser system, there are several details that have limited the wide spread use of optical phase conjugation in laser systems. The first and most limiting factor is the number of nonlinear processes available with which to create the phase-conjugate wave.

Of the processes available for dynamic phase conjugation, only stimulated scattering and four-wave mixing are viable for laser applications. Furthermore, efficient phase conjugation for Q-switched solid-state lasers is limited to stimulated scattering processes rather than four wave mixing process. This limitation is due to the necessity to have coherent pump waves for four-wave mixing processes. Thus the use of a four wave mixing process requires most of the energy of the laser to be used in creating the PCM rather than being used as laser output. Other known types of nonlinearities are not considered viable due either to their complicated nature or the limitation in speed of the process.

Of the available stimulated scattering processes, by far the most common and most useful is the Brillouin nonlinearity. In most materials the Brillouin gain exceeds that of other nonlinear process for pulse lengths from one to 100 ns, and it has been

shown that in many instances SBS produces a back-scattered wave that is nearly phase-conjugate to the incident wave. The physics of SBS will be discussed in Chapter 2, but it is useful to note here the limitations that have been discovered (mostly by experiment) and the ambiguity in the literature concerning the phase-conjugate ability of SBS.

1.3 Optical phase conjugation by SBS in the literature

The study of SBS phase conjugation is logically divided into steady-state and transient effects. Until recently it was thought that the phase-conjugate aspects of the beam depended at most weakly on the transient nature of the nonlinearity. It was known that operating in the transient regime produced a higher value of SBS threshold,² but otherwise it was generally thought that the phase-conjugate nature of the Stokes wave was unaffected except for the degradation attributable to competing nonlinear processes such as self-focusing and breakdown of the medium.⁶¹⁻⁶³ Recently however, it has been shown experimentally that pulses with leading edges that have rise times that are significantly shorter than the phonon lifetime can produce Stokes waves with significant nonconjugate components.⁶⁴ The reason for this failure of SBS as a phase-conjugate mirror is still unknown.

One well known transient effect that does not appear to affect the phase-conjugate ability of the SBS process, but has implications for its use in phase-conjugate lasers, is the phase wave or phase jump.⁶⁵⁻⁷² The phase wave is a result of an abrupt change in the amplitude and phase of the initiating radiation during the SBS process. These changes in phase and amplitude of the initiating radiation result in a change in phase and amplitude of the Stokes wave exiting the Brillouin medium. While the presence of these fluctuations has prompted one researcher to quip (quite correctly) that "stimulated scattering does not have a steady-state",⁶⁸ for a very wide range of pulse lengths the approximation of steady-state is valid. These fluctuations, and a method for minimizing them, are discussed in Chapter 5.

There are clearly some very important transient effects that occur during SBS; however, in the present context of phase conjugation, the ability (or inability) of SBS to produce an accurate phase-conjugate wave appears to be weakly tied to the transient response of the process. Most known limitations of optical phase conjugation by SBS have been found experimentally in the regime of steady-state SBS.

One of these limitations to optical phase conjugation by SBS is seen when using a random phase aberration to increase the quality of phase conjugation. In general a better conjugate reproduction of the incident beam is obtained if the beam is highly aberrated. Thus a beam with little aberration is not as well conjugated by SBS as one with large aberration. The theoretical basis for this is well established in the literature^{2,6} and will be address in the following chapter. Since the quality of conjugation is dependent upon the aberration of the beam, it is common for a beam to be passed through a glass plate with random phase aberrations prior to being sent into the SBS phase-conjugate mirror. Such a plate is termed a *phase plate* in the literature and indeed it has been shown that by some measures, higher quality phase conjugation results from the use of a phase plate.

Although the use of phase plates can increase the quality of phase conjugation as it is usually measured in the laboratory, experiments,^{39,73,74} numerical simulations^{75,76} and theoretical calculations⁷⁷⁻⁸¹ have shown that using a random phase plate will result in the Stokes beam having the attributes of the complex conjugate of the phase of the incident beam, but the intensity will be characterized by a speckle pattern whose spatial frequency is approximately that of the mean spatial frequency of the phase aberration of the phase plate. For most applications this means that the use of a random phase plate is an unacceptable method for increasing the quality of a phase-conjugate mirror.

In many instances of practical interest the beam requiring phase conjugation is not aberrant with high spatial frequencies in phase or amplitude. Generally, in the design of phase-conjugate lasers, the aberrations that one wishes to correct are characterized by low order Seidel aberrations.^{27,82,83} These smooth aberrations have a distinctly different effect on the quality of the Stokes beam generated by SBS than those random aberrations created by a phase plate. Unfortunately the issue of the quality of optical phase conjugation by SBS for these type of aberrations is clouded by the literature, where reports of mutually contradictory results are common. From a search of the literature one may conclude that high-quality optical phase conjugation by SBS of beams with low-order smooth aberrations is either trivial, very difficult or impossible.^{36-39,84-92}

One final difficulty in the study of SBS stems from the difficulty of solving the applicable equations. Due to the inherent complexity of the equations much of the theoretical work assumes either an undepleted pump or a plane wave geometry, and

usually both of these approximations are applied. In reality seldom does the undepleted pump approximation apply and almost never is a plane wave used for optical phase conjugation by SBS. It is almost universal that when stimulated Brillouin scattering is used for optical phase conjugation the beam is focused into the active medium and the incident wave is strongly depleted. The universality of the use of a focusing lens stems from the high intensities required to reach SBS threshold in a confined space. Also, there is enhanced discrimination against nonconjugate Stokes waves obtained when the beam is brought to a focus in the medium; this will be addressed in Chapter 4.

It is tempting to think that since the highest intensities of a focused beam occur within a few Rayleigh ranges of the focus (a region where the wave is a good approximation to a plane wave), modeling a focused beam by a plane wave with a restricted interaction region is adequate. However it is not generally true that a focused beam may be modeled by a plane wave as is often thought. A simple demonstration of the necessity of modeling the focused geometry, rather than the plane wave geometry, when a beam is focused into the medium may be seen by examining the dependence of wavelength and interaction length on the threshold behavior of the SBS process in the two cases.

In the plane wave geometry the threshold intensity of SBS is not dependent upon the wavelength of the incident beam and is linearly dependent on the length of the medium.³ However, in the case of focused beams SBS threshold is proportional to the wavelength of the incident beam, independent of the focal length of the focusing lens and only weakly dependent on the length of the Brillouin medium, provided that the entire focal region is contained in the Brillouin medium (see Appendix A). These and several other aspects of focused beams that are explored in detail in the following chapters show that an understanding of optical phase conjugation by SBS for laser applications demands an understanding of the process of SBS in focused geometries with pump depletion.

1.4 Overview of research

The remainder of this work is devoted to a detailed report of the research performed on stimulated Brillouin scattering in the context of use as a mechanism for phase conjugation for Q-switched solid-state laser applications. Chapter 2 contains a brief review of the well known theory of stimulated Brillouin scattering and how it

leads to optical phase conjugation, followed by a description of how new insight was gained through application of a different theoretical formalism . Then a detailed description of the modeling effort used to assist in understanding SBS in the focused geometry is presented, followed by a review of the predictions of the numerical simulations.

Chapter 3 is a detailed discussion of the distribution of energy in the Brillouin medium when using focused beams. The results of computer models developed in Chapter 2 are discussed as well as experimental data confirming the predictions.

In Chapter 4, SBS phase conjugation of beams with smooth aberrations is discussed. Both theory and experiment are presented that lend insight into the limits of SBS phase conjugation and how nonconjugate Stokes waves can grow in situations where there are multiple intensity maxima along the beam path.

The transient phenomena of phase waves in SBS is discussed in Chapter 5. Experiments show that the linewidth of the Stokes wave may be narrowed by the suppression of phase waves. This suppression is achieved by carefully choosing the length of the interaction region.

Finally in Chapter 6 the design of an all solid-state phase-conjugate laser is presented. The design is based on all of the information on optical phase conjugation by SBS available in the literature and from the research presented in chapters 2 through 5. A new oscillator design is coupled with an SBS phase-conjugate mirror to produce single-longitudinal mode, near diffraction-limited beams with pulse lengths ranging from tens to hundreds of nanoseconds. A brief conclusion of the work follows in Chapter 7.

Chapter 2

Theory and Modeling of SBS Phase Conjugation

As noted in Chapter 1, one of the issues complicating our understanding of SBS phase conjugation is the complexity of the equations describing the process. The complex nature of the nonlinear interaction has not allowed extensive theoretical investigations of SBS in the focused-beam geometry. Those few investigations that are reported in the literature are derived in the limit of the undepleted pump approximation, where the effect of the Stokes wave in depleting the pump is ignored.⁷⁷⁻⁸¹ The undepleted pump approximation limits the applicability of the theory to cases where the intensity of the SBS scattering is less than a few percent of the intensity of the incident wave, which is not the regime commonly of interest to the optics community. Theories developed without utilizing the undepleted pump approximation almost exclusively employ infinite plane wave assumptions, thus eliminating all transverse effects from the model.

To investigate SBS in a manner that includes pump depletion researchers have turned to numerical methods. However, the Brillouin interaction is so complex that as a rule the only successful modeling techniques have involved only two of the four dimensions. Transient models use time and one space dimension (the coordinate in the direction of propagation) and steady-state models use two spatial dimensions, one in the direction of propagation and one in the transverse dimension. With one notable exception,⁹² these two dimensional steady-state modeling efforts have not considered the case of focused beams in the interaction region. As noted earlier, it is precisely this geometry that is used almost exclusively in optical phase conjugation by SBS.

This chapter is devoted to the derivation and numerical solution of the equations describing the SLS process. The usual plane-wave formalism found in the literature is presented first; then an alternative formalism is presented. This alternative formalism more accurately describes the SBS process and highlights the limitations of the plane-wave formalism. We then describe how this alternative theoretical formalism was used for numerical modeling of the SBS process in three

dimensions. This modeling effort has provided considerable insight into the process of SBS with focused beams.

2.1 SBS theory

Stimulated Brillouin scattering is created by the nonlinear interaction of a light wave (called the pump wave, \tilde{E}_p) with a second light wave (the Stokes wave, denoted \tilde{E}_s) through a sound wave, $\tilde{\rho}$. In a naive sense, the Stokes wave is simply the pump wave reflected off of an acoustic wave in the medium; a form of Bragg scattering. Since the sound wave is moving, the scattered Stokes wave is shifted in frequency from the pump wave (Doppler shifted). The amount that the Stokes wave is shifted in frequency from the pump is dependent upon the angle of the scattering; in the usual case of backscattering the shift depends upon the speed of sound in the medium and the wavelength of the exciting radiation. In a more rigorous sense, the Stokes wave is the amplification of spontaneous noise by the Brillouin interaction.

The derivation of the equations governing SBS are presented in detail in several places, so I will not rigorously derive them here. I will present a brief overview using a plane-wave formalism based on the complete derivation found in reference [3] to establish the foundation for original work presented later.

In the plane-wave formalism the two optical fields are given by

$$\tilde{E}_p(z,t) = [E_p(z,t)e^{-i(kz+\omega_p t)} + \text{c.c.}] \quad (2.1)$$

and

$$\tilde{E}_s(z,t) = [E_s(z,t)e^{i(kz-\omega_s t)} + \text{c.c.}] \quad (2.2)$$

Since the two optical waves are coupled through the acoustic wave, we will assume that the acoustic wave follows the interference between the optical fields so that the material density $\tilde{\rho}$ is given by

$$\tilde{\rho}(z,t) = \rho_o + [\rho(z,t)e^{-i(qz+\Omega t)} + \text{c.c.}] \quad (2.3)$$

Where the frequency of the sound wave is the difference between the frequency of the pump wave and the Stokes wave

$$\Omega = \omega_p - \omega_s, \quad (2.4)$$

and ρ_o is the mean density of the medium. We assume that the pump and Stokes waves are counter propagating so that the propagation vector can be written as a scalar:

$$q = k_p + k_s \approx 2k. \quad (2.5)$$

Here we make the implicit assumption that $k_p = k_s = k$ and that the pump wave is traveling in the -z direction.

The acoustic wave equation that $\tilde{\rho}$ obeys is given by

$$\frac{\partial^2 \tilde{\rho}}{\partial t^2} - \frac{\Gamma_B}{q^2} \nabla^2 \frac{\partial \tilde{\rho}}{\partial t} - v^2 \tilde{\rho} = \frac{-\gamma_e q^2}{4\pi} (E_p E_s^* e^{-i(qz + \Omega t)} + \text{c.c.}), \quad (2.6)$$

where Γ_B is the Brillouin linewidth, γ_e is the electrostrictive constant of the medium and Ω_B is the Brillouin frequency of the medium defined by

$$\Omega_B = qv, \quad (2.7)$$

and v is the speed of sound in the medium. The driving term in the acoustic wave equation is derived from the divergence of the force per unit volume on the material.

Substituting the assumed form of $\tilde{\rho}$ given in equation (2.3) into the acoustic wave equation, and assuming the slowly varying envelope approximation, equation (2.6) becomes

$$-2i\Omega \frac{\partial \rho}{\partial t} + (\Omega_B^2 - \Omega^2 - i\Omega\Gamma_B)\rho + 2iqv^2 \frac{\partial \rho}{\partial z} = \frac{-\gamma_e q^2}{4\pi} E_p E_s^*. \quad (2.8)$$

Since hypersonic phonons are strongly damped, we will ignore the spatial derivative in equation (2.8). Furthermore, since we will be considering the steady-state Brillouin interaction, we may drop the time derivative also. With these two simplifications equation (2.8) reduces to

$$\rho = \frac{-\gamma_e q^2}{4\pi} \left(\frac{E_p E_s^*}{\Omega_B^2 - \Omega^2 - i\Omega\Gamma_B} \right). \quad (2.9)$$

The nonlinear polarization that acts as a driving term for the optical wave equation is

$$\tilde{P}_{\omega}^{\omega} = \frac{1}{4\pi\rho_o} \gamma_e \tilde{\rho} \tilde{E}. \quad (2.10)$$

However, since we are only concerned with acoustic waves that can couple to the two optical fields, we will write only the part of the nonlinear polarization that is phase matched to one of the optical fields. Thus the applicable part of the nonlinear polarization is

$$\tilde{P}_{\omega}^{\omega} = \frac{\gamma_e}{4\pi\rho_o} \left(\tilde{\rho}^* \tilde{E}_p + \tilde{\rho} \tilde{E}_s \right). \quad (2.11)$$

In all cases considered here we will be concerned with SBS amplification of waves that are generated from noise within the medium. Considering only the amplification of noise, and not waves that are externally generated at some arbitrary frequency, allows us to simplify equation (2.9) and consider only on-resonance scattering. The validity of this assumption is based on the fact that many frequencies are present at the level of noise in the medium, but the light having the frequency of Ω_B will see the highest gain and will therefore dominate the SBS process. Under this condition equation (2.11) reduces to

$$\tilde{P}_{SBS}^{\omega} = \left(\frac{i\gamma_e^2 q^2}{16\pi^2 \rho_o \Omega_B \Gamma_B} \right) \left(|E_s|^2 \tilde{E}_p - |E_p|^2 \tilde{E}_s \right). \quad (2.12)$$

For later use I will define here the first factor in brackets on the right hand side of equation (2.12) as the on-resonance Brillouin contribution to the third order

nonlinear susceptibility. This the portion of $\chi^{(3)}$ due to the (on-resonance) Brillouin interaction can be written as

$$6i\chi_{SBS}^{(3)} = \frac{i\gamma_e^2 q^2}{16\pi^2 \rho_o \Omega_B \Gamma_B}. \quad (2.13)$$

In defining $\chi_{SBS}^{(3)}$, we have left the imaginary nature explicit to avoid confusion during later discussions. Besides being imaginary, it is important to note that the value of $\chi_{SBS}^{(3)}$ is not extremely large compared to other contributions to $\chi^{(3)}$. An estimate of the value of $\chi_{SBS}^{(3)}$ for CCl_4 (one of the preferred Brillouin media) reveals that the on-resonance Brillouin contribution to $\chi^{(3)}$ is on the order of ten times larger than the Kerr-type nonlinear contribution.

Using equation (2.12) as the source term for the nonlinear wave equation one may derive the coupled equations for resonant, steady-state SBS under the slowly varying amplitude approximation:

$$\frac{dE_p}{dz} = \frac{\gamma_e^2 q^2 \omega}{16\pi^2 \rho_o n c \Omega_B \Gamma_B} |E_s|^2 E_p, \quad (2.14.a)$$

$$\frac{dE_s}{dz} = \frac{\gamma_e^2 q^2 \omega}{16\pi^2 \rho_o n c \Omega_B \Gamma_B} |E_p|^2 E_s. \quad (2.14.b)$$

In writing equations (2.14) we have assumed that to a very good approximation $\omega_p \approx \omega_s = \omega$.

In the undepleted pump limit the right hand side of equation (2.14.a) is set to zero leaving an analytical solution to equation (2.14.b);

$$E_s = E_o \exp\left[6\chi_{SBS}^{(3)} |E_p|^2 z\right]. \quad (2.15)$$

It is this simple solution that occurs in the undepleted pump limit that makes it such an appealing, if unrealistic, approximation to work under.

Equations (2.14) show that the SBS process is a pure gain process. That is, it is automatically phase matched and there is no discrimination or enhancement of one

wave over another due to phase-matching requirements. In the next section we will develop a theoretical basis for the discrimination against Stokes modes that are not correlated with the pump field.

2.2 SBS phase conjugation

While the above derivation assists in understanding the SBS process, it does little to help in understanding why SBS can lead to phase conjugation. Prior to 1972 it was known that SBS occurred primarily in the direction counter-propagating to the incident wave, but this effect may be explained by the fact that for a wave of limited transverse extent the product in the exponent of equation (2.15) is maximized along the path of the incident wave. The discovery in 1972 that SBS produced phase conjugation led Zel'dovich et al.⁶ to establish a theoretical basis for the effect, utilizing a statistical argument to account for the higher gain experienced by the phase-conjugate wave. Since the discrimination against nonconjugate components is central to an investigation of phase-conjugate fidelity, it is useful to briefly outline why the conjugate wave sees gain in excess of the nonconjugate components.

The origin of optical phase conjugation by SBS lies in the fact that not only is the intensity of the waves important, but the correlation between the scattered and incident waves is also important. Since SBS begins with noise in the medium, there are sufficient spatial components in the field to create any arbitrary wavefront. However, the components that make up the phase-conjugate wave will see higher gain than nonconjugate waves. This is because in a nonuniform beam the conjugate wave will retrace the path of the incident beam, matching the intensity distribution exactly, resulting in a higher intensity length product than the nonconjugate waves.

To understand this process it is useful to consider the two waves of section 2.1 in terms of intensity rather than electric fields. Consider the pump and Stokes waves as having nonuniform transverse intensity profiles denoted by I_p and I_s , respectively. The total power in each beam at some fixed point in the medium is given by

$$P_{p,s} = \int I_{p,s} d^2r. \quad (2.16)$$

In terms of the powers in the beams equation (2.14.b) may be written as

$$\frac{dP_s}{dz} = g \frac{P_p P_s}{A} \frac{\langle I_p I_s \rangle}{\langle I_p \rangle \langle I_s \rangle}, \quad (2.17)$$

where g is the SBS intensity gain, A is the total area of integration and

$$\langle I_{p,s} \rangle = \frac{\int I_{p,s} d^2r}{A}. \quad (2.18)$$

If I_p and I_s are completely uncorrelated (or if they are both spatially uniform) then $\langle I_p I_s \rangle = \langle I_p \rangle \langle I_s \rangle$. Defining $\langle I_s \rangle = \alpha \langle I_p \rangle$ for simplicity, we see that $\langle I_p I_s \rangle = \alpha \langle I_p \rangle^2$. If however, I_p and I_s are correlated (for example if $I_s = \alpha I_p$), then $\langle I_p I_s \rangle$ is greater than $\langle I_p \rangle \langle I_s \rangle$, and the cross correlation function, given by the last term in equation (2.17), is greater than unity;

$$C = \frac{\langle I_p I_s \rangle}{\langle I_p \rangle \langle I_s \rangle} > 1. \quad (2.19)$$

In the case of a severely aberrated beam, the transverse variations in the intensity may obey Gaussian statistics⁹³ and $\langle I^2 \rangle = 2\langle I \rangle^2$. Therefore in the case that $I_s = \alpha I_p$, $\langle I_p I_s \rangle = \alpha \langle I_p^2 \rangle = 2\alpha \langle I_p \rangle^2$. Thus the portion of the scattered wave that is the phase-conjugate of the incident wave in this case will have a cross correlation coefficient of $C = 2$, and will see an exponential gain that is a factor of two higher than the uncorrelated components. Thus one expects that the beam scattered in the backward direction by SBS will be dominated by the component that is the phase-conjugate of the incident wave.

This analysis leads one to believe that up to some limiting point, the more severely aberrated the incident wave the higher the discrimination against nonconjugate components and the better the phase conjugation. This reasoning is the origin of the use of the phase plate to enhance phase conjugation as described in Chapter 1. Unfortunately, as noted earlier, the presence of small scale phase distortions on the incident beam leads to small scale intensity variations on the Stokes beam. A detailed analysis of this effect has been presented by Baranova and

Zel'dovich⁸⁰ and can be understood even within the assumption of an undepleted pump.

2.3 An alternative theoretical formalism for SBS

The theoretical derivation of the SBS process presented in section 2.1 showed that the SBS process in and of itself does not discriminate against Stokes waves that are not correlated with the pump wave. That is, SBS is a pure gain process. Section 2.2 reviewed how a pure gain process can produce a Stokes wave that is strongly correlated with the pump wave. In this section we present an alternative theoretical formalism that demonstrates that the SBS equations themselves predict the process of optical phase conjugation if transverse variations of the waves are considered in the derivation of the coupled amplitude equations.

To develop the formalism we assume a homogeneous, nonlinear, time-independent medium. The wave equation for an electric field traveling in this medium is given by

$$\nabla^2 \tilde{E} - \frac{\epsilon}{c^2} \frac{\partial^2 \tilde{E}}{\partial t^2} = \frac{4\pi}{c^2} \frac{\partial^2 \tilde{P}}{\partial t^2}, \quad (2.20)$$

where as usual ϵ is the square of the index of refraction and c is the speed of light.

Let us assume that the electric field in the medium consists of a pump wave and a Stokes wave that are generally counter propagating. Thus the field in the medium is adequately described by two counter-propagating waves with independent and slowly varying envelopes that are a function of all three spatial coordinates:

$$\tilde{E} = \left(E_p(\mathbf{r}, z) e^{-i(kz + \omega_p t)} + E_s(\mathbf{r}, z) e^{i(kz - \omega_s t)} \right) + \text{c.c.} \quad (2.21)$$

We now write the steady-state driven wave equation for the field described by equation (2.21). We assume the slowly varying envelope approximation and separate the portions of the nonlinear polarization that are phase matched to the two parts of the electric field and treat them as independent driving terms. This allow us to write two coupled wave equations, each one describing the propagation of one of the constituent fields. These equations are

$$\nabla_T^2 E_p - 2ik \frac{\partial E_p}{\partial z} = \frac{-4\pi\omega^2}{c^2} P_{-ik}^{NL} \quad (2.22.a)$$

and

$$\nabla_T^2 E_s + 2ik \frac{\partial E_s}{\partial z} = \frac{-4\pi\omega^2}{c^2} P_{+ik}^{NL}, \quad (2.22.b)$$

where $P_{\pm ik}^{NL}$ refers to the phase matched portion of the nonlinear polarization, we assume that $\omega_p = \omega_s = \omega$, and as before ∇_T^2 is the transverse portion of the Laplacian operator.

We now consider a modal decomposition of the transverse components of the pump and Stokes fields. For the moment we will leave the basis set arbitrary, but require that the individual functions of the basis set be orthonormal and individually satisfy the homogenous wave equation. Thus we may write the pump and Stokes waves as a superposition of the basis sets A and B ,

$$E_p(\mathbf{r}, z) = \sum_{\alpha} a_{\alpha}(z) A_{\alpha}(\mathbf{r}, z) \quad (2.23.a)$$

and

$$E_s(\mathbf{r}, z) = \sum_{\alpha} b_{\alpha}(z) B_{\alpha}(\mathbf{r}, z). \quad (2.23.b)$$

Substituting equations (2.23.a) and (2.23.b) into equations (2.22.a) and (2.22.b), and utilizing the fact that both A_{α} and B_{α} are solutions to the homogeneous wave equation, the coupled equations describing the propagation of the wave described by equation (2.21) become

$$2ik \sum_{\alpha} A_{\alpha} \frac{\partial a_{\alpha}}{\partial z} = \frac{4\pi\omega^2}{c^2} P_{-ik}^{NL} \quad (2.24.a)$$

and

$$2ik \sum_{\alpha} B_{\alpha} \frac{\partial h_{\alpha}}{\partial z} = \frac{-4\pi\omega^2}{c^2} P_{+ikz}^{NL}. \quad (2.24.b)$$

A similar derivation to that described in section 2.1 shows that the phase matched portion of the nonlinear polarization under the slowly varying envelope approximation, assuming on-resonance SBS, is given by

$$P_{SBS}^{NL} = i6\chi_{SBS}^{(3)} \left[|E_s(\mathbf{r}, z)|^2 E_p(\mathbf{r}, z) - |E_p(\mathbf{r}, z)|^2 E_s(\mathbf{r}, z) \right]. \quad (2.25)$$

By substituting equations (2.23) into equation (2.25) we may write the phase matched portions of the nonlinear polarization in terms of the two basis sets used for the decomposition of the electric fields. Upon doing this, we may multiply each of equations (2.24) by a single member of the applicable basis set (A_n^* or B_n^*) and integrate over all of transverse space, utilizing the orthonormality of the functions to produce the equations

$$\frac{\partial a_n}{\partial z} = \frac{12\pi\omega}{\sqrt{\epsilon}c} \chi_{SBS}^{(3)} \sum_{jkl} a_j b_k^* b_l \int_{-\infty}^{\infty} d^2r A_j B_k^* B_l A_n^* \quad (2.26.a)$$

and

$$\frac{\partial b_n}{\partial z} = \frac{12\pi\omega}{\sqrt{\epsilon}c} \chi_{SBS}^{(3)} \sum_{jkl} b_j a_k^* a_l \int_{-\infty}^{\infty} d^2r B_j A_k^* A_l B_n^*. \quad (2.26.b)$$

To continue the development of the model it is now necessary to choose basis sets for the decomposition. Since our research concerns focused Gaussian beams we will choose the Hermite-Gaussian functions as the basis set. The Hermite-Gaussian functions are chosen instead of the Laguerre-Gaussian functions for the basis set because the type of aberrations that we will wish to model are not necessarily cylindrically symmetric and therefore lend themselves to decomposition into Hermite-Gaussian more readily than Laguerre-Gaussian functions.

In one of the two transverse dimensions the normalized Hermite-Gaussian modes for the pump wave are given by⁹⁴

$$A_n(x, z) = \left(\frac{2}{\pi}\right)^{1/4} (2^n n! w(z))^{-1/2} e^{i(n+1/2)\psi(z)} H_n\left(\frac{\sqrt{2}x}{w(z)}\right) \exp\left[-i\frac{kx^2}{2R(z)} - \frac{x^2}{w(z)^2}\right]. \quad (2.27.a)$$

For the Stokes wave we choose the basis set made up of the complex conjugates of the modes of the pump wave. These are given by

$$B_n(x, z) = \left(\frac{2}{\pi}\right)^{1/4} (2^n n! w(z))^{-1/2} e^{-i(n+1/2)\psi(z)} H_n\left(\frac{\sqrt{2}x}{w(z)}\right) \exp\left[i\frac{kx^2}{2R(z)} - \frac{x^2}{w(z)^2}\right]. \quad (2.27.b)$$

Here $w(z)$, $R(z)$ and $\psi(z)$ have their usual meanings of spot size, radius of curvature of the wave front and Guoy phase angle respectively, given by

$$w(z) = w_o \sqrt{1 + \left(\frac{z}{z_R}\right)^2},$$

$$R(z) = z + \frac{z_R^2}{z}$$

and

$$\psi(z) = \tan^{-1}\left(\frac{z}{z_R}\right).$$

As usual, w_o is the spot size at the beam waist and z_R is the Rayleigh range given by

$$z_R = \frac{\pi w_o^2}{\lambda}.$$

Since the transverse coordinates are orthogonal, in two dimensions the basis sets are given by

$$A_{n,m}(\mathbf{r}) = A_n(x)A_m(y)$$

and

$$B_{n,m}(\mathbf{r}) = B_n(x)B_m(y).$$

For notational simplicity I will develop the rest of the model in only one of the two transverse dimensions.

Having chosen a basis set, the product under the integral in equations (2.26) can be written explicitly as

$$\begin{aligned} A_j B_k^* B_l A_n^* &= \left(\frac{2}{\pi}\right) (2^{j+k+l+n} j! k! l! n!)^{-1/2} \left(\frac{1}{w(z)}\right)^2 \\ &\times H_j\left(\frac{\sqrt{2}x}{w(z)}\right) H_k\left(\frac{\sqrt{2}x}{w(z)}\right) H_l\left(\frac{\sqrt{2}x}{w(z)}\right) H_n\left(\frac{\sqrt{2}x}{w(z)}\right) \exp\left(\frac{-4x^2}{w(z)^2} + i[j+k-l-n]\psi(z)\right) \end{aligned} \quad (2.28.a)$$

and

$$\begin{aligned} B_j A_k^* A_l B_n^* &= \left(\frac{2}{\pi}\right) (2^{j+k+l+n} j! k! l! n!)^{-1/2} \left(\frac{1}{w(z)}\right)^2 \\ &\times H_j\left(\frac{\sqrt{2}x}{w(z)}\right) H_k\left(\frac{\sqrt{2}x}{w(z)}\right) H_l\left(\frac{\sqrt{2}x}{w(z)}\right) H_n\left(\frac{\sqrt{2}x}{w(z)}\right) \exp\left(\frac{-4x^2}{w(z)^2} - i[j+k-l-n]\psi(z)\right). \end{aligned} \quad (2.28.b)$$

Since the integral is over the transverse dimensions and the Hermite-Gaussian functions are separable, we can perform the integration in equations (2.26) explicitly and define an overlap integral by

$$\begin{aligned} \xi_{jkl n} &= \left(\frac{2}{\pi}\right) (2^{j+k+l+n} j! k! l! n!)^{-1/2} \\ &\times \int_{-\infty}^{\infty} dx' H_j(\sqrt{2}x') H_k(\sqrt{2}x') H_l(\sqrt{2}x') H_n(\sqrt{2}x') \exp(-4x'^2), \end{aligned} \quad (2.29)$$

where

$$x' = \frac{x}{w(z)}.$$

Equations (2.26) can now be written in final form as

$$\frac{\partial a_n}{\partial z} = \left(\frac{12\pi\omega}{\sqrt{\epsilon}c} \right) \left(\frac{1}{w(z)} \right) \chi_{SBS}^{(3)} \sum_{jkl} a_j b_k^* b_l \xi_{jkl n} e^{i(j-k-l-n)\psi(z)} \quad (2.30.a)$$

and

$$\frac{\partial b_n}{\partial z} = \left(\frac{12\pi\omega}{\sqrt{\epsilon}c} \right) \left(\frac{1}{w(z)} \right) \chi_{SBS}^{(3)} \sum_{jkl} b_j a_k^* a_l \xi_{jkl n} e^{-i(j+k-l-n)\psi(z)} \quad (2.30.b)$$

Equations (2.30) are the steady-state coupled SBS equations in two dimensions. In three dimensions this system of equations is given by

$$\begin{aligned} \frac{\partial a_{n,m}}{\partial z} &= \left(\frac{12\pi\omega}{\sqrt{\epsilon}c} \right) \left(\frac{1}{w_x(z)} \right) \left(\frac{1}{w_y(z)} \right) \chi_{SBS}^{(3)} \\ &\times \sum_{jklpqr} a_j b_k^* b_l r \xi_{jkl n} \xi_{pqr m} e^{i(j+p+k+q-l-r-n-m)\psi(z)} \end{aligned} \quad (2.31.a)$$

and

$$\begin{aligned} \frac{\partial b_{n,m}}{\partial z} &= \left(\frac{12\pi\omega}{\sqrt{\epsilon}c} \right) \left(\frac{1}{w_x(z)} \right) \left(\frac{1}{w_y(z)} \right) \chi_{SBS}^{(3)} \\ &\times \sum_{jklpqr} b_j a_k^* a_l r \xi_{jkl n} \xi_{pqr m} e^{-i(j+p+k+q-l-r-n-m)\psi(z)} \end{aligned} \quad (2.31.b)$$

Note that in contrast to the development in section 2.1, here all of the transverse effects are included. These transverse effects are not only those attributable to diffraction, but also include the very complicated effects of nonlinear gain.

There are three important things to note in equations (2.31). The first thing to note is that Stokes modes that are conjugate to the pump modes will see higher gain than those that are not. That is, whenever there is an instance where $j=k=l=n$ or $p=q=r=m$, the value of the overlap integral is maximum. Stokes modes that are not conjugate to modes that exist in the pump beam have a reduced value of the overlap integral, and therefore see less gain than those modes whose conjugate does exist in the pump beam.

The second important conclusion that can be drawn from an examination of equations (2.31) is that there are quite obviously some phase-matching requirements

and these phase matching requirements can also help to ensure that modes correlated with the pump wave are amplified more than those uncorrelated modes. Note however, that the phase matching requirements are imposed internally on each of the waves independently, so that the phase of the Stokes is unaffected by the phase of the pump and vice versa.

The third important thing to note in equations (2.31) is that every Stokes mode is coupled to every other Stokes and pump mode through the Brillouin nonlinearity. Therefore all modes affect the phase and amplitude of all other modes. In the case of SBS for optical phase conjugation, this coupling between modes results in the imposition of noise on the conjugate modes due to the presence of nonconjugate modes. As will be seen later, when the amplitude of the conjugate mode dominates, this noise can still be seen in the phase of the mode.

Developing the SBS equations in the manner described here allows us to see that SBS can lead to phase conjugation in the context of the coupled amplitude equations, without recourse to statistical arguments such as those presented in section 2.2. The discrimination against nonconjugate components is accomplished by the reduced value of the overlap integral for cases where the indices $(j,k,l,n$ or $p,q,r,m)$ are not the same and via the imposition of phase matching requirements between Stokes modes.

In closing this section we note that the process of phase conjugation can be inferred from an examination of equations (2.31); however the development here in no way invalidates the statistical argument presented in section 2.2. Our development of the SBS equations is complementary to that work, and all of the analysis of Zel'dovich et al. presented in section 2.2 is also valid in the context of equations (2.31).

2.4 Modeling of the SBS process

As noted earlier, the SBS equations do not appear to have a simple analytical solution. If one wishes to investigate transverse, temporal or pump depletion effects it appears that one must turn to numerical methods. Recent numerical work on the transient nature of SBS has provided great insight into certain phase effects in SBS;^{68,70,95} however the investigation of effects that are dependent upon the transverse beam profile have been limited.^{75,76,92} Furthermore it appears that the spatial effects of the stochastic initiation of SBS have yet to be investigated at all.

In this section we present results of the numerical solutions to equations (2.31) under conditions often encountered in the laboratory. In particular, the beams modeled will be Gaussian in intensity and can be smoothly aberrated in phase; this corresponds to the case most often encountered in SBS laser systems. Although the computational time required is enormous, the numerical modeling effort has proved to be a significant tool in understanding the SBS process.

In modeling the SBS process we numerically solve equations (2.31) with one slight modification. We assume that there is no coupling between modes in orthogonal transverse dimensions higher than order zero. That is, we consider all modes $(n,0)$ and $(0,m)$, but we will not in general consider modes (n,m) where $n,m \neq 0$. This is equivalent to assuming that the SBS process treats each transverse dimension independently for modes of order greater than zero. This is not strictly true, but we find it to be a valid approximation for a very wide variety of circumstances commonly encountered in the laboratory.

Understanding that the single index on the coefficients implies the lowest order mode in the orthogonal dimension, we will define the SBS coupling constant by

$$K = \frac{12\pi\omega}{\sqrt{\epsilon}c} \xi_{50000}. \quad (2.32)$$

Equations (2.31) may then be written in the form used for our numerical analysis as

$$\frac{\partial a_n}{\partial z} = K \left(\frac{1}{w_x(z)} \right) \left(\frac{1}{w_y(z)} \right) \chi_{SBS}^{(3)} \sum_{jkl} a_j b_k^* b_l \xi_{jkl n} e^{i(j+k-l-n)\psi(z)} \quad (2.33.a)$$

and

$$\frac{\partial b_n}{\partial z} = K \left(\frac{1}{w_x(z)} \right) \left(\frac{1}{w_y(z)} \right) \chi_{SBS}^{(3)} \sum_{jkl} b_j a_k^* a_l \xi_{jkl n} e^{-i(j+k-l-n)\psi(z)}, \quad (2.33.b)$$

where the possibility of astigmatic modes is shown explicitly by writing the spot sizes of the orthogonal transverse dimensions separately.

The coordinate system and physical picture used for the modeling are shown in Figure 2.1. The choice of the origin at the focus of the pump beam rather than one end of the Brillouin medium is made to facilitate the modal decomposition. The modes used as a basis set for the decomposition are completely specified by equations (2.27), provided we know the spot size at the beam waist w_o . Since we are interested in investigating focused Gaussian beams, we have defined the basis set by the spot size at the focus of the pump beam. The spot size at the focus of a lens of focal length f is related to the beam size at the entrance to the focusing lens by⁹⁴

$$w_o = \frac{f\lambda}{\pi w(f)}. \quad (2.34)$$

We now turn to the actual numerical integration of equations (2.33). In principle the numerical solution of two-point boundary value problems using equations of this form is straightforward. There are several methods that have been developed for the solution of coupled nonlinear differential equations;⁹⁶ however, as with most problems of interest, there are some subtleties in the solution of equations (2.33). Additionally it is of interest not simply to find a solution to the equations at the boundaries, but it is important in our research to also know the solution at every point within the medium. Additionally, we wish to investigate the effects due to the distributed noise within the medium.

The method devised to meet all of the requirements is based on a recursive use of the Runge-Kutta method of numeric integration with a fixed step size. The medium is divided into a longitudinal grid of 2,500 steps and equation (2.33.a) is integrated from the front of the medium to the back. The integration is the simultaneous integration of N coefficients and the value of each of the N coefficients at each point in the medium is stored along with an additive noise of random phase with amplitude equal to 10^{-6} of that of the pump. Equation (2.33.b) is then integrated from the back of the medium to the front in the presence of the pump. After completing the integration of the Stokes wave, the pump wave is again integrated through the medium; however prior to this integration an algorithm is used to attempt to adjust the Stokes wave for the effects of pump depletion. This sequence is repeated until the total energy in the system is conserved, a process that normally takes between 20 and 50 iterations.

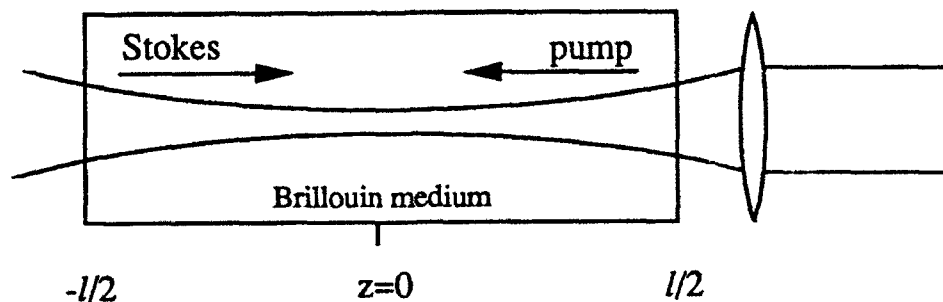


Figure 2.1. The physical geometry and the coordinate system assumed in the model.

Unfortunately, due to the intensity maximum at the focus of the system it is impossible to simply choose a pump value of interest and integrate the equations. It is necessary instead to solve the equations for the system starting well below the level where pump depletion becomes important, and then slowly increase the pump power. Thus the solution at each new intensity relies on the solution of the previously solved lower intensity situation. The necessity of finding solutions at many pump powers combined with the enormous number of terms necessary for accurate predictions is responsible for the large amount of CPU time needed to arrive at a solution.

We have found that under most situations of interest in our research, ten Hermite-Gaussian modes is an adequate number to describe the stimulated Brillouin scattering resulting from a pump that is initially described by a Gaussian beam of lowest order. Even with this small number of modes in the basis set, to solve the ten coupled equations (each having 2000 terms) at an intensity level that is well into the region of pump depletion takes approximately 45 days of CPU time on an IBM RISC 6000 computer.

Fortunately we have found that due to parity considerations, the growth of the odd numbered modes is very small compared to the even numbered modes and therefore in many cases it is only necessary to explicitly integrate the first five even numbered modes. Under these circumstances the necessary CPU time is reduced to approximately ten days.

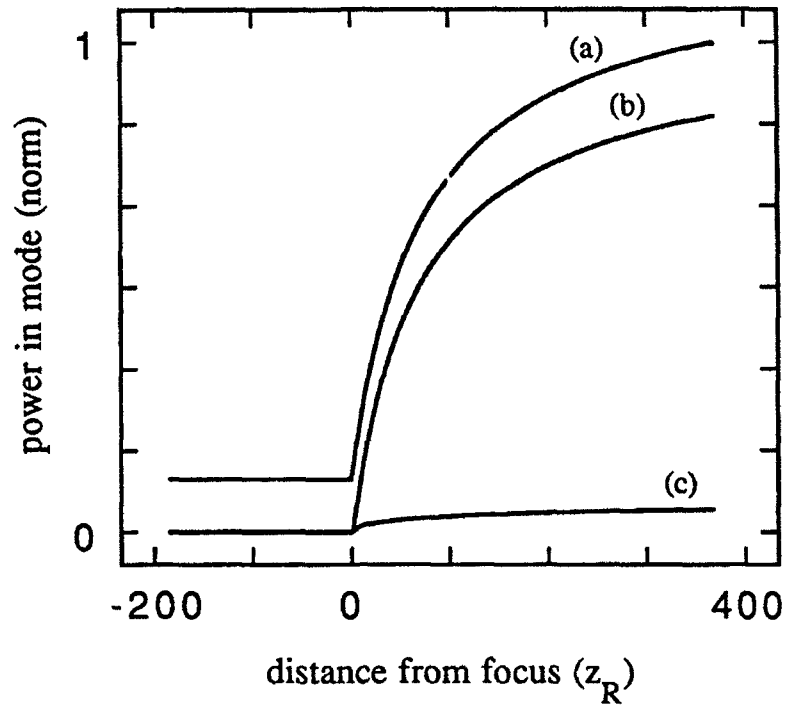


Figure 2.2. Power in the (0,0) mode of the pump beam (a), and the (0,0) and (0,2) modes of the Stokes beam (b and c) as a function of distance within the Brillouin medium during SBS. The situation modeled is for ten times above threshold.

2.5 Initial results of the modeling effort

Although excruciatingly slow in its numerical solution, the model described above accurately predicts the behavior of the fields in a Brillouin medium in a focused geometry under many situations. The evolution of the power in the first two even numbered modes of the Stokes wave for an incident focused Gaussian beam is shown in Figure 2.2. Also shown in Figure 2.2 is the evolution of the power in the mode of the incident beam that was input into the medium (the (0,0) mode). The phase-conjugating ability of SBS is clearly seen by the dominance of the (0,0) mode in the Stokes beam. The power in the remaining modes of the basis set is too small to be of any significance on the scale shown in Figure 2.2. In Figure 2.2 the abscissa is written in terms of the Rayleigh range of the incident beam and the ordinate is

normalized to the input power of the pump. The situation modeled is that shown in Figure 2.1.

There are two parameters that characterize plots of the type shown in Figure 2.2. The first is the length of the medium relative to the Rayleigh range of the incident beam. This parameter has a large effect both on the behavior of the power transfer between the incident and Stokes beams and on the ability of the process to produce a phase-conjugate of the incident wave.

The second important parameter is the power in the incident beam. That is, it is important to know by how much the incident beam power exceeds the threshold for SBS. It is common among researchers in the field to quote the power in a beam as being some value *times threshold*, where it is understood that the threshold referred to is the threshold for SBS. What is implicit in this statement is an understanding of what the SBS threshold is; unfortunately there is no consensus in the literature as to what exactly defines SBS threshold.

For theoretical investigations one normally assumes that SBS threshold occurs at the point where the product of the Brillouin gain and the on-axis pump intensity integrated over the length of the medium reaches a certain value (usually ~25-30). For engineering expediency the SBS threshold is often defined as the point at which the Stokes power leaving the medium reaches 10% of the value of the incident beam. While there are several disadvantages to this latter definition, the "10% criteria" has the advantage of being directly measurable in the laboratory. As long as one ignores the semantic problem of being able to have SBS occur below SBS threshold, the 10% criteria is quite useful and we will therefore adhere to that convention. The interaction shown in Figure 2.2 is for an incident beam that is ten times over threshold.

From Figure 2.2 it is obvious that most of the power is extracted from the incident beam in the region in front of the focus. This has important implications that will be addressed fully later. However, SBS is actually the result of the selective amplification of noise within the medium and must be viewed from that perspective.

In order to demonstrate the noise amplification aspect of SBS, in Figure 2.3 we have plotted the first three even modes of the Stokes beam for the same situation shown in Figure 2.2 on a semi-log scale. Figure 2.3 clearly shows that almost all of the amplification of the initiating noise occurs at or near the focus and that very little actually occurs away from the focal region; this is of course expected from an

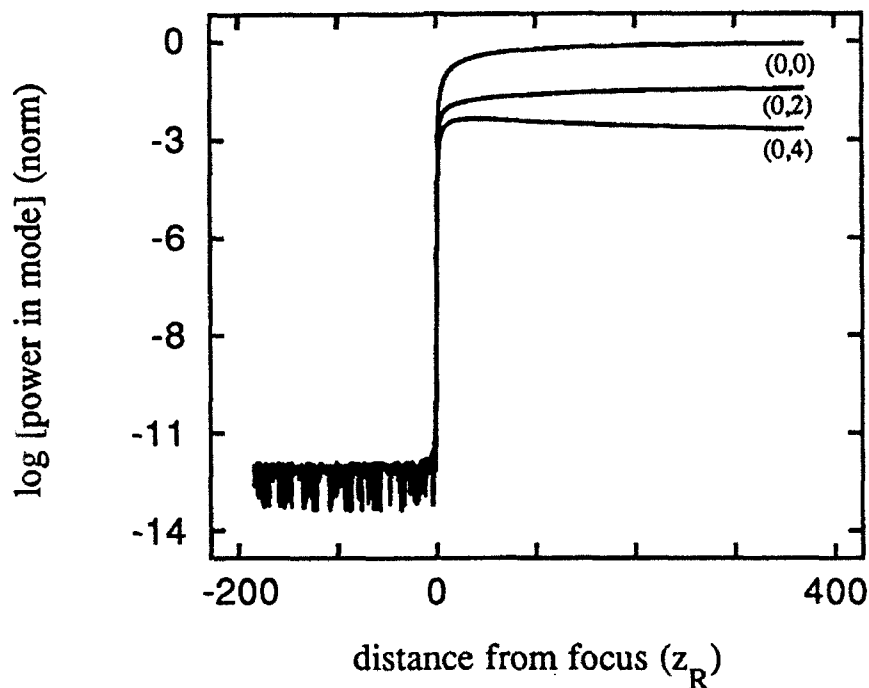


Figure 2.3. Plot of the log of the power in the first three even modes of the Stokes wave showing the amplification of noise and discrimination against nonconjugate modes. The incident beam was made up entirely of the (0,0) mode.

intuitive understanding of SBS. Furthermore, Figure 2.3 confirms that most of the discrimination against nonconjugate modes occurs at the focus. A full discussion of the implications of extended focal regions and short interaction lengths will be presented in Chapter 3.

2.6 Noise initiation of SBS

The inclusion of distributed noise in our model is one of the unique and most important aspects of our theoretical investigation. Some recent research has focused on the temporal aspects of the distributed nature of the noise in SBS,^{70,95} but little attention has been given to the spatial aspects.

In our model the amplitude of the noise in the Stokes wave at every point in the medium is fixed at 10^{-6} of the pump amplitude at that point, and given a random

phase. The integration of equations (2.33) is then allowed to progress; however every time the pump amplitude changes the noise amplitude is varied to keep the ratio constant at 10^{-6} . By using a distributed noise source we may investigate exactly where SBS starts in the focused geometry and what regions are important in the development of the phase of the Stokes beam.

Note that we have chosen to keep the noise amplitude fixed rather than use the more realistic model of a random amplitude with a mean of 10^{-6} of the pump. We do this so that conclusions about the SBS initiation process are not clouded by normal statistical fluctuations. Under ideal circumstances one would wish to use a stochastic phase and normal Gaussian amplitude distribution. However, given the length of time required for one simulation, it would be impossible to perform enough simulations to ensure that normal statistical fluctuations were not biasing the conclusions. Therefore we use a constant amplitude for the noise and follow the effects of the noise by examining the phase of the wave.

The effects of the noise on the amplitude of the Stokes beam are clearly seen in the portion of Figure 2.3 where $z < 0$, but it is the phase of the Stokes beam that yields the most information about the initiation process. Figure 2.4 shows the phase of the lowest order mode of the Stokes beam far below SBS threshold and at ten times threshold (only every fifth point has been plotted for purposes of clarity). The arrow in Figure 2.4(a) indicates the phase of the noise at the point at the far end of the Brillouin medium.

Figure 2.4(b) demonstrates that even very high above SBS threshold, the phase of the rear-most point determines the phase of the Stokes beam. From a naive point of view one would expect this to be true, since the integral of the product of the gain and the intensity over the length of the medium is the greatest for the maximum value of z . It is surprising however, that even ten times above threshold the phase of the Stokes beam is determined by the noise at the rear-most point, a point where the pump intensity is orders of magnitude lower than near the focus. Judging from the evolution of the amplitude shown in Figure 2.3, one may have thought that the initiating noise occurred much closer to the focus when the pump is far above threshold. Of course had random intensity been modeled into the noise, the point of initiation could have been slightly different, since a peak in the intensity of the noise could dominate over the length factor.

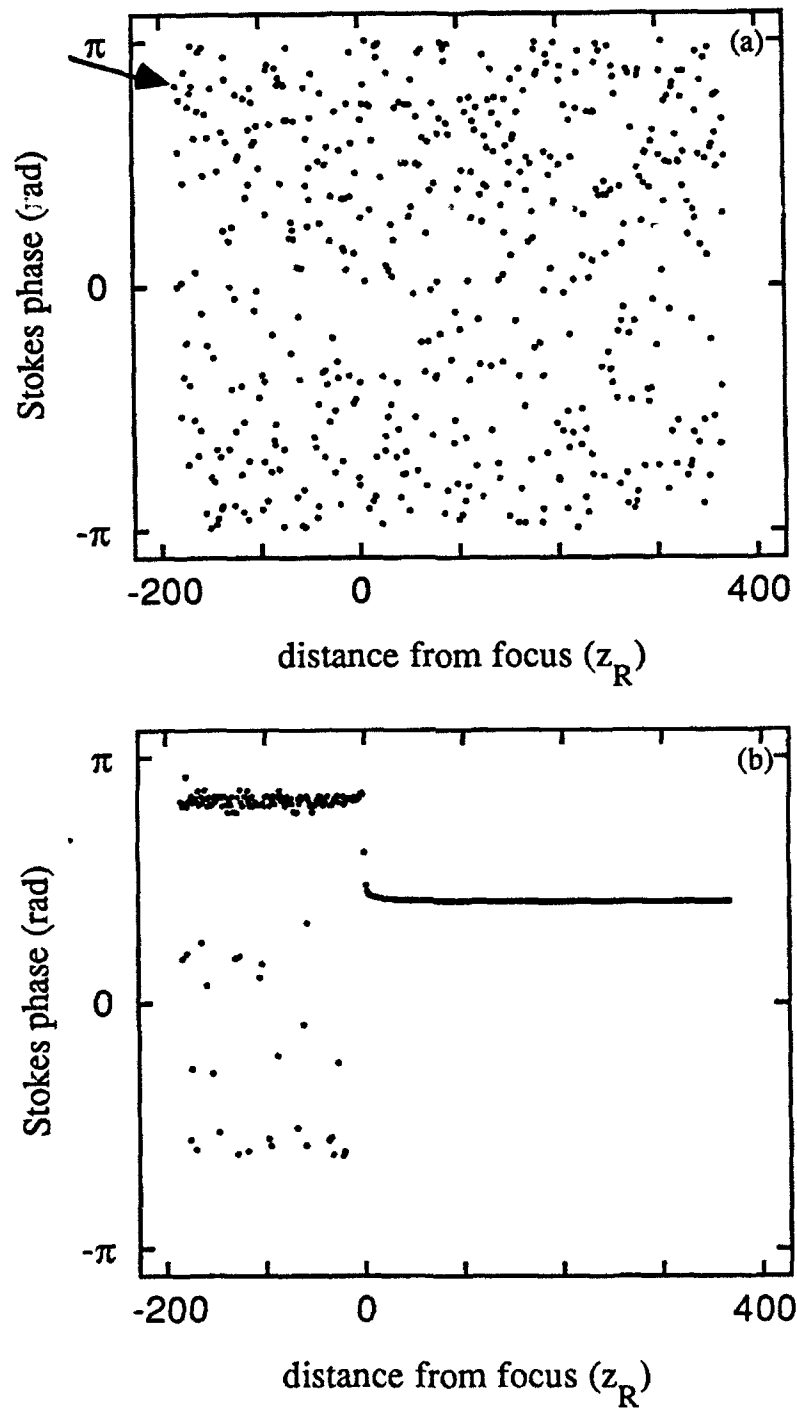


Figure 2.4. The phase of the lowest order mode of the Stokes radiation far below SBS threshold (a) and ten times above SBS threshold (b). The arrow in (a) indicates the phase of the noise at the point at the back end of the Brillouin medium

2.7 Phase pulling of the Stokes modes

Besides the determination of the origin of the phase of the Stokes beam, it is interesting to note in Figure 2.4(b) that the phase of the coefficient of the Stokes wave undergoes a phase shift as it propagates through focus. The magnitude of this phase shift depends in detail on the phase and magnitude of the other Stokes modes and varies with the intensity of the pump. If no modes other than the mode conjugate to the pump are allowed to propagate in the simulation, the coefficient of the Stokes wave undergoes no phase shift at all.

The origin of this phase shift is the coupling between modes mentioned in section 2.3. An examination of equations (2.31) reveals that even when one mode is dominant, the phases and amplitudes of all modes (including the dominant mode) are dependent upon the phases and amplitudes of all of the other modes. The more dominant a single mode is, the less effect the coupling between modes will have on the phase and amplitude of the dominant mode. In the case of the pump wave, where the mode structure is imposed externally, the phase shifts of the coefficients of the pump mode are very small upon propagation through the medium.

In the case considered in Figure 2.4(b), the phase of the coefficient of the Stokes wave moves in the same direction as the Guoy phase shift. Thus the Stokes wave has a total phase shift on the order of $3\pi/2$ as it propagates from the back of the medium to the front.

To demonstrate the effect that noise modes in the Stokes beam have on the mode conjugate to the pump wave we have solved equations (2.33) for a variety of different initial phases of the nonconjugate Stokes modes, keeping the initial phase of the conjugate mode fixed. We do this by forcing both the phase and the amplitude of the initiating radiation to be fixed for each mode throughout the medium. The noise in the TEM_{00} Stokes mode was fixed with zero phase and amplitude 10^{-6} of the pump. The noise in the other Stokes modes was fixed at 10^{-6} of the value of the pump in amplitude, but the phase was varied from zero to 2π . The results of these simulations are shown in Figure 2.5. In Figure 2.5 the phase of the coefficient of the mode conjugate to the pump mode (TEM_{00} mode) is plotted as a function of the initial phase of the other Stokes modes. It is clear from Figure 2.5 that even though the TEM_{00} mode dominates the Stokes wave (~80% of the power is in the TEM_{00} mode), its phase is determined in part by the amplitude and phase of all of the other

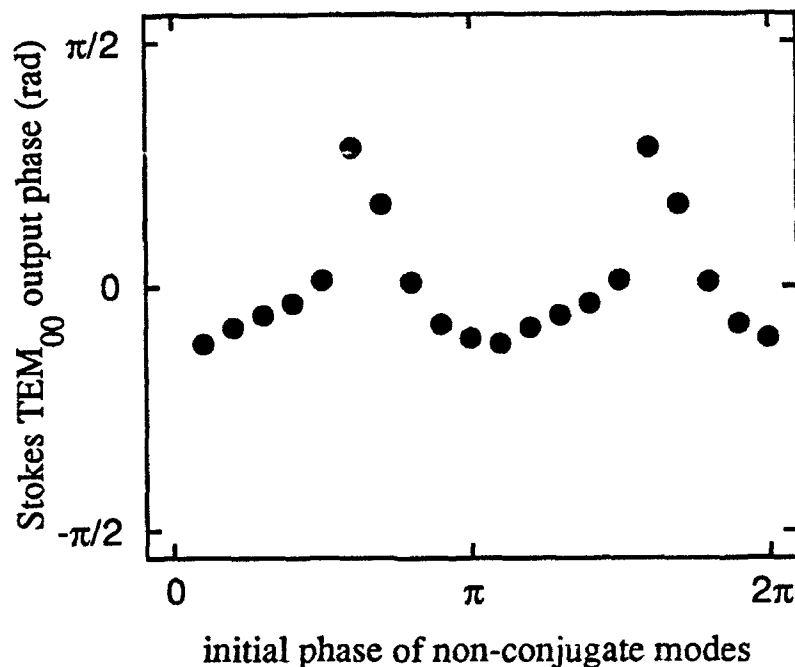


Figure 2.5. Demonstration of the effects of noise modes on the phase of the Stokes mode that is conjugate to the pump. The phase of the initiating radiation was held constant for the TEM_{00} mode and varied for the phase of the nonconjugate modes.

Stokes modes. Naturally, had the pump wave contained modes other than the TEM_{00} mode, they would have affected the phase and amplitude of the Stokes wave as well.

It is surprising that the nonconjugate, non-phase matched modes could have such a large effect on the Stokes wave. However, a similar behavior is observed for all modes in the region of high Brillouin gain. That is, a phase shift is observed at the focal point whose magnitude is determined by the magnitudes and phases of all of the other modes allowed to propagate.

A careful study of these phase shifts shows that they are the result of all of the modes attempting to shift their phase to maximize the gain. That is, the phase of each mode is shifted to maximize the constructive effect of all of the non-phase matched terms, a sort of competition for gain. Since all of the non-phase matched terms are also combined with a reduced overlap integral, one must wonder whether the effect of

the non-phase matched terms is of much importance. Our research has shown that the non-phase matched terms are extremely important.

To demonstrate the importance of the non-phase matched terms in determining the SBS gain of any given mode we will examine the b_0 , b_1 and b_2 modes of the Stokes beam in the simple case of a lowest order Gaussian beam focused into a Brillouin medium. First let us assume that only the a_0 mode of the pump beam is allowed to propagate, and then examine the first three terms in each of the differential equations describing the first three Stokes modes.

The three differential equations are:

$$\frac{\partial b_0}{\partial z} = K \left(\frac{1}{w_x(z)} \right) \left(\frac{1}{w_y(z)} \right) \chi_{SBS}^{(3)} |a_0|^2 \{ b_0 \xi_{0000} + b_1 \xi_{1000} e^{-i\psi(z)} + b_2 \xi_{2000} e^{-2i\psi(z)} \} \quad (2.35.a)$$

$$\frac{\partial b_1}{\partial z} = K \left(\frac{1}{w_x(z)} \right) \left(\frac{1}{w_y(z)} \right) \chi_{SBS}^{(3)} |a_0|^2 \{ b_0 \xi_{0001} e^{i\psi(z)} + b_1 \xi_{1001} + b_2 \xi_{2001} e^{-i\psi(z)} \} \quad (2.35.b)$$

$$\frac{\partial b_2}{\partial z} = K \left(\frac{1}{w_x(z)} \right) \left(\frac{1}{w_y(z)} \right) \chi_{SBS}^{(3)} |a_0|^2 \{ b_0 \xi_{0002} e^{2i\psi(z)} + b_1 \xi_{1002} e^{i\psi(z)} + b_2 \xi_{2002} \}. \quad (2.35.c)$$

To understand these equations it is important to know the values of the overlap integral ξ_{jkn} . The values of the overlap integrals in equations (2.35) are:

$$\begin{aligned} \xi_{0000} &= .56 \\ \xi_{2000} &= -.20 \\ \xi_{1001} &= .28 \\ \xi_{2002} &= .21, \end{aligned}$$

with all of the others being zero due to parity considerations (see Appendix C).

Replacing the overlap integrals with their actual values produces the following set of coupled equations:

$$\frac{\partial b_0}{\partial z} = K \left(\frac{1}{w_x(z)} \right) \left(\frac{1}{w_y(z)} \right) \chi_{SBS}^{(3)} |a_0|^2 \{ (.56)b_0 - (.20)b_2 e^{-2i\psi(z)} \} \quad (2.36.a)$$

$$\frac{\partial b_1}{\partial z} = K \left(\frac{1}{w_x(z)} \right) \left(\frac{1}{w_y(z)} \right) \chi_{SBS}^{(3)} |a_0|^2 \{ (.28)b_1 \} \quad (2.36.b)$$

$$\frac{\partial b_2}{\partial z} = K \left(\frac{1}{w_x(z)} \right) \left(\frac{1}{w_y(z)} \right) \chi_{SBS}^{(3)} |a_0|^2 \{ (-.20)b_0 e^{2i\psi(z)} + (.21)b_2 \}. \quad (2.36.c)$$

Examination of equations (2.36) would lead one to believe that the lowest order mode would dominate a rigorous integration of the SBS equations under these conditions. The value of the overlap integral for the phase matched term of the b_0 mode is twice that of the other two modes and would see the highest gain. The b_1 coefficient has the next highest gain and the b_2 coefficient sees the least gain of the three. In this case of a focused Gaussian beam, the phase angle is changing rapidly in the region of highest gain and therefore one would think that the importance of the non-phase matched terms is even less than indicated by the value of the overlap integral.

Rigorous integration of equations (2.36) shows that indeed the b_0 mode dominates the Stokes beam as expected. The value of the b_0 mode is an order of magnitude larger than that of the next largest coefficient. However, the next largest coefficient is that of the b_2 mode; the value of the coefficient b_1 is fully three orders of magnitude below that of the coefficient b_2 when the equations are integrated well above SBS threshold.

This surprising result is due to the fact that as the modes propagate, they change phase to enhance their gain through the non-phase matched terms. This may be described as *phase pulling* and is the origin of the phase shift exhibited in Figure 2.4. The b_1 mode sees such little gain because the coefficient for the non-phase matched term connecting the b_1 mode to the b_0 Stokes mode is zero. In the case of only three propagating modes, there is no phase of the b_1 mode that can in any way enhance the gain over the basic phase matched term. The situation of reduced gain due to the lack of an overlap integral connecting them with the b_0 Stokes mode is the same for all of the odd numbered modes.

If instead of a pure a_0 mode pump beam there were odd numbered pump modes present, naturally there would be non-phase matched terms in the equation for the odd numbered Stokes coefficients. However, there would still be no coupling between even and odd numbered Stokes modes except through the pump beam.

The phase shifts on the Stokes modes as they propagate through a region of high gain are then due to the process of phase pulling. This process will produce an intensity dependent phase shift on each mode of the Stokes beam as the phases adjust themselves for maximum gain. In the process of SBS, this will appear as phase noise on the Stokes beam.

The process of phase pulling may be intuitively understood by noting that in the example just considered, all of the even modes have either a local maximum or a local minimum at the same transverse coordinate as the maximum of the mode conjugate to the pump. Simply by shifting the phase of the b_0 mode and/or all of the other even numbered modes, all of these inflection points may be made to add constructively; this is the process of phase pulling. If instead of the mode amplitudes one were examining the SBS process in terms of the intensity structure, the process of phase pulling would be described as gain guiding. However, the presence of the overall shift of phase of the dominant fundamental mode is not predicted by a simple gain guiding argument.

While the analysis of phase pulling provides important insight into the physics of SBS, the importance of this induced phase shift in stimulated Brillouin scattering for laser applications is debatable. Since the absolute phase of the Stokes wave is of little interest one can argue that an arbitrary shift is unimportant; however, this process does add phase noise to the Stokes beam. This phase noise is dependent upon the amplitude and phase of the nonconjugate modes, thus one may assume that there are transient effects that reduce the coherence of the Stokes wave as the intensity of the pump wave changes in time. Phase pulling effects related to the coupling between Stokes modes may be very important in the determination of the noise properties of a Brillouin amplifier however, where the phase of the Stokes wave may be of great importance.

2.8 The Brillouin gain parameter

Before concluding a discussion of the modeling effort we will briefly investigate the response of the Brillouin gain parameter to variations in the pump power.

We may rewrite the undepleted pump solution for the Stokes wave (equation (2.15)) in terms of the intensity in the familiar manner:

$$I_s(z) = I_o e^{\eta(z)} \quad (2.37)$$

and define the Brillouin gain parameter as

$$\eta(z) = \int_{-l/2}^z g I_p(z') dz', \quad (2.38)$$

where again g is the Brillouin gain, $I_p(z)$ is the intensity of the pump wave in the medium and I_o is the intensity of the spontaneous scattering in the medium. Since it is often the total value of the Brillouin gain parameter that is of interest, for notational convenience we will define

$$\eta(l/2) = G. \quad (2.39)$$

Note that this definition of the Brillouin gain parameter is different than that normally defined in the literature. Normally the quantity $I_p(z)$ is defined as the undepleted pump intensity; here we have used the actual (depleted) value of $I_p(z)$ in the integral.

As mentioned above, the intensity of the spontaneous scattering in the medium is on the order of 10^{-12} of the intensity of the pump wave. The stimulated Brillouin scattering intensity becomes on the order of the pump intensity when $G \approx 27$. Thus a value of $G \approx 25-30$ is often quoted as a theoretical threshold for SBS. The question may be asked what happens when the pump power is increased after G becomes on the order of 25? That is, what effect does pump depletion have on the Brillouin gain parameter?

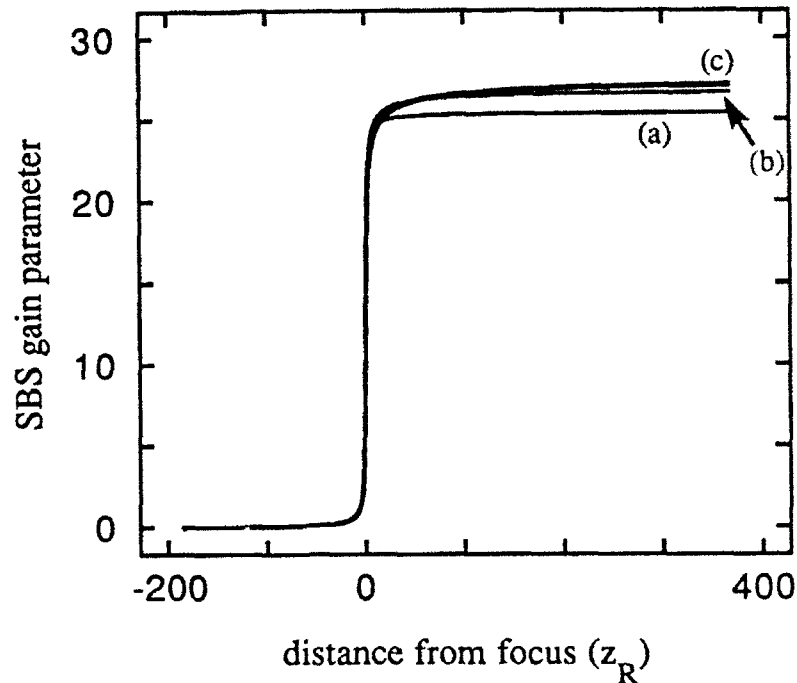


Figure 2.6. Evolution of the Brillouin gain parameter $\eta(z)$ as a function of distance within the medium. The values of the pump intensity are: (a) threshold ($G=25.37$), (b) five times above threshold ($G=26.63$), (c) ten and fifteen times above threshold ($G=27.01$ and $G=27.15$).

The model we have developed is specifically designed to investigate the distribution of the intensity within the Brillouin medium during SBS, so it is natural to use the simulation to investigate the value of the Brillouin gain parameter throughout the medium at different intensities of the pump.

Figure 26 shows the evolution of the on-axis value of $\eta(z)$ in the Brillouin medium for four values of pump intensity ranging from SBS threshold to 15 times above threshold. The value of G for each case increased as the pump intensity was increased, but clearly not linearly. In fact, the difference between the final value of the Brillouin gain parameter for ten and 15 times above threshold ($\sim 0.5\%$) is not noticeable on the scale used in Figure 2.6.

Since it is obvious from Figure 2.6 that G does not increase linearly with increased pump intensity, we may conclude (since the Brillouin gain is a constant) that the longitudinal intensity profile of the pump wave has been modified by the SBS process. That is, above SBS threshold a significant amount of power gets extracted from the pump wave before the focal point. As the pump intensity is increased, the amount of power extracted from the pump wave by the Stokes wave at points in front of the focus becomes proportionally larger, so that an increase in incident pump intensity does not result in a proportional increase in G . With extensive modeling we have shown that the power of the waves in a focused Brillouin interaction has a characteristic functional form as a function of longitudinal coordinate z .

To demonstrate the functional form of the power in the pump wave as a function of the longitudinal coordinate, in Figure 2.7 we have plotted the power in the

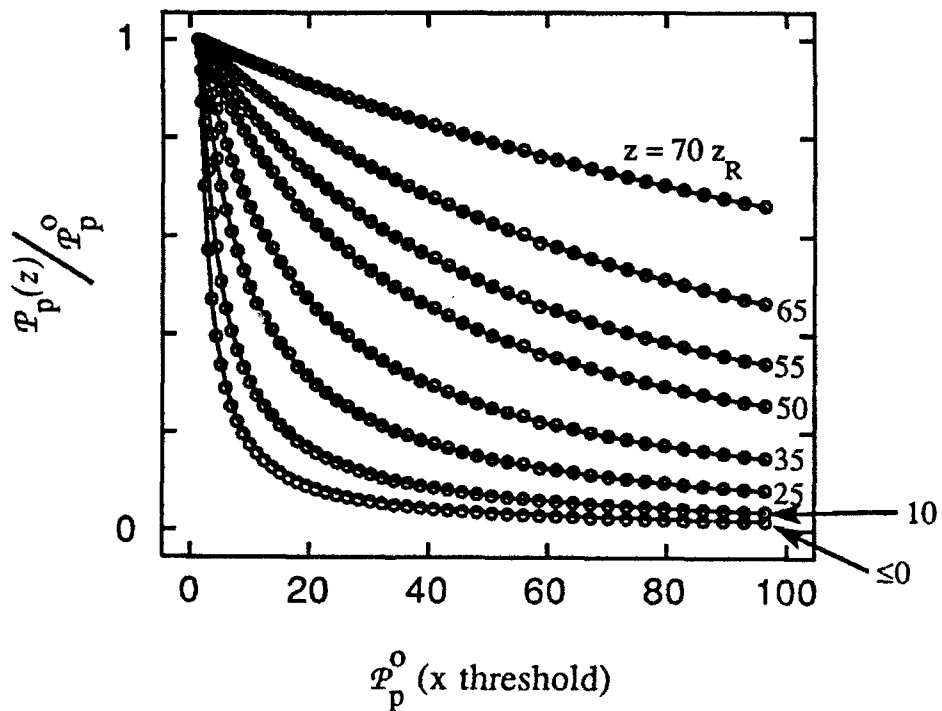


Figure 2.7. Power in the pump beam at different points in the Brillouin medium plotted as a function of the input pump power. The points are derived from simulation and the lines are fit to equation (2.40).

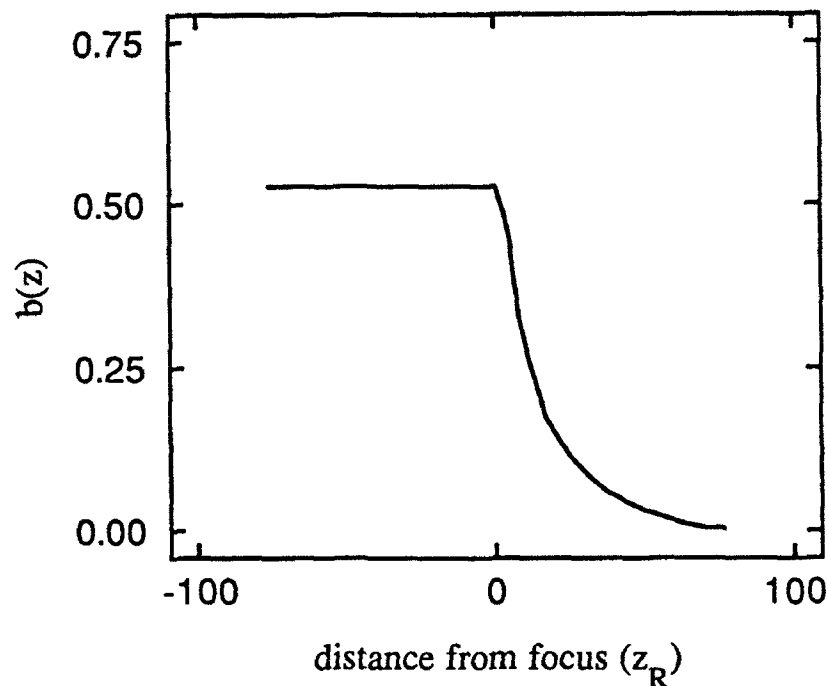


Figure 2.8. The saturation parameter plotted as a function of position in the Brillouin medium. From the front of the medium to the focus $b(z)$ is almost exponential; past the focus $b(z)$ is a constant.

pump wave ($\mathcal{P}_p(z)$) at several different points in the medium versus the input pump power. The points in Figure 2.7 are derived from simulations using the model described above and the lines are a fit to the equation

$$\frac{\mathcal{P}_p(z)}{\mathcal{P}_p^0} = \frac{1}{a(z) + b(z)\mathcal{P}_p^0}, \quad (2.40)$$

where $\mathcal{P}_p^0 = \mathcal{P}_p(l/2)$ and $a(z)$ and $b(z)$ are constants determined by the position in the Brillouin medium. Equation (2.40) shows that from the perspective of the pump beam, the SBS process looks like a reverse saturable-absorber.

Equation (2.40) is only valid above SBS threshold and therefore the constant $a(z)$ is of little importance. If the value of \mathcal{P}_p^0 was defined such that at SBS threshold $\mathcal{P}_p^0 = 0$, then the value of $a(z)$ would be unity. The z -dependent parameter $b(z)$ in equation (2.40) is of importance however. The parameter $b(z)$ indicates the strength

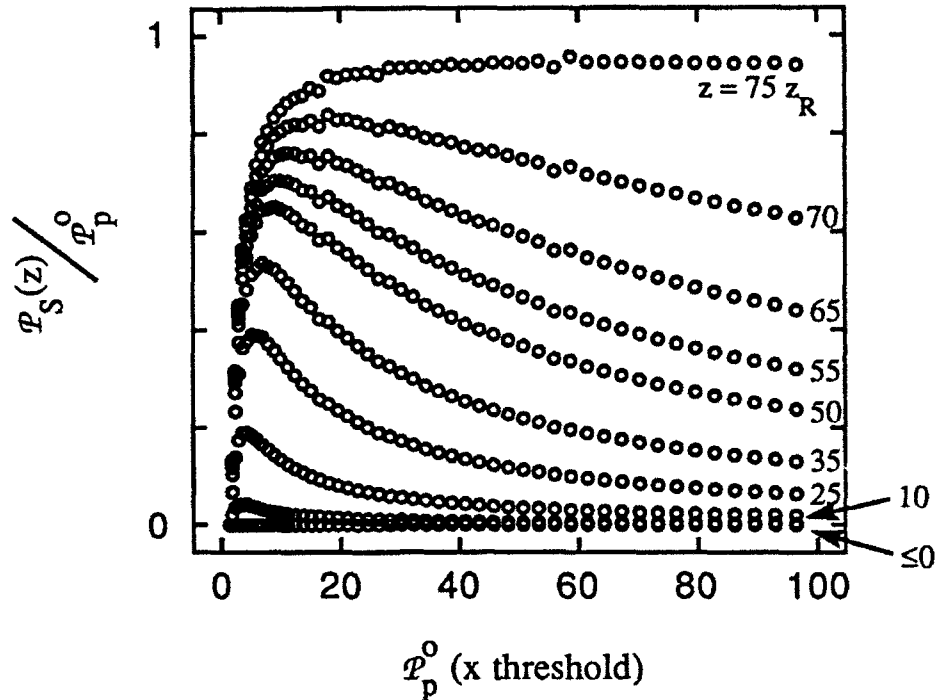


Figure 2.9. Power in the Stokes beam at different points in the Brillouin medium plotted as a function of the input pump power.

of the saturation of the SBS process at that point in the medium, and we will therefore refer to it as the Brillouin saturation parameter. The Brillouin saturation parameter is plotted in Figure 2.8 as a function of position in the medium. The actual value of $b(z)$ will vary with varying focal geometries, but the functional form is constant. The functional form of $b(z)$ is not easily fit, but we find that the form is almost exponential from the entrance to the medium to the focal point, where it becomes a constant.

Unfortunately, the functional form of the Stokes wave as a function of position and pump power is not so easy to analyze. As yet we have found no simple, universal dependence of the power in the Stokes wave on the parameter \mathcal{P}_p^0 . A plot of the normalized power in the Stokes wave as a function of \mathcal{P}_p^0 and position in the medium is shown in Figure 2.9.

2.9 Conclusions

In this chapter the development of a new formalism has provided considerable insight into the process of SBS. Most of the insight is the result of considering the transverse effects that are often ignored during an analysis of the SBS process. Among other things, we have demonstrated that the process of SBS phase conjugation can be understood in the context of the coupled wave equations without recourse to statistical arguments such as have been relied upon in the past. Furthermore, we have shown that there is coupling between modes within the Stokes and the pump beams through the Brillouin interaction. We have also shown that this interaction leads to the shifting of the phase of the Stokes modes upon propagation through a region of high gain, a process we have termed phase pulling.

While the development of a new theoretical approach has given insight into the SBS process that was not available before, the complexity of the equations is still formidable enough that recourse to numerical solutions is necessary. The development of a three dimensional simulation of the SBS process using focused Gaussian beams has allowed us to investigate many aspects of the physical nature of stimulated Brillouin scattering. Some results of the modeling effort confirm previous analytical work while other results represent new understanding of the SBS process.

In particular the presence of phase shifts on the Stokes beam modes induced by the process of phase pulling has been demonstrated. Also, the simulations have demonstrated that the Brillouin gain parameter G does not increase linearly with increased pump power once SBS threshold is reached, and above threshold, the SBS process mathematically resembles a reverse saturable absorber for the pump wave at any point in the medium.

In the following chapters the results of simulations using the model described above will be compared to experimental data. The combination of data and modeling will prove to lend even further insight into the SBS process.

Chapter 3

Energy Distribution in the Interaction Region

In attempting to understand the process of optical phase conjugation by stimulated Brillouin scattering one may surmise that it is of paramount importance to know how the energy is distributed in the interaction region. Knowledge of the distribution of the energy within the interaction region can help us to understand how and why SBS sometimes fails to create the phase-conjugate of the incident wave. In the focused geometry, this knowledge can also be used to help understand the importance of such parameters as the length of the Brillouin medium relative to the Rayleigh range, as well as assist in understanding how very high intensities may exist in some Brillouin interactions without evidence of competing nonlinear processes.

As important as this knowledge is to understanding SBS and the associated phenomenon of phase conjugation, there has been surprisingly little published research on the subject of the distribution of the energy in the interaction region. In fact, we can find no published research that addresses the issue of the distribution of the energy during SBS in the focused geometry at all. One of the reasons for this lacuna in the literature is the difficulty in simultaneously addressing the issues of complex geometry, pump depletion and phase conjugation. Another reason may be that many researchers in the field believe that they already know qualitatively where the energy is during SBS with focused beams.

The complexity of the SBS process with focused beams has been addressed in Chapter 2, and we will use the model described there to investigate the distribution of the energy during SBS. However, it is useful to investigate briefly the latter reason noted for the lack of research on the subject. It is useful because there are good physical reasons why many researchers believe they understand the energy distribution in the interaction region to some extent, even without performing rigorous calculations or extensive experiments.

3.1 Intuition and experience

While there are a few published reports that indicate the importance of the regions far from the focus in the process of phase conjugation,⁹⁷⁻⁹⁹ a case can be made that when using focused beams, the entire process of SBS is confined to a region that extends approximately three Rayleigh ranges on either side of the focus. This restriction of the interaction region to approximately three confocal parameters is thought to be strictly true close to SBS threshold, but even above threshold one may think it to be an acceptable approximation. The restriction is based on a calculation of the on-axis Brillouin gain parameter for focused Gaussian beams.

For a Gaussian beam focused into a Brillouin medium of infinite extent the integral in equation (2.38) for the on-axis portion of the beam is (to within a constant)

$$\int_{-z}^z \frac{dz'}{1 + (z'/z_R)^2} = \frac{2}{z_R} \tan^{-1}(z/z_R), \quad (3.1)$$

where z_R is the Rayleigh range as usual. When all space is considered, the limits of integration are from $-\infty$ to ∞ and the value of the integral is simply π/z_R . When the limits of integration are only three Rayleigh ranges on each side of the focal point, the value of the integral is $(0.8)\pi/z_R$. Since fully 80% of the value of the undepleted gain occurs within three Rayleigh ranges of the focus, it is common to refer to the interaction region as being approximately six Rayleigh ranges (or three confocal parameters) in length. Therefore, as long as the focal point of the system is well within the Brillouin medium it is usually assumed that the "three confocal parameter approximation" is valid.

Although the analysis leading to the limitation of the interaction region is carried out in the undepleted pump approximation, the intensity of the pump beam is an order of magnitude less at the point three Rayleigh ranges from the focus than at the focus. So it is not unreasonable to assume that while the longitudinal intensity profile within three confocal parameters of the focus may be complicated during the SBS process, regions outside of a few confocal parameters play an insignificant role in the formation of the Stokes wave. An experimental study of the dependence of SBS threshold on cell length appears to confirm this conjecture,¹⁰⁰ and some researchers have even proposed that the interaction length of the SBS process is less

than one Rayleigh range when the pump power is close to SBS threshold, and approximately three Rayleigh ranges in length far above threshold.¹⁰¹

In the rest of this chapter we will investigate the distribution of the energy in the Brillouin medium both experimentally and theoretically. We will show that contrary to popular opinion, regions well outside of the focal region play a significant role in the formation of the Stokes wave, even when the intensity is several orders of magnitude below that at the focus.

3.2 Simulations of SBS using focused beams

In performing computer simulations of the SBS process using focused Gaussian beams there are three parameters that characterize the interaction region. The first is the Rayleigh range, the second is the length of the medium and the third is the position of the focal point inside the medium. Usually, the region more than a few Rayleigh ranges past the focus ($z \leq -3z_R$) is of little importance, as can be seen from an examination of Figure 2.3. Therefore generally one can characterize the Brillouin interaction region by the distance from the focus to the front of the medium ($0 \leq z \leq l/2$) and the Rayleigh range. The only other parameter necessary to completely characterize the Brillouin interaction is the incident power of the pump wave relative to SBS threshold.

We have performed numerous simulations of the process of SBS with focused beams using the model described in Chapter 2 and we find that, contrary to the argument presented in section 3.1, a significant portion of the SBS process is attributable to the region far away from the focus. Furthermore, in situations similar to those often encountered in the laboratory, almost all of the energy is extracted from the pump beam in regions where the pump intensity is more than 100 times lower than at the focus.

There are two geometries of interest in our research. The first geometry of interest is what we may call the *long* Brillouin medium, where the medium is several hundred Rayleigh ranges in length. The second geometry of interest, the *short* medium, is characterized by a Brillouin medium of a few tens of Rayleigh ranges in length.

Results of the simulation of SBS in a Brillouin medium that is considerably longer than the Rayleigh range is shown in Figure 3.1. In Figure 3.1 the normalized power in the Stokes wave is plotted as a function of distance in the medium for a

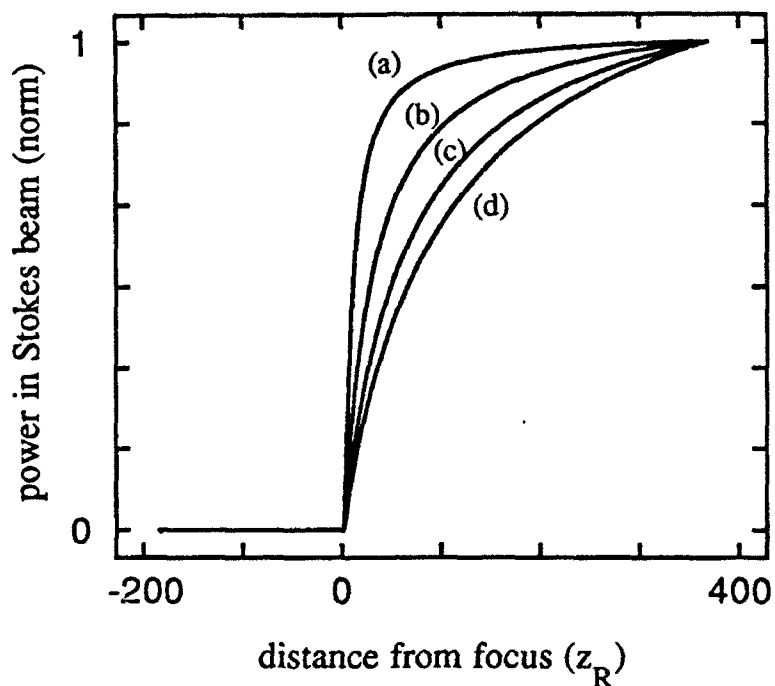


Figure 3.1. The power in the Stokes wave plotted as a function of position in the medium for four different pump powers: (a) SBS threshold, (b) five times above threshold, (c) ten times above threshold and (d) 15 times above threshold. The power in each case is normalized to the total Stokes power exiting the medium ($z=l/2$).

variety of incident pulse energies. Note from Figure 3.1 that at ten times SBS threshold, half of the power is transferred to the Stokes wave (and therefore is extracted from the pump wave) at points greater than 50 Rayleigh ranges from the focus. This means that at only ten times above threshold, half of the energy is extracted by SBS at positions where the undepleted pump intensities range from 2,500 to 160,000 times lower than the intensity at the focus.

From one perspective the extraction of the pump power at points far from the intensity maxima at the focus is surprising. However it is not so surprising when SBS is viewed as the amplification of noise. As can be seen from Figure 2.6, at all values of pump power almost all of the amplification of the Stokes wave occurs in the region near the focus. Once the process of SBS has started (i.e. threshold is reached), the

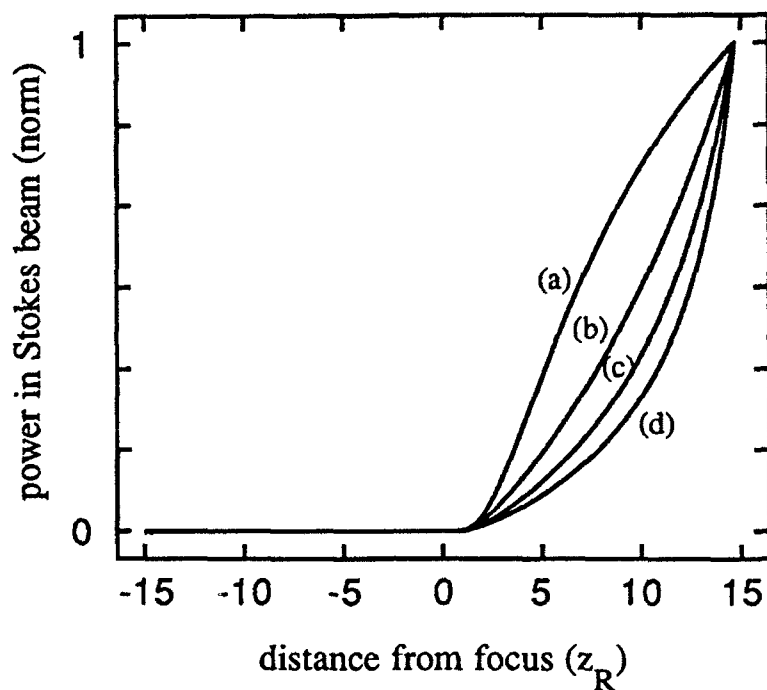


Figure 3.2. The normalized power in the Stokes wave plotted as a function of position for a short medium. The four different pump intensities are: (a) SBS threshold, (b) five times above threshold, (c) ten times above threshold and (d) 15 times above threshold. The power in each case is normalized to the total Stokes power exiting the medium ($z=l/2$).

remainder of the Brillouin medium for $z>0$ no longer sees the noise in the medium at a value of 10^{-12} the intensity of the pump beam. Instead the seed value is that of the noise already amplified by the focal region. Therefore, well above threshold, the SBS process in the region $z>0$ may be viewed as the amplification of the Stokes wave produced in the region $z\sim 0$.

While it is not uncommon to find a long Brillouin medium, it is much more usual in the laboratory to find a short Brillouin medium. In many laboratory situations the physical size of the beam used for SBS is quite small and therefore the Rayleigh range for most situations is such that the length of the Brillouin medium is on the order of tens of Rayleigh ranges instead of hundreds. Such is the case in our

laboratory, where the beam diameter from our laser at the e^{-2} intensity point is about 1.5 mm. This is a typical beam size for a commercially available solid-state laser.

When the length of the Brillouin medium is on the order of tens rather than hundreds of Rayleigh ranges, the length of the medium becomes a factor in the distribution of energy within the medium, even close to SBS threshold. Thus for a short medium the functional form of the energy in the Stokes beam can change from a concave slope, as shown in Figure 3.1, to a convex slope. This change in the nature of the curve is due to the fact that once the portion of the Brillouin medium in contact with the front of the cell has become important, there is no more medium in the positive z direction for the extraction process to move into. To maintain $G \sim 25-30$ it is then necessary for the pump to be depleted in a shorter space. The results of a simulation of this situation are presented in Figure 3.2.

As a general rule, the power distribution in a short medium begins to resemble the power distribution in a long medium for values of the incident pump below SBS threshold.

From Figures 3.1 and 3.2 we may also determine the functional form of the pump beam power within the medium. To within an additive constant, the functional form of the power in the pump beam as a function of position in the medium is the same as that for the Stokes beam, assuming that the transverse profile of the Stokes beam is the same as that of the pump beam.

Having determined the power distribution in the Brillouin interaction region, it is now important to look at the intensity distribution. This is important not only because SBS is an intensity dependent process, but because the issue of the effects of competing nonlinear processes must be addressed. Figure 3.3 is a plot of the on-axis intensity of the pump beam as a function of position through the medium for the same situation graphed in Figure 3.2. Note that the maximum intensity of the pump beam always occurs at the focus. Furthermore note that increasing the input intensity from threshold to 15 times above threshold only slightly increases intensity at the focus (the actual increase is $\sim 10\%$). So while the process of SBS keeps most of the power away from the focal region, the maximum intensity is still at $z=0$. Therefore the process of SBS does not create secondary intensity maxima away from the focus that may lead to poor phase conjugation (this will be discussed in the next chapter), while still shielding the focus from very high intensities that may lead to competing nonlinear effects such as self-focusing or breakdown of the material.

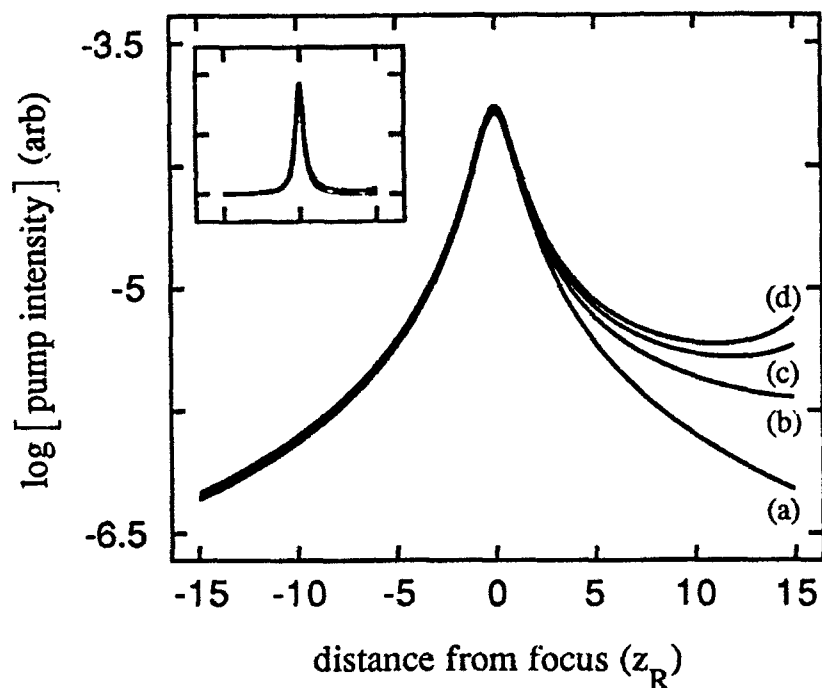


Figure 3.3. Intensity of a focused pump beam as a function of position in the Brillouin medium. The incident pump energies are: (a) threshold, (b) five times above threshold, (c) ten times above threshold and (d) 15 times above threshold. The inset is the same graph on a linear scale.

The screening of the focal region by the SBS process has been proposed in the past by some experimentalists. This seemed the only logical explanation for the high quality SBS phase conjugation that can be achieved with pump beams whose power is far in excess of the critical power for self focusing.^{12,16,24,25} Our modeling work has shown that this screening is predicted by theory and that the power distribution in the Brillouin medium is not confined to the focal region as is sometimes thought. We now turn to the experimental verification of our model to confirm the predictions presented in this section.

3.3 Experimental investigation of the energy distribution

The apparatus used to experimentally determine the distribution of the energy in the interaction region during stimulated Brillouin scattering is shown schematically

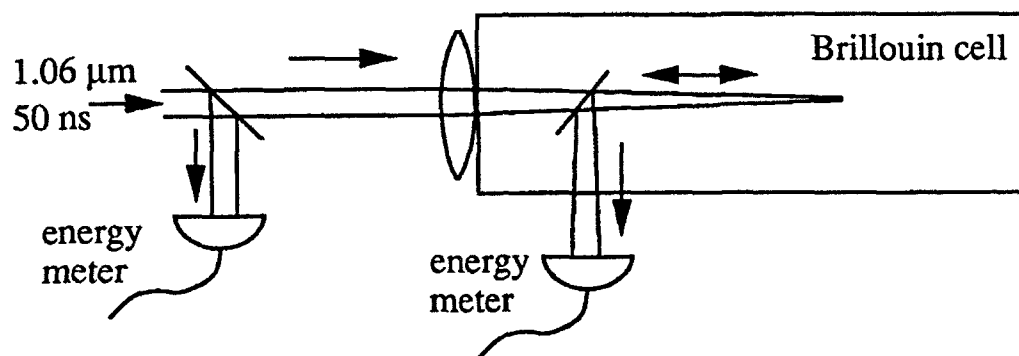


Figure 3.4. Experimental arrangement for determining the energy in the Brillouin interaction region for focused beams.

in Figure 3.4. Single 50 ns pulses from a single longitudinal, single transverse mode Nd:YAG laser were directed through a lens and into a rectangular glass cell. Inside the cell was a liquid Brillouin medium and a beam splitter that could traverse the length of the cell. The thickness of the beam splitter was $\sim 100 \mu\text{m}$ and the reflectivity was measured as ~ 0.005 , so that the presence of the beam splitter inside the medium did not significantly perturb the SBS process. Outside the cell an energy detector was mounted on an optical rail parallel to the cell and positioned such that any Stokes light reflected from the beam splitter within the cell was absorbed by the device.

Simultaneous measurements were made of the incident energy and the energy reflected from the beam splitter inside the medium. These measurements were taken with the beam splitter placed in several positions within the cell. Various incident energy levels and lens focal lengths were investigated as well as several different Brillouin media. Typical experimental results are shown in Figure 3.5, where in this case the Brillouin medium used was acetone. Also plotted in Figure 3.5 are the predictions of the model developed in section 2.3 of Chapter 2 for the physical geometry of the experiment. The model is completely specified by the experiment and there are no free parameters.

3.4 Conclusions

As is clearly demonstrated in Figure 3.5, for a focused pump geometry most of the energy of the pump wave is transferred to the Stokes wave significantly away

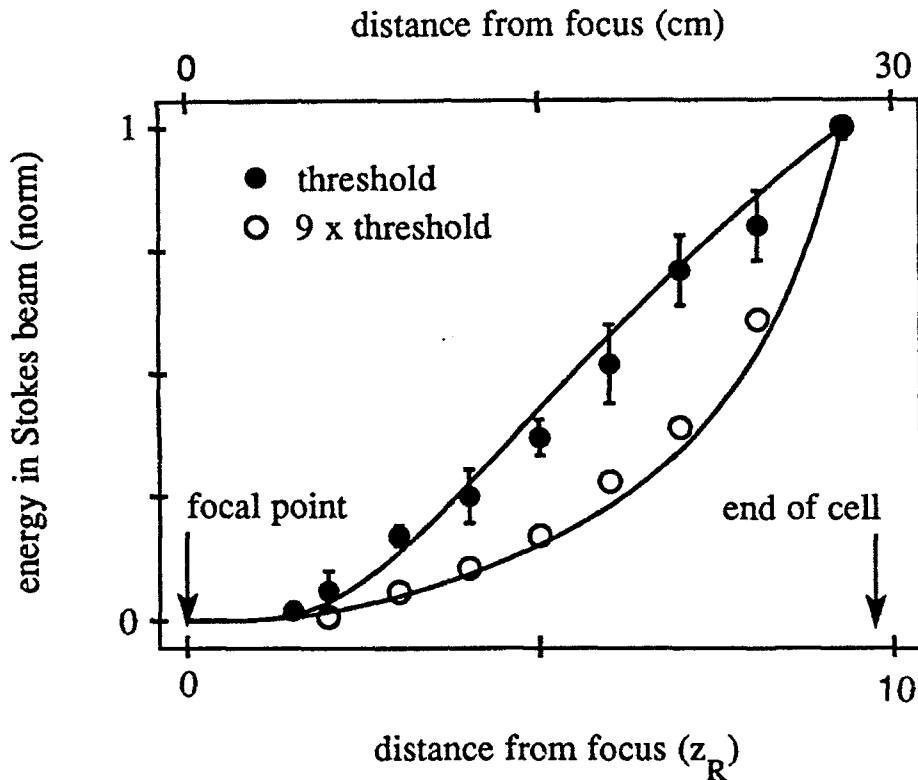


Figure 3.5. Dependence of the energy in the Stokes beam as a function of position in the medium. The data points are the result of experiment; the lines are from computer simulations. For the case of three times above threshold, the error bars are significantly smaller than the data points.

from the focal point of the lens, as is predicted by theory. From the results of experiments and simulations we conclude that it is not valid to use the criteria of three confocal parameters to estimate the SBS interaction region as is sometimes thought, even when the pump power is very close to SBS threshold. Additionally, we see that the characteristic length of the pump depletion region when using focused Gaussian beams is approximately equal to the focal length of the focusing lens; this will become important in the analysis presented in Chapter 5.

Finally, the excellent agreement between experiment and simulation validates the model for use in other predictions. The availability of a three dimensional model that can accurately predict the SBS interaction using focused beams has been very

useful in understanding the failure of SBS to produce a phase-conjugation wave under certain circumstances. This will be discussed in the next chapter.

Chapter 4

SBS Phase Conjugation of Beams with Smooth Aberrations

Up to this point we have only briefly discussed the phase-conjugating ability of stimulated Brillouin scattering. In Chapter 1 we investigated the ability of phase conjugation to correct for phase aberrations. In Chapter 2 we reviewed the theory that predicts enhanced gain during the SBS process for the wave whose amplitude is the complex conjugate of the incident beam. We also demonstrated in Figure 2.3 that when the pump wave is described by a lowest order Gaussian mode, most of the discrimination against nonconjugate waves in the Stokes beam occurs at or near the focal constriction. In this chapter we will discuss the ability (or inability) of SBS to produce a phase-conjugate wave when the incident beam is aberrated in a manner similar to that produced by solid-state laser amplifiers.

4.1 Smooth aberrations and phase conjugation

For the purpose of this work we will class aberrations as either *smooth* or *inhomogeneous*. The terms smooth and inhomogeneous refer to the phase of the slowly varying amplitude as measured from a plane wave. Often in the Russian literature the term "speckle inhomogeneous" is used to describe a beam with complex phase aberrations. This term actually refers to the intensity profile produced upon propagation of a beam with complex phase aberrations.

From the analysis of section 2.2 it is clear that at least within the undepleted pump approximation, the more aberrated the pump wave the more efficient the SBS process will be in creating a phase-conjugate wave. However, many of the potential applications of optical phase conjugation by SBS involve pump beams that are not aberrated in an inhomogeneous manner. Of particular interest here is the application of optical phase conjugation by stimulated Brillouin scattering to correct for aberrations induced by a typical solid-state laser amplifier.

As a wave propagates through a modern solid-state laser amplifier, the aberrations induced by the medium are almost always smooth in nature. Due to the very high quality of most optical amplifiers, almost all of the distortions can be traced to the thermal stresses induced by the optical pumping.^{82,83,90} It is these smooth aberrations that the solid-state laser community wishes to use optical phase conjugation to correct, using a multi-pass scheme similar to that shown in Figure 1.2.

To investigate stimulated Brillouin scattering using beams with smooth aberrations it is necessary to choose a representative aberration. Ideally one may wish to individually investigate each of the Seidel aberrations, however this is impractical. Therefore we will concentrate on the single smooth aberration of astigmatism.

Astigmatism is chosen as the representative smooth aberration for several reasons. Some of these reasons are: astigmatism is easy and inexpensive to create in the laboratory, it is easy to quantify practically and theoretically, and astigmatism is easily inserted into the simulation described in Chapter 2. Finally, astigmatism is the primary aberration found on the beams amplified by slab laser amplifiers. Since slab amplifiers are the design of choice by the laser community for the amplification of very high power pulses, there has been much anticipation within the community that optical phase conjugation will be able to correct for the distortion induced by these amplifiers. To date there have been several attempts to use optical phase conjugation in SBS in slab lasers, and several instances of failure.

For several years there has been interest in SBS phase conjugation of beams with smooth aberrations, and astigmatic beams in particular. The investigations reported in the literature are usually experimental and have produced a series of inconsistencies. Depending on the source, one may conclude from the literature that SBS cannot,^{37-39,85,88} might not,^{36,86} or can^{84,89-92} produce a high quality phase-conjugate beam from an astigmatic pump.

Assuming that even a few of the conflicting reports are accurate, there are clearly some conditions under which it is possible to produce a phase conjugate wave of an astigmatic beam via SBS. Just as clearly there are some conditions under which one cannot. Since there are so many reports of both good and bad SBS phase conjugation of astigmatic beams, one can assume that it is not some subtle difference in experimental technique that accounts for the varying results. Rather, it is more probable that the SBS phase conjugation of astigmatic beams is of good quality up to

a certain amount of astigmatism, and then the phase-conjugate ability of the PCM fails in a very specific manner.

Upon the study of the possible explanations for the disparity in the literature there are two areas that emerge as the probable culprits. The first is the manner in which an experimentalist quantifies astigmatism. The second is the manner in which the experimentalist measures the quality of the Stokes beam. These issues will be addressed in the following two sections.

4.2 Characterization of astigmatic beams

The first issue in the investigation of astigmatic beams is to unambiguously define and quantify the astigmatism present on a given beam. Since conventional aberration theory was developed in the context of incoherent imaging systems there is some ambiguity in the use of the term when applied to coherent, collimated Gaussian beams.

Consider the case of an astigmatic Gaussian laser beam incident upon a lens. The lens focuses the beam into a Brillouin cell for the purpose of creating a wave phase-conjugate to the incident wave. This is the most often used configuration for SBS and we shall call the lens/cell arrangement a phase-conjugate mirror. As a general rule, the beam that is incident upon the PCM is not an image in the usual sense and therefore the astigmatism present on the beam is difficult to define using the terms usually used. That is, there is no entrance pupil, reference sphere or field angle in the classical sense because usually the lens diameter is significantly larger than the beam diameter.

To alleviate the problem of the definition of astigmatism we consider a hypothetical "perfect" image with which to compare the actual wavefront. This perfect image is simply a plane wave of infinite extent. The problem of defining astigmatism is then a matter of simply defining the extent of the beam in the transverse dimension.

Since the amount of astigmatism depends quadratically on the distance from the beam axis, the determination of the extent of the beam in the transverse dimension is crucial. In keeping with the normal definition of Gaussian beams, we have chosen the beam diameter to be the full width at the e^{-2} intensity point. While this seems reasonable, it is by no means a universal convention. For example, had one used a commercially available fringe analysis program (as some experimentalists in the field

have) the aperture would not be defined in this manner unless special precautions were taken. Normally one would use a much larger aperture and therefore the value of astigmatism by our definition would be significantly less than that defined by a fringe analysis for the same wavefront. The inconsistency in the definition of the aperture is almost assuredly one of the elements contributing to the contradictory experimental results reported in the literature.

Having chosen a (somewhat arbitrary) definition for the amount of astigmatism on a given beam we must now briefly investigate the measurement of the astigmatism. One method of quantifying how much astigmatism is present on a beam is interferometrically; however there are several drawbacks to interferometry. It is easier and less expensive to infer the amount of astigmatism on a beam by measuring the separation of the foci after passing through a lens. In fact, for measurements of the SBS process, one can use the lens focusing the light into the SBS medium to induce the astigmatism and to infer the amount of astigmatism. Astigmatism is induced by tilting the lens in one dimension, and the amount of induced astigmatism is calculated from a measurement of the separation of the foci.

When using a tilted lens to induce the astigmatism one must take great care to minimize the introduction of other Seidel aberrations. Specifically, great care must be taken to ensure that the beam is centered on the lens so as to minimize the amount of coma induced. For all of the experiments presented here, close examination of the focal region ensured that the induced astigmatic aberration was far in excess of other types of aberrations.

The relationship between the amount of astigmatism on a beam and the separation between the foci may be derived from the standard equations of geometrical optics and is outlined in Appendix B. Using our conventions, the wavefront aberration is related to the separation between foci by

$$\Delta f = \frac{2\pi}{n} z_R W_\lambda, \quad (4.1)$$

where Δf is the distance between the foci, z_R is the Rayleigh range, n is the index of refraction of the medium, and the wavefront aberration W_λ is in wavelengths of the light (i.e. "waves of astigmatism").

For any definition of the beam diameter other than the e^{-2} intensity point, the equation for the wavefront aberration may be determined by the distance between foci from the equation

$$W_\lambda = \frac{nD^2\Delta f}{8f^2\lambda}, \quad (4.2)$$

where f is the focal length of the lens used to create the two foci and D is the beam diameter.

As noted above, there is little doubt that some of the confusion in the literature over the ability of SBS to produce a phase-conjugate beam from an astigmatic pump is due to the manner in which the researchers quantified the astigmatism on the pump beam. The quantity of astigmatism on an incident beam is reported in a variety of manners in the literature. Seldom is it possible to extract the actual amount of astigmatism in a manner useful in comparing two reports. Some of the methods various researches have used in reporting the astigmatism on a beam are: results from commercially available fringe analysis programs, reporting the placement and focal length of cylindrical lenses in the beam path, and the tilt (in degrees) of the lens used to induce the astigmatism. None of these are useful in a comparative sense if one does not know unambiguously the diameter of the incident beam.

Having settled on a method to produce and quantify the astigmatism of Gaussian beams, we now turn to methods to measure the quality of the beam produced by the phase-conjugate mirror. Besides the ambiguity in the amount of aberration present, it is the manner in which the beam quality of the Stokes beam is measured that probably accounts for much of the confusion in the literature.

4.3 Measuring the quality of phase-conjugate mirrors

It may seem obvious that prior to discussing the ability of a process to produce a high quality beam one should understand what criteria are going to be used in determining the beam quality. Unfortunately, like the quantification of the amount of astigmatism on the pump beam, the methods for determining the quality of the Stokes beam vary.

From a theoretical point of view the question of phase-conjugate beam quality is not too difficult. Since a theorist can define the pump beam unambiguously, any

number of criteria are suitable to determine the "phase-conjugate ability" of a given system. For example, in the context of the simulations presented in Chapter 2, we have chosen to define the beam quality of the Stokes beam by the amount of power in the mode conjugate to the pump mode, normalized to the total power in the Stokes beam. That is, if the Stokes wave contains no power in the mode conjugate to the pump beam it has a beam quality of zero and the phase conjugation is poor. If on the other hand the Stokes wave is made up entirely of the mode conjugate to the pump beam's mode, the beam quality is unity and the phase conjugation is good. Experimentalists have a more difficult problem in defining the phase-conjugating ability of a phase-conjugate mirror.

Depending upon the desired knowledge (and budget), experimentalists determine the quality of the Stokes wave in one of three ways: interferometry, analysis of the energy distribution in the near-field of the aberrant optic and analysis of the energy distribution in the far-field of the aberrant optic.

Interferometry and fringe analysis is often the best method for determining the beam quality of the Stokes beam. However, interferometry alone is not sufficient to characterize the phase-conjugate ability of a PCM, since the energy distribution of the Stokes wave is important as well as the phase. In solid-state laser applications, it can be argued that in some cases the Stokes intensity distribution is more important than the phase.

Of particular importance to our research is the energy distribution of the Stokes wave. It has been shown that even when SBS fails to produce a high quality Stokes wave, the phase of the Stokes beam is conjugate to the pump to better than $\lambda/4$.³⁹

Since the intensity distribution of the Stokes beam in the near-field of the phase-conjugate mirror is of most importance in our research, we have primarily relied on the qualitative measure of comparing the intensity profiles of Stokes beams with astigmatism present on the pump to those produced without the aberration.

To investigate the quality of phase conjugation of astigmatic beams by SBS we used the apparatus shown in Figure 4.1. A near diffraction limited beam from a Nd:YAG laser was focused through a lens into a cell filled with a Brillouin-active medium. The Stokes light was imaged through a beamsplitter onto a CCD array attached to a computer with frame-grabbing software. The image plane was approximately five centimeters in front of the focusing lens. The focusing lens was

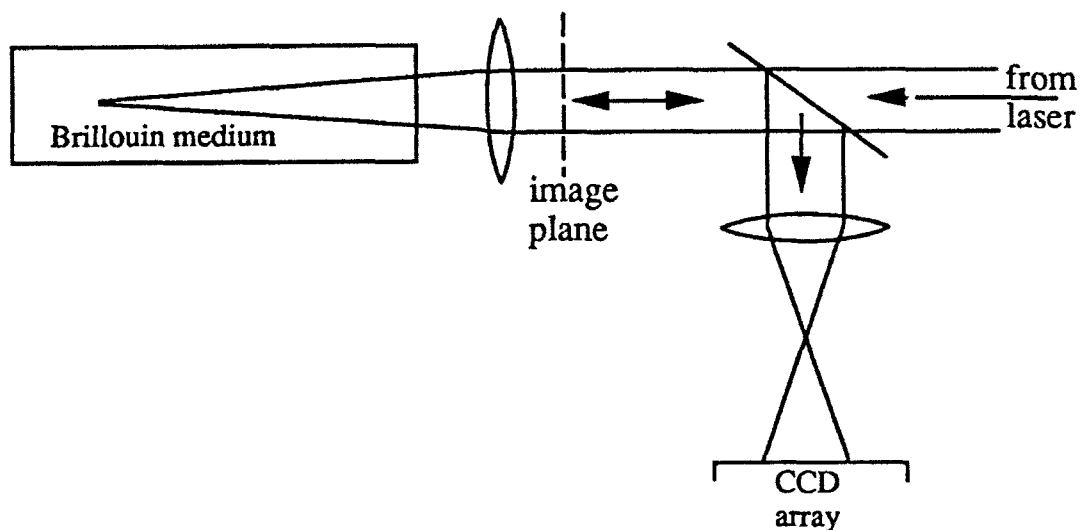


Figure 4.1. Experimental arrangement for investigating the near-field beam quality of an SBS Stokes beam.

mounted on a rotation stage so that astigmatism could be introduced onto the beam after the image plane, but before the SBS cell, when desired. Comparison of near-field beam profiles of the Stokes beam with and without astigmatism present on the incident beam were used to qualitatively investigate the accuracy of the phase conjugation.

As a quantitative measurement we have used the energy distribution of the Stokes wave in the far-field of the aberrant optic using the apparatus shown in Figure 4.2. The Stokes beam was sampled by the beamsplitter, as in the near-field measurements, but was then focused through a pinhole whose diameter was close to the diffraction limit of the incident laser beam. The ratio of the energy in the entire Stokes beam to that transmitted through the pinhole was then used as a measure of the quality of the Stokes beam.

While the use of the apparatus described above to measure the far-field beam quality is useful, it is often not the best way to describe the ability of a process to produce a phase-conjugate wave. To illustrate this point consider a hypothetical phase-conjugate mirror that produces a counter-propagating Hermite-Gaussian (0,1) mode for an input (0,0) mode pump beam. Since the Hermite-Gaussian functions are orthogonal, we may say that the quality of this phase-conjugate mirror is zero. That

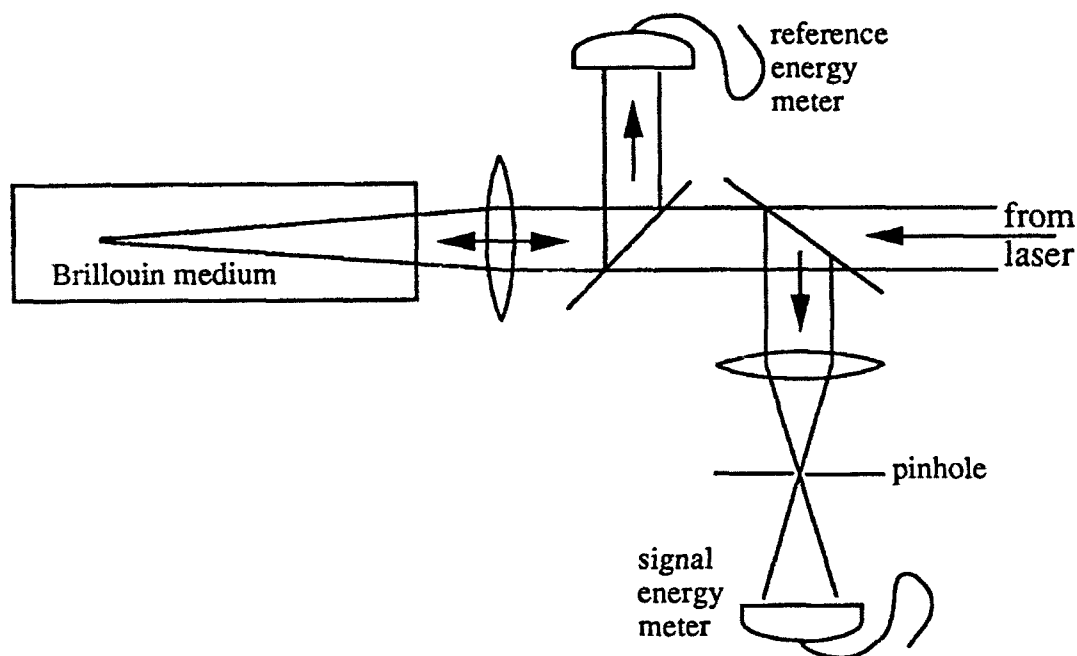


Figure 4.0. Apparatus for phase-conjugate beam quality measurement in the far-field of the aberrant optic.

is, it produces none of the mode that is phase-conjugate to the incident beam. Unfortunately a simple calculation will show that about 67% of this nonconjugate mode will be transmitted through a diffraction limited pinhole. In the parlance of the field, the reflected beam would be measured at ~ 1.5 "times diffraction limited". Any measurement less than about 2.5 times the diffraction limit is considered to be very good. As this example illustrates, it is probable that the variety of methods used to determine the beam quality of the Stokes beam is the second reason for the disparity of results reported in the literature.

Having investigated two of the most probable reasons for the conflicting reports in the literature, we will now turn to the report of our original work investigating the SBS phase conjugation of astigmatic beams. We have used the two methods of near and far-field energy measurements to determine the beam quality of the Stokes wave.

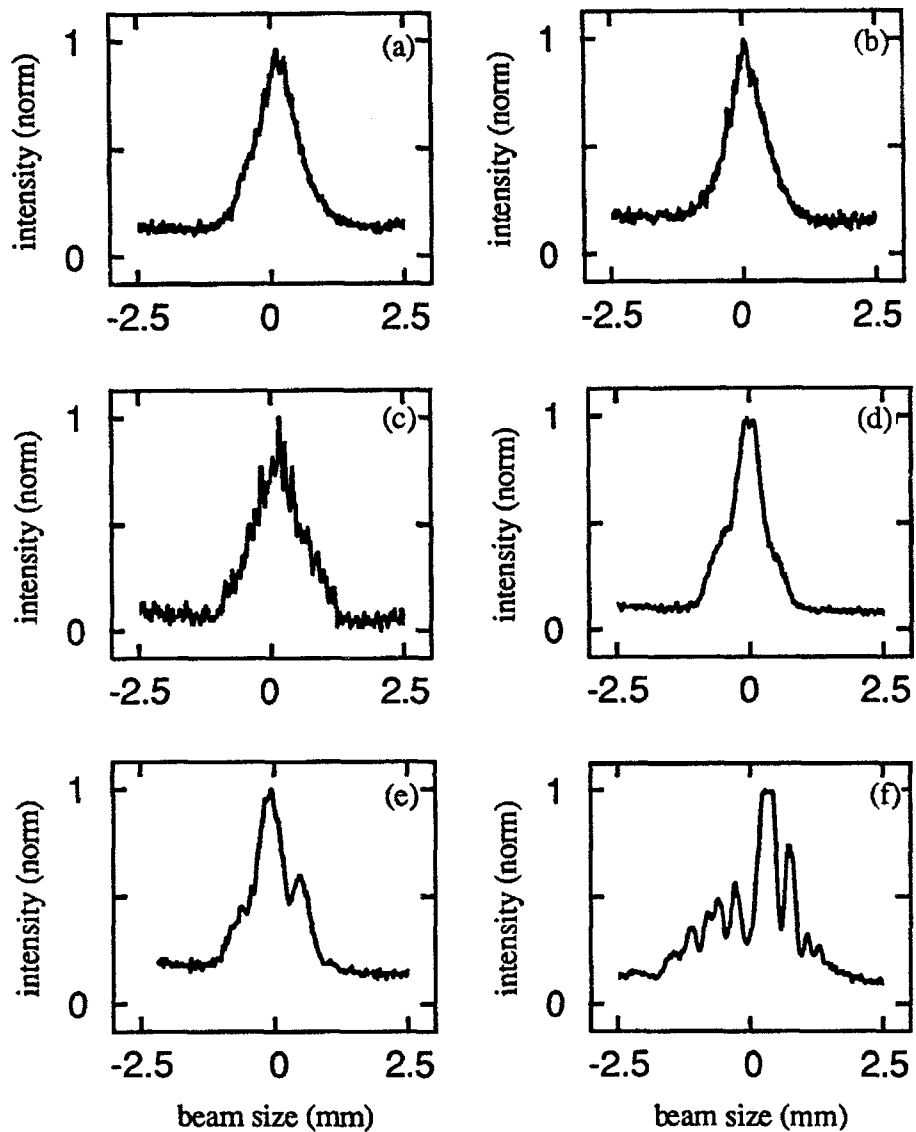


Figure 4.3. Intensity profiles of: (a) the pump beam, (b) the Stokes beam with no astigmatism on the pump, and (c)-(f) the Stokes beam with astigmatism present on the pump beam. Figures (c) through (f) show the effect on the Stokes beam of an increase in the pump power from near SBS threshold in (c) to approximately 10 times SBS threshold (f). SBS threshold is defined as the input pump power necessary to create a Stokes wave containing one tenth the power in the pump; the Stokes wave in (c) contained 0.05 of the pump power.

4.4 Experimental investigation of SBS with astigmatic beams

The apparatus shown in Figure 4.1 was used to study the intensity profile of the Stokes beam in the near-field of the aberrant optic. Figure 4.3 (a) shows the intensity profile of the pump beam at the image plane shown in Figure 4.1. Figure 4.3 (b) shows a typical profile of the Stokes beam from the SBS interaction when the pump is focused by the lens into the Brillouin medium with no astigmatism. Fitting each of these two beams to a Gaussian form using nonlinear least-squares fitting shows that each of the beams has a Gaussian shape with spot size given by $0.75 \pm .05$ mm, indicating virtually perfect phase conjugation of the pump beam.



Figure 4.4. Photograph of Stokes beam when the pump beam is astigmatic and high above threshold.

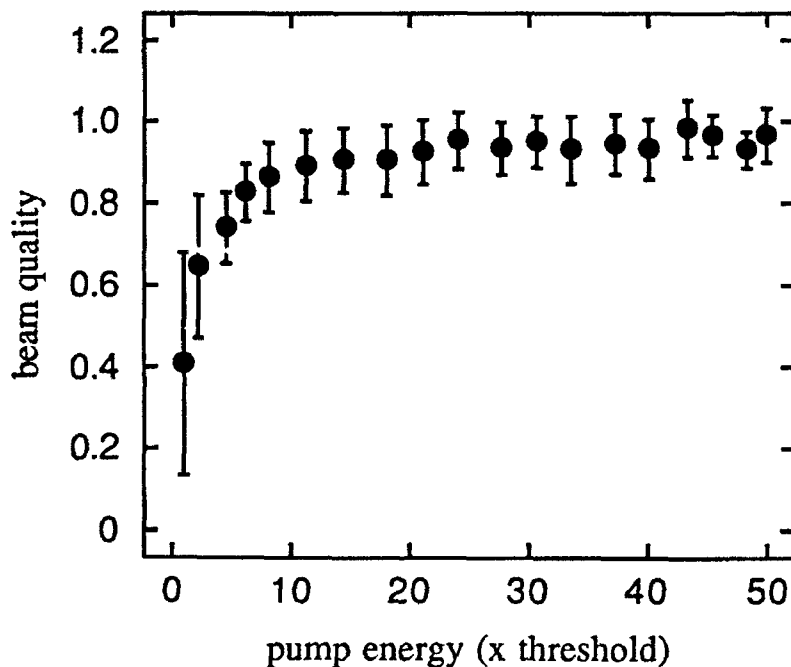


Figure 4.5. Stokes beam quality as a function of pump energy for the case of pump beam with no astigmatism. The measurements were taken with the apparatus shown in Figure 4.2.

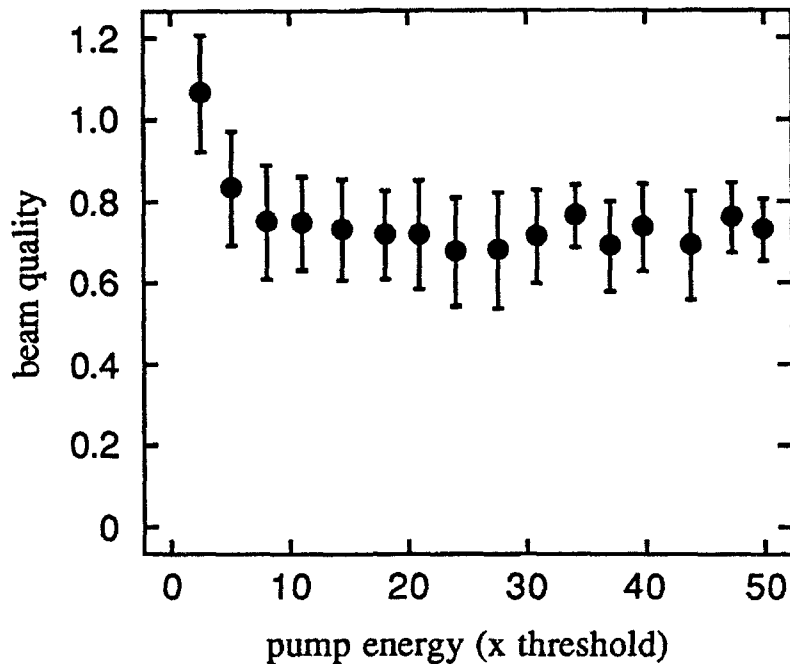


Figure 4.6. Stokes beam quality as a function of pump energy for an astigmatic pump beam. SBS threshold is defined in terms of the unaberrated beam.

Figures 4.3(c) through 4.3(f) each show a typical intensity profile of the Stokes beam under the same conditions as in Figure 4.3(b), but with the focusing lens tilted so that the beam entering the Brillouin cell was astigmatic. The incident beam intensity was different in each of the four cases shown for the astigmatic pump, ranging from below SBS threshold in Figure 4.3(c) (reflectivity ~ 0.05) to approximately 10 times SBS threshold in Figure 4.3(f). The intensity modulation evident from the profile in Figures 4.3(e) and (f) is only in one dimension. The orthogonal dimension shows no distortion when compared to the pump profile; this can be seen from the photograph in Figure 4.4.

Representative far-field measurements of the beam quality using the apparatus shown in Figure 4.2 are shown in Figures 4.5 and 4.6. The Brillouin medium in this case was SnCl_4 . Figure 4.5 contains the data derived from far-field measurements

when the pump beam is not astigmatic. As expected, the beam quality increases with increasing pump energy until almost perfect beam quality is achieved.

Figure 4.6 contains the data derived from far-field measurements when the pump beam is astigmatic. In this case threshold is defined by the unaberrated beam's threshold, which is approximately three times lower than the SBS threshold for the astigmatic beam. There are two important things to note about the data in Figure 4.6. The first is that the beam quality decreases with increasing pump energy. The second important feature of Figure 4.6 is that the beam quality can be well above unity.

The ability to measure beam quality greater than unity again demonstrates the difficulties in attempting to quantitatively measure the beam quality using this method. If the Stokes beam has a larger diameter (in one or both dimensions) than the pump beam, as is often the case when the pump beam is astigmatic, the Stokes beam will focus to a smaller spot size than the pump beam. This situation leads to proportionally more energy being transmitted through the pinhole for the case of an aberrated pump beam than for one with no aberration, even though the beam quality may actually be lower in the former case. Given this situation, the data derived from the far-field measurements are at best qualitative in nature.

The point at which the intensity profile of the Stokes beam breaks up into discrete intensity maxima as seen in Figure 4.3 (e) and (f) varies depending upon the Brillouin medium, the intensity of the pump and the amount of astigmatism. However, the first sign of distortion of the Stokes beam is usually an elongating of one dimension similar to that noted in reference [38]. Increased pump intensity and/or increased astigmatism then causes the Stokes beam to have the characteristic multiple intensity maxima as seen in Figure 4.3(e) and (f). At very high pump intensities or with large amounts of aberration, the number of intensity maxima increases substantially, and becomes similar to the Stokes beam profile seen when only a cylindrical lens is used to focus the pump beam into the Brillouin medium.¹⁰²

Upon attempting to quantify the effect of an astigmatic pump beam on the resulting Stokes beam, it becomes obvious that there is an additional reason for the conflicting reports in the literature. It appears from our research that the amount of astigmatism that can be corrected by the SBS process without introducing intensity maxima of the type displayed in Figure 4.3 (e) and (f) depends upon the specifics of the focusing geometry and the choice of the Brillouin medium. That is we can find

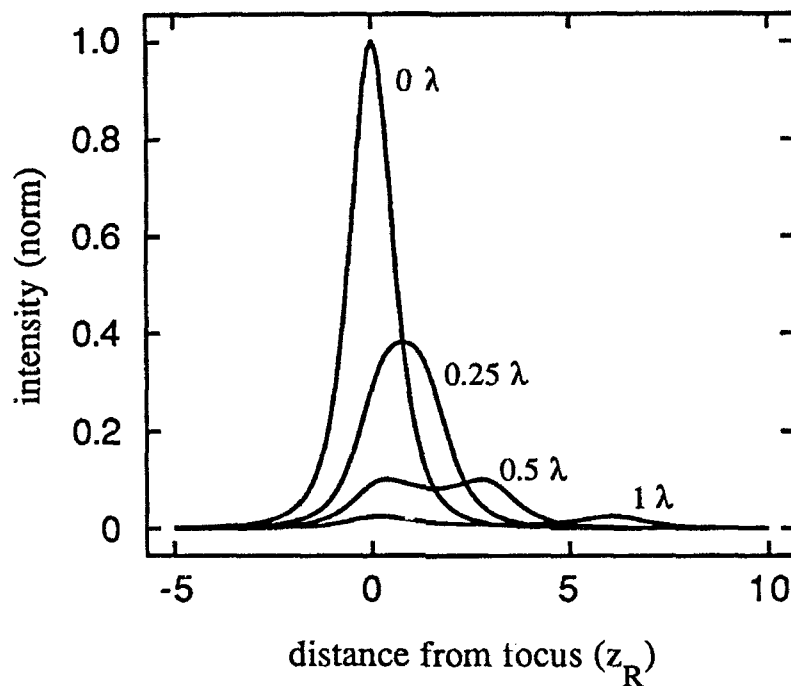


Figure 4.7. Normalized on-axis intensity for focused beams with different amounts of astigmatism. High quality SBS phase conjugation is not seen for beams with astigmatism $\geq 0.5\lambda$. Pump beams with only one intensity maximum along the direction of propagation ($\leq 0.25\lambda$ astigmatism) produce a Stokes beam with an intensity profile that is a very good approximation to the pump beam.

no parameter that will unambiguously determine when the process of optical phase conjugation by SBS will fail to produce a Gaussian Stokes beam.

It is not even accurate to say that the Stokes beam generated by different focusing geometries and media follow the same transition to poor phase conjugation. In most instances as the input energy is increased, the intensity of the Stokes beam will progress from Gaussian, to elongated in one dimension, and finally to rippled. In some instances however, the Stokes intensity makes an immediate transition from Gaussian to that of Figure 4.3 (e). The best one can say about the SBS phase conjugation of astigmatic beams is that the more astigmatism present on the incident beam, the more transverse intensity modulation present on the Stokes beam.

Likewise, the higher the input intensity above threshold, the more intensity ripples present on the Stokes beam.

The one constant appears to be that when there are not two discernible intensity maxima along the axis of propagation, the quality of the phase conjugation is very high. That is, the focusing of a Gaussian beam that has no phase distortion is very well conjugated by SBS. One may of course consider the act of focusing a beam a phase distortion; however this type of distortion results in only a single intensity maximum along the path of the beam's propagation. Thus it is accurate to say that the presence of spherical aberration and defocus do not adversely effect the phase-conjugating ability of the SBS process.

It has been proposed in the past that up to approximately one wave of astigmatism can be well conjugated;^{39,88} however we have found that even very small amounts of astigmatism ($\sim \lambda/2$) cannot be well conjugated in some instances. For example, the Stokes beam profiles shown in Figure 4.3(e) and (f) were produced by SBS with a pump wave with on the order of one half wave of astigmatism in SnCl_4 .

To estimate the maximum astigmatism that can be corrected we may determine the point at which two intensity maxima exist along the path of the focused beam. The intensity profiles of three focused astigmatic beams are shown in Figure 4.7 along with the plot of the intensity of a beam without astigmatism. From Figure 4.7 we may conclude that $\lambda/4$ waves of astigmatism can be well conjugated by the SBS process, but $\lambda/2$ cannot be well conjugated under some circumstances. This prediction agrees well with our laboratory experience; under no circumstances have we seen any degradation of the Stokes wave for 0.25λ or less of astigmatism on the pump beam.

The sensitivity of the quality of the Stokes wave to the focusing geometry and choice of Brillouin medium makes it difficult to experimentally determine the etiology of poor phase conjugation of astigmatic beams by SBS. The lack of a universal dependence on such parameters as the level of distortion or input intensity above threshold leaves no recourse except to numerical analysis.

4.5 Modeling of SBS with astigmatic pump beams

It has been proposed in the past that the failure of SBS to produce the accurate phase-conjugate wave of an astigmatic pump beam is due to separate intensity

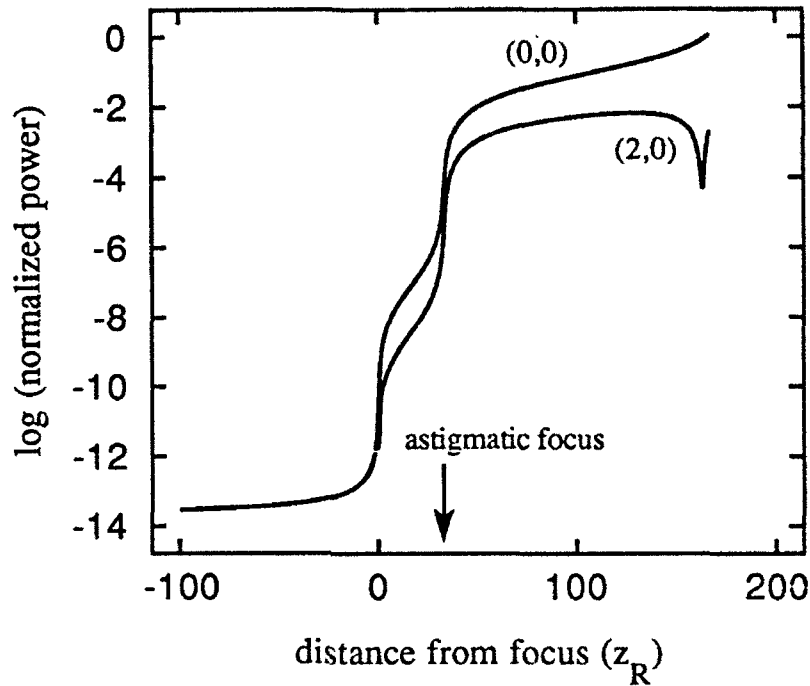


Figure 4.8. Evolution of the first two Hermite-Gaussian modes of the Stokes wave for the case of an astigmatic pump 55 times the SBS threshold. The importance of both focal regions is clearly evident.

maxima along the pump beam path. The speculation has been that as the focus farthest from the entrance to the medium becomes unimportant in the SBS process, nonconjugate modes in one dimension are not discriminated against in the region of very high gain at the location of the other focus.^{39,91,92} While it is common to refer to the focal region as a region in which nonconjugate modes are discriminated against, there is no basis for this statement in the usual understanding of SBS (i.e. the approximation of an undepleted, infinite plane-wave pump). If one ignores the non-phase matched terms in the SBS equations the overlap integrals determine the gain of each mode and nothing else. In this case, since the overlap integrals are not a function z , a focal constriction is of no value in the discrimination against nonconjugate modes.

To investigate the role that the two foci play in the formation of the Stokes beam, the simulation introduced in Chapter 2 was used to model SBS with an

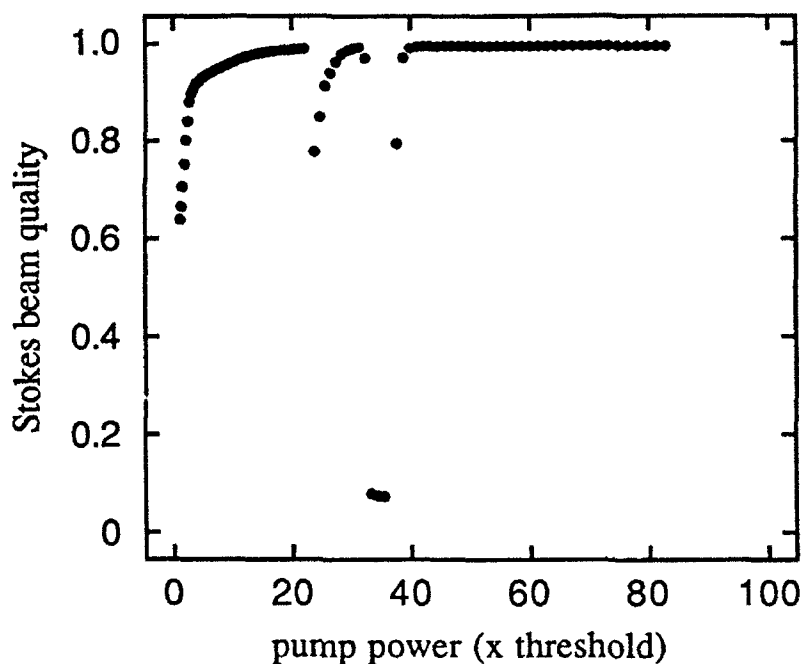


Figure 4.9. Stokes beam quality as a function of pump power for a pump beam containing 3λ astigmatism. The beam quality is defined as the power in the mode conjugate to the pump mode, normalized by the entire Stokes power. These results are derived from the simulation described in Chapter 2.

astigmatic pump beam. The model described in Chapter 2 is especially suited for modeling the SBS process with focused, astigmatic pump beams since the possibility that the pump beam was astigmatic was specifically left open in the derivation of equations (2.33).

Figure 4.8 is a plot of the normalized power in the mode conjugate to the pump and the second most energetic mode for the case of 55 times SBS threshold. Obviously the back focus plays a major role in the SBS process even very far above threshold, contrary to previous speculation. Of course, from the discussion of the Brillouin gain parameter in Chapter 2 one may have suspected that the entire beam path is always important in the formation of the phase-conjugate wave.

It is also interesting to note in Figure 4.8 that the majority of the discrimination against the b_2 coefficient occurs at the focus in the dimension of interest (i.e. the back focus). The front-most focus provides almost the same amplification for both modes.

The issue of Stokes beam quality in the simulation is addressed in Figure 4.9. Figure 4.9 is a plot of the Stokes beam quality, as defined by the normalized power in the mode conjugate to the pump beam, for the case of a pump beam with five waves of astigmatism. Note that at approximately 20 times the SBS threshold the phase-conjugate beam quality begins to experience some reduction at certain intensities of the pump. However, the fundamental mode eventually dominates.

The results presented in Figures 4.8 and 4.9 show that at some pump energies the beam quality of the Stokes beam generated by an astigmatic pump beam can be degraded. Also the simulations show that at all times both foci contribute to the formation of the Stokes beam. Why the Stokes beam degrades at only some energies, even when both foci clearly participate in the formation of the Stokes beam, is not immediately obvious and can only be seen by carefully examining the SBS equations derived in Chapter 2.

4.6 The etiology of poor phase conjugation with astigmatic pump beams

The experimental evidence as well as the results of simulations show that when multiple intensity maxima are present along the path of the pump beam poor phase conjugation can result in some instances. As demonstrated in Figure 4.8 however, this poor phase conjugation is not due to a lack of importance of one of the foci. On the contrary, even very far above SBS threshold both foci participate in the formation of the Stokes wave.

Since it is the presence of a second region of high intensity that causes amplification of noise modes, it is useful to study the difference between the two points of high Brillouin gain: one at the focus in the dimension of interest and one in the orthogonal dimension. For purposes of clarity in the following discussion, we will assume that an astigmatic beam is focused into a Brillouin medium and that the focal point closest to the lens (the sagittal focus) is not in the dimension of interest. That is, the Guoy phase shift does not occur at the sagittal focus in the dimension that we are studying. The tangential focus (the farthest from the lens) does contain the Guoy phase term in the dimension of interest.

As derived in Chapter 2, the equations describing the evolution of the coefficients for the Stokes beam are given by

$$\frac{\partial b_n}{\partial z} = K \left(\frac{1}{w_x(z)} \right) \left(\frac{1}{w_y(z)} \right) \chi_{SBS}^{(3)} \sum_{jkl} b_j a_k^* a_l \xi_{jkl n} e^{-i(j+k-l-n)\psi(z)}, \quad (4.3)$$

with a similar equation for the coefficients of the pump wave. The two important points to note here are that every mode in the Stokes wave is coupled to every other mode in the Stokes wave, as well as to every mode in the pump beam, and that there are explicit phase terms in the equation.

Examination of equations (4.3) reveals that there is only one difference between the equations for the coefficients of the Stokes modes at the sagittal and tangential foci. At the sagittal focus the phase angle is almost a constant, $\psi(z) \sim \pi/2$. At the tangential focus, the phase angle is rapidly changing. Beyond this difference, equations (4.3) are identical in the region of the two foci, provided that they are separated sufficiently to introduce two discrete intensity maxima.

To investigate the evolution of the Stokes beam in the region of the sagittal focus let us examine the set of coupled equations describing the coefficients of the Stokes modes in the region of the Sagittal focus. To minimize the complexity we will examine only the first three Hermite-Gaussian modes, and initially we will consider only the case of the undepleted pump. From the discussion in Chapter 2 we know that a system described by a single pump mode and a Stokes wave containing only the first three modes can be described by the equations:

$$\frac{\partial b_0}{\partial z} = K \left(\frac{1}{w_x(z)} \right) \left(\frac{1}{w_y(z)} \right) \chi_{SBS}^{(3)} |a_0|^2 \{ (.56)b_0 - (.20)b_2 e^{-2i\psi(z)} \}, \quad (4.4.a)$$

$$\frac{\partial b_1}{\partial z} = K \left(\frac{1}{w_x(z)} \right) \left(\frac{1}{w_y(z)} \right) \chi_{SBS}^{(3)} |a_0|^2 \{ (.28)b_1 \}, \quad (4.4.b)$$

$$\frac{\partial b_2}{\partial z} = K \left(\frac{1}{w_x(z)} \right) \left(\frac{1}{w_y(z)} \right) \chi_{SBS}^{(3)} |a_0|^2 \{ (-.20)b_0 e^{2i\psi(z)} + (.21)b_2 \}. \quad (4.4.c)$$

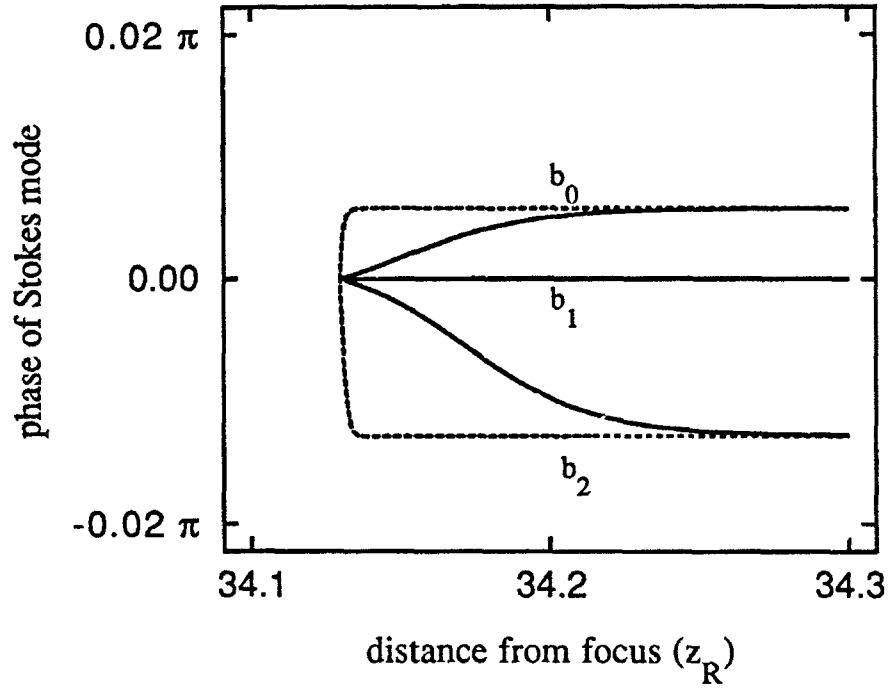


Figure 4.10. The phase evolution of the Stokes modes at the sagittal focus under the undepleted pump approximation. The solid lines are calculated at SBS threshold, the dashed lines are calculated at 10 times above threshold.

Since $\psi(z) \sim \pi/2$, these equations may be approximated by:

$$\frac{\partial b_0}{\partial z} = K \left(\frac{1}{w_x(z)} \right) \left(\frac{1}{w_y(z)} \right) \chi_{SBS}^{(3)} |a_0|^2 \{ (.56)b_0 + (.20)b_2 \}, \quad (4.5.a)$$

$$\frac{\partial b_1}{\partial z} = K \left(\frac{1}{w_x(z)} \right) \left(\frac{1}{w_y(z)} \right) \chi_{SBS}^{(3)} |a_0|^2 \{ (.28)b_1 \}, \quad (4.5.b)$$

$$\frac{\partial b_2}{\partial z} = K \left(\frac{1}{w_x(z)} \right) \left(\frac{1}{w_y(z)} \right) \chi_{SBS}^{(3)} |a_0|^2 \{ (.20)b_0 + (.21)b_2 \}. \quad (4.5.c)$$

It is a trivial matter to solve these equations numerically. As one may expect, given some initial phase the coefficients b_0 and b_2 change phase upon propagation until both have the same phase (phase pulling). The coefficient b_1 does not change phase and grows more slowly than the other two modes.

In the case of a real astigmatic beam, the phase angle at the sagittal focus is not identically zero. In the case of the simulation the results of which were presented in Figures 4.9 and 4.8 (i.e. 3λ of astigmatism), the sagittal focus was modeled approximately 34 Rayleigh ranges in front of the tangential focus. The phases of the three modes determined by solving equations (4.5) under these conditions are shown in Figure 4.10. For the purpose of this simulation, the phases of all three Stokes modes were chosen initially to be zero. As seen in Figure 4.10, the phases adjust themselves for maximum gain and then stay constant upon propagation. Due to the enhanced gain for the Stokes mode conjugate to the pump, the phase-conjugating ability of this system is quite high ($\sim .85$) at all levels of the pump intensity.

Without a change in the pump wave, there can be no instability in the Stokes wave. That is, in the undepleted pump approximation there is no process that can change the structure of the Stokes wave. A small perturbation of one mode will be accompanied by the adjustment in the phase of the other modes; the situation is quite stable. Thus phase pulling and the large value of the overlap integral for the b_0 mode ensure discrimination against nonconjugate modes even when the region of high gain is well away from the focal constriction.

Equations (4.5) clearly show that the poor phase conjugation that results from a second region of high intensity where $\psi(z) \sim \pi/2$ is only possible in the context of the depleted pump. Increasing the pump power in the context of the undepleted pump only decreases the length necessary to reach equilibrium value of the phases of the coefficients, but the ratios of the amplitudes of the coefficients stay constant.

The full undepleted pump equations for SBS with the Hermite-Gaussian modes are a series of six coupled nonlinear differential equations with eight complex terms each. What is surprising is not that there are regions where the solution is unstable, but rather that there are regions where the solution is stable. With increasing pump power the coupling between the odd and even modes through the pump modes becomes important, as well as the enhancement between modes of like parity. At some point it is inevitable that the gain for a nonconjugate mode will

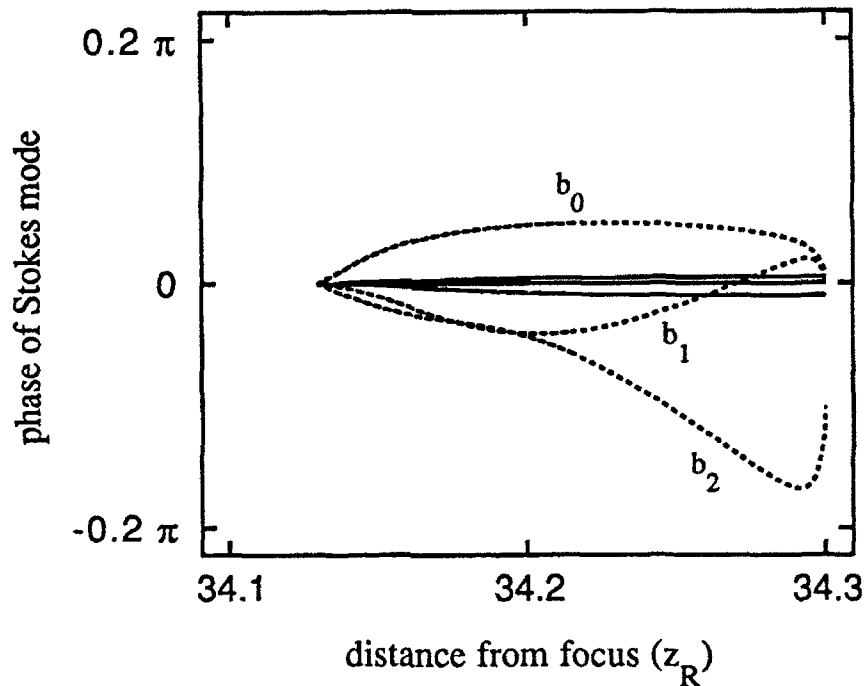


Figure 4.11. The phase evolution of the Stokes modes at the sagittal focus with pump depletion. The solid lines are calculated at SBS threshold, the dashed lines are calculated at ten times above threshold. At ten times above threshold, the system is close to an unstable region, where the phase-conjugate quality quickly degrades.

exceed the gain for the conjugate mode. One may think of the process as a transition into regions of spatial instability.

Figure 4.11 shows the phases of the three Stokes modes for the same case as shown in Figure 4.10, but with the full effects of pump depletion included. The quality of phase conjugation in the case presented in Figure 4.11 is still quite high (~ 78), however this is a value for the pump power that is almost unstable. Slightly more pump power and the numerical simulation does not converge with this limited number of modes.

From the results just presented we may surmise that the poor phase conjugation of astigmatic beams by SBS is a direct result of the effects of pump depletion. Pump depletion causes the system to evolve from one that can be

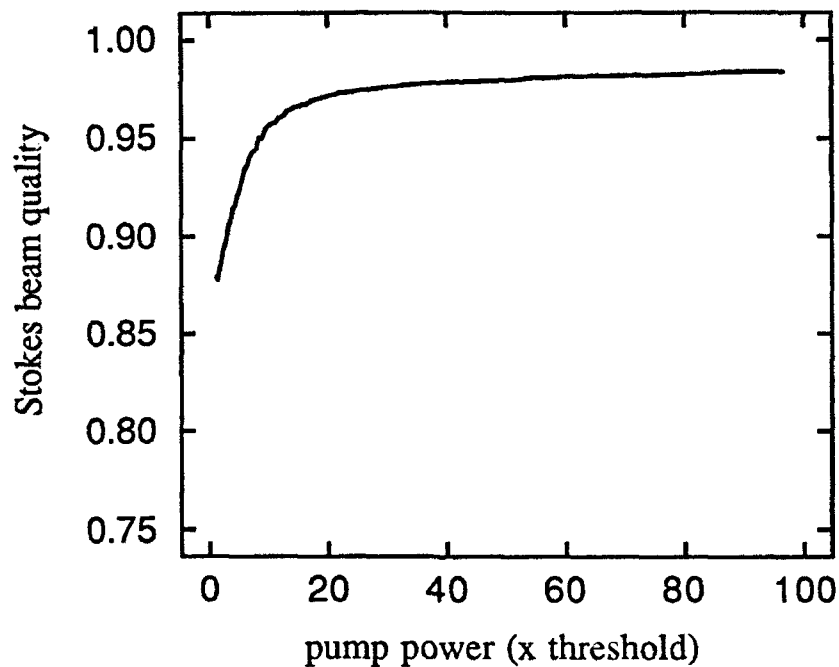


Figure 4.12. Theoretical beam quality of the Stokes beam as a function of pump power.

described by N differential equations, $N/2$ of which are coupled in a simple manner, to a system described by $2N$ differential equations, all of which are coupled in a very complicated manner. Additionally, the overlap integral ensures that in the case of a single mode pump wave, only a few of the terms are important in the undepleted pump approximation. This is not the case in the depleted pump regime, where the growth of Stokes modes impresses a new modal structure on the pump. An alternative way of viewing the importance of pump depletion is to say that the presence of pump depletion transforms the equation for the amplitude of the Stokes wave from being linear in the field amplitude to nonlinear in the field amplitude.

Pump depletion also plays a significant role in the instance of a beam without aberration. It is universally true that for an unaberrated Gaussian beam, the phase-conjugate quality of the Stokes beam, as measured in the far-field, is increased as the pump power is increased. The beam quality saturates at some high value when the

pump power is well into the pump depletion regime. This can be seen experimentally in Figure 4.5. Figure 4.12 demonstrates that this behavior is expected theoretically.

There are two remaining questions to be addressed: 1) Why does this instability occur only when the phase angle $\psi(z) \sim \pi/2$ and 2) why do the experimental results not show an aperiodic evolution from good to poor phase-conjugation of the pump beam as predicted by the simulations?

4.7 The effects of the Guoy phase shift and n_2

First we will address the issue of why poor phase conjugation occurs only at a point where the pump beam is not undergoing a rapid shift in the phase angle. In the case of a focused beam (without astigmatism) the phase angle $\psi(z)$ is rapidly changing at the point of highest gain (i.e. the focal point). Even the sign of $\psi(z)$ changes as the beam propagates through the focal point. Due to this rapid change in the phase angle, the process of phase pulling discussed in Chapter 2 will require a rapid constant change in all of the phases of the Stokes modes; the only combination of modes that is phase matched for all z are those for which $j=k=l=n$. Thus we have the discrimination against nonconjugate modes due to the presence of the overlap integral, as well the rapidly changing phase in z that keeps other modes from being efficiently phase matched along the entire region of high gain.

The scenario of an astigmatic beam is entirely different. When there is sufficient astigmatism on the beam to produce two separate regions of high intensity, the phase angle in one dimension is approximately constant for the entire region of high gain where one of the foci is located. Thus the phase of noise modes do not have to change rapidly as they propagate through the focus for them to have a stable relationship to the pump beam and other Stokes modes. Since the value of $\psi(z)$ is approximately constant, non-phase matched terms have a much better chance of being nearly phase matched as the Stokes wave propagates. The coupling between all of the modes will eventually lead to a spatially unstable solution if the coupling constant is large enough (i.e. if the pump intensity is high enough). It is inevitable that at some pump intensity, the nonconjugate Stokes modes will dominate the Stokes wave at the point at which it exits the medium.

It is important to remember that the excess growth of the noise modes will occur only in the case of a depleted pump. In the case of an undepleted pump the overlap integral dominates the terms in the equations for the coefficients of the Stokes

wave and essentially linear gain is experienced at the sagittal focus. Therefore in the case of an undepleted pump beam the discrimination that occurs at the tangential focus is sufficient to produce high quality phase conjugation.

The remaining question to be answered is why the aperiodic transition from poor to good phase conjugation that is evident in the simulation is not evident in the laboratory. There is also the related problem that the onset of spatial instability in the simulations occurs at significantly higher pump energies than in the laboratory.

It is possible that the aperiodic transition from good to poor Stokes beam quality may be explained by the limited number of modes used in the simulation. As shown experimentally, increased pump power results in an increase in the number of intensity maxima on the Stokes beam. If there are not enough modes present in the simulation to accurately describe the physical system, it is possible that a stable solution may exist within the limited number of modes available. It is also possible that there are other important nonlinear effects present in the physical system that are not in the simulation.

Of the possible effects that may cause the process of SBS not to behave in the manner predicted by theory, the intensity dependent refractive index due to the non-Brillouin part of $\chi^{(3)}$ is probably the most likely cause (Kerr nonlinearity). A simple calculation of the power in a beam during the SBS process shows that in almost all cases, the incident power exceeds the critical power for self focusing. Because the power in the pump beam is modified by the Brillouin interaction, it is generally thought that the onset of SBS keeps the effects of any *nonlinear* phase effects below the level of importance. Indeed, Maier et al. have shown that the onset of SBS terminates the self-focusing process in nonlinear media.¹⁰³ Additionally, the excellent level of phase conjugation that occurs in SBS for focused unaberrated beams leads one to believe that the lower intensities at the foci of an astigmatic beam should not cause the failure of optical phase conjugation by SBS; if any effects are apparent it should be the increased beam quality due to the lower focal intensities.

The results of simulations that were presented in Chapter 2 also lend credence to speculation that effects due to the Kerr nonlinearity are unimportant. The virtual clamping of the Brillouin gain parameter with increased intensity shows that the intensity length integral does not venture significantly over the SBS threshold value. Since the value of $\chi_{SBS}^{(3)}$ is typically many times larger than the non-Brillouin part of

$\chi^{(3)}$ (which we will denote $\chi_{Kerr}^{(3)}$) one would not suspect that there would be significant competing effects.

Accepting these arguments as valid, a case can also be made that there are significant nonlinear effects present during the ongoing SBS process. As noted above, different media produce widely varying results when astigmatic beams are used for SBS. Also, it has been noted by Milam et al.¹⁰⁴ that although the on-axis intensity for an astigmatic beam is trivially calculable, the threshold behavior of SBS with increased astigmatism is material dependent, and in no known case does the threshold follow the predicted functional form.

To determine the effects of the Kerr-type nonlinearity on the SBS process and the formation of the phase-conjugate Stokes wave, the real part of $\chi^{(3)}$ was added to the simulation described in Chapter 2. The addition of the real portion of $\chi^{(3)}$ to the simulation developed earlier is straightforward; however the additional CPU time required to reach a solution is increased dramatically.

With the addition of $\chi_{Kerr}^{(3)}$ terms, the complete nonlinear polarization that becomes the driving term for the nonlinear wave equation is

$$P^{NL} = 6(\chi_{Kerr}^{(3)} + i\chi_{SBS}^{(3)})(E_p E_s E_s^* - E_s E_p E_p^*) + 3\chi_{Kerr}^{(3)}(E_p E_p E_p^* + E_s E_s E_s^*). \quad (4.6)$$

Incorporating this expression for the nonlinear polarization into the derivation described in section 2.3 produces a modified version of equations (2.33). The N coupled equations that must be integrated are then

$$\begin{aligned} \frac{\partial a_n}{\partial z} = & K \left(\frac{1}{w_x(z)} \right) \left(\frac{1}{w_y(z)} \right) \\ & \times \sum_{jkl} \xi_{jkl n} e^{i(j+k-l-n)\psi(z)} \left\{ (\chi_{SBS}^{(3)} - i\chi_{Kerr}^{(3)}) a_j b_k b_l^* - (1/2) i\chi_{Kerr}^{(3)} a_j a_k a_l^* \right\} \end{aligned} \quad (4.7.a)$$

and

$$\begin{aligned} \frac{\partial b_n}{\partial z} = & K \left(\frac{1}{w_x(z)} \right) \left(\frac{1}{w_y(z)} \right) \\ & \times \sum_{jkl} \xi_{jkl n} e^{i(j+k-l-n)\psi(z)} \left\{ (\chi_{SBS}^{(3)} + i\chi_{Kerr}^{(3)}) b_j a_k a_l^* + (1/2) i\chi_{Kerr}^{(3)} b_j b_k b_l^* \right\}. \end{aligned} \quad (4.7.b)$$

Approximate values for the ratio $\chi_{SBS}^{(3)} / \chi_{Kerr}^{(3)}$ are given in Table 4.1 for a number of common Brillouin media. The values of $\chi_{SBS}^{(3)}$ were calculated using equation (2.13) and the values of $\chi_{Kerr}^{(3)}$ were derived from the literature.¹⁰⁵

Since the previous chapters have relied on the accuracy of the simulation to predict the steady-state behavior of SBS it is important to investigate the effect of the addition of $\chi_{Kerr}^{(3)}$ to the simulation on the unaberrated pump beam prior to investigating the effects on the astigmatic beam. Figure 4.13 is a plot of the power in the two lowest order Stokes modes for the case considered experimentally in Chapter 3. In Figure 4.13 the solid line is the case presented in Chapter 3 that was shown to agree well with experiment. The dotted line shows the results of adding the Kerr nonlinearity to the simulation with $\chi_{Kerr}^{(3)} = \chi_{SBS}^{(3)}/10$. As can be noted from an examination of Table 4.1, the value of $\chi_{Kerr}^{(3)} = \chi_{SBS}^{(3)}/10$ is typical of many Brillouin media, and an order of magnitude larger than the value for acetone, the medium used in the experiments described in Chapter 3.

Figure 4.13 demonstrates quite clearly that for a beam with no significant aberration the inclusion of the effects of $\chi_{Kerr}^{(3)}$ is not very important. This behavior may be expected from our intuitive understanding of the discrimination mechanism at the focus. The addition of non-phase matched terms complicates the equations, but at the focus the rapid shift of the Guoy phase angle can keep these non-phase matched terms from becoming too important compared to the real part of the coefficients.

For the sagittal focus of an astigmatic beam, the situation has not changed from the case considered without $\chi_{Kerr}^{(3)}$ terms, except that it has become orders of magnitude more complicated. When the $\chi_{Kerr}^{(3)}$ terms are included in the SBS equations, there are significantly more non-phase matched terms, and similarly a

medium	$\chi_{SBS}^{(3)} / \chi_{Kerr}^{(3)}$
N ₂ (1500 psi)	15
CS ₂	40
CCl ₄	50
Acetone	550
SiO ₂	1500

Table 4.1. The ratio $\chi_{SBS}^{(3)} / \chi_{Kerr}^{(3)}$ for some common Brillouin media.

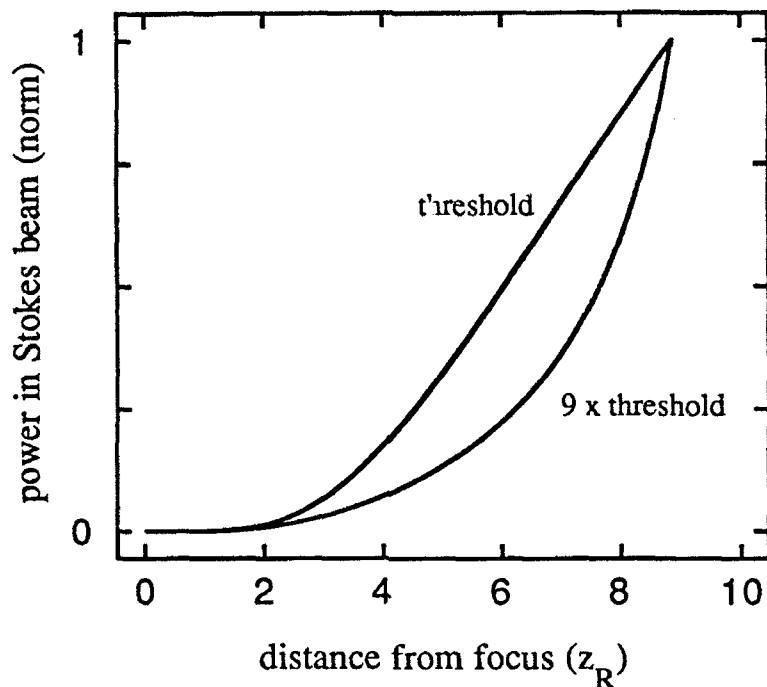


Figure 4.13. Effect of adding a Kerr-type nonlinearity to the simulation of SBS for beams without astigmatism. For each input level of the pump power there are two lines plotted: one for the case of $\chi_{Kerr}^{(3)} = 0$ and one for the case of $\chi_{Kerr}^{(3)} = \chi_{SBS}^{(3)}/10$. The almost perfect superposition of the two curves demonstrates that the effects of the Kerr nonlinearity are negligible for beams without astigmatism. The case presented here is that of the experiment presented in Chapter 3.

significantly larger number of possibilities for unstable growth of nonconjugate modes at a region of high gain where $\psi(z) \approx \text{constant}$.

Due to the complicated nature of the nonlinear process when $\chi_{Kerr}^{(3)}$ terms are included it is difficult to look into the region of instability due to the large number of modes required for the convergence of the simulation. We can estimate the importance of the $\chi_{Kerr}^{(3)}$ terms however, by determining at what point the first three Hermite-Gaussian modes become inadequate to describe the SBS process. For the case of $\chi_{Kerr}^{(3)} = 0$ the onset of spatial instability begins at over 100 times the threshold for SBS. When $\chi_{Kerr}^{(3)} = \chi_{SBS}^{(3)}/10$, the first evidence of spatial instability is at approximately 25 times SBS threshold. Furthermore, with the addition of the $\chi_{Kerr}^{(3)}$

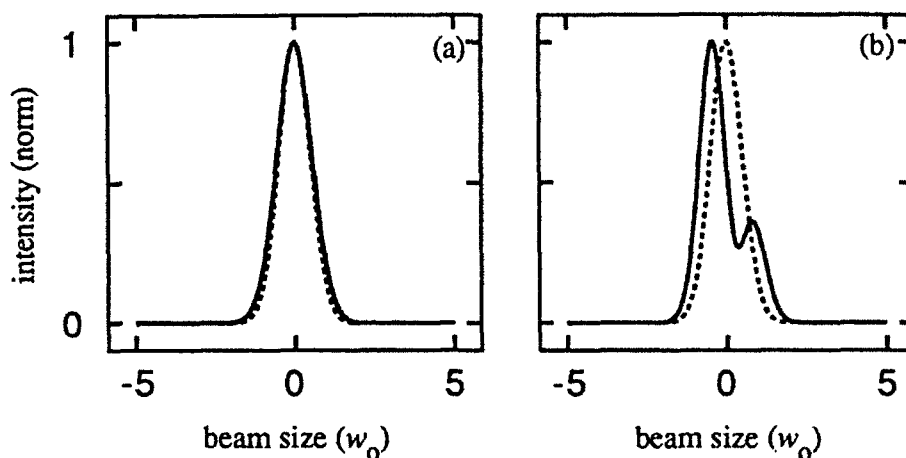


Figure 4.14. Theoretically predicted Stokes beam profiles for a pump beam with no astigmatism (a) and a beam with astigmatism (b), at a pump power near the onset of spatial instability. The dashed lines are the profile of the pump beam.

terms, once the simulation reaches a region of instability the solution never returns to a point where the mode that is conjugate to the pump dominates.

Having added the effects of $\chi_{\kappa_{irr}}^{(3)}$, we may now look at the predicted Stokes beam profile at some level above SBS threshold near the region of spatial instability. Figure 4.14 shows the predicted Stokes intensity profile when the pump is not aberrated, and the Stokes beam profile produced when the pump beam is astigmatic. Referring back to the experimental data presented in Figure 4.3 demonstrates an excellent agreement between theory and experiment.

4.8 Discussion

As is demonstrated in Figure 4.14, the deterioration of the Stokes beam that is observed in the laboratory when an astigmatic pump is used to create SBS is predicted by theory. The reduction in the threshold for the spatial instability derived by adding $\chi_{\kappa_{irr}}^{(3)}$ to the simulation is however, not sufficient to explain the transition to poor SBS phase conjugation observed very near SBS threshold.

There are two plausible explanations that could account for the rapid degradation of the Stokes beam into nonconjugate modes that is seen in experiment

but not seen in the simulation. One reason for the inconsistency may be the inaccurate knowledge of the actual values of $\chi_{Kerr}^{(3)}$ and $\chi_{SBS}^{(3)}$. Values of $\chi_{Kerr}^{(3)}$ in the literature routinely vary by an order of magnitude. Also, it is known that even slight contamination of a Brillouin medium can significantly decrease the value of $\chi_{SBS}^{(3)}$.¹⁰⁶ The combination of an error in the calculation of $\chi_{SBS}^{(3)}$ and the actual value of $\chi_{Kerr}^{(3)}$ could lead to a ratio of $\chi_{SBS}^{(3)} / \chi_{Kerr}^{(3)} \sim 1$ or even lower. Thus the value of $\chi_{Kerr}^{(3)} = \chi_{SBS}^{(3)} / 10$ used in our simulations may be too high. Simulations of astigmatic beams with higher values of $\chi_{Kerr}^{(3)}$ show that an increase in the ratio $\chi_{Kerr}^{(3)} / \chi_{SBS}^{(3)}$ results in a decrease in the pump power necessary to reach the point of spatial instability.

In addition to an inaccurate value of $\chi^{(3)}$, the threshold for spatial instability may be significantly reduced due to the presence of high-order modes on the pump beam. These high order modes can come from imperfect optics or, more likely, from thermal aberrations in the Brillouin medium. The presence of high-order pump modes provides a path for enhanced coupling between conjugate and nonconjugate pump and Stokes modes.

A final possible reason that the simulations and experiments are not completely in agreement may be that the steady-state theory is not applicable in the case of regions of high SBS gain without a Guoy phase shift. That is, the possibility of spatio-temporal instabilities must be considered in regions of high gain and small phase shift. Such a region is present in the case of a focused astigmatic beam.

Temporal instabilities due to frequency-degenerate counter-propagating beams in Brillouin media have been observed in the past.¹⁰⁷⁻¹⁰⁹ Likewise, utilizing a plane-wave theory, temporal-spatial instabilities have been predicted in media with a Kerr nonlinearity.¹¹⁰ These spatio-temporal instabilities grow linearly in space and exponentially in time. Unfortunately, the numerical investigation of spatio-temporal instabilities using focused beams is well beyond our currently available computing power.

There exists no firm theoretical basis for the claim of a temporal-spatial instability during SBS with astigmatic pump beams. It is interesting to note however, that Gaeta et al.¹⁰⁸ have observed a spatial instability in the Stokes wave during SBS while investigating counter-propagating frequency-degenerate waves. This instability was observed in the form of six beams of Stokes-shifted radiation surrounding the central intense spot when the beams were above SBS threshold. Thus, in a single dimension the instability has a shape similar to that shown in Figure 4.3(e). Under

similar experimental conditions, Kulagin et al.¹⁰⁹ saw no such instability; the chief difference in the experiments being the focusing of the beams into the media in the latter case. Thus the spatial instability was seen when there was no focusing of the pump beams, and not seen when there was focusing.

4.9 Conclusions

In this chapter, we have investigated the SBS phase conjugation of astigmatic beams. We have proposed possible reasons for the conflicting reports in the literature as to the effects of inducing astigmatism on the pump beam. Experimentally we have demonstrated that there is no obvious fundamental parameter by which to control the growth of nonconjugate beams when the pump beam is astigmatic. We have demonstrated however, that when there are not two separate intensity maxima along the incident beam path, phase conjugation by SBS is consistently of very high quality. Additionally, when the power in the astigmatic pump beam is very close to threshold usually the quality of phase conjugation is much better than when the energy in the pump beam is several times SBS threshold.

Theoretically, we have demonstrated that the spatial instability of the Stokes wave cannot be present without the effects of pump depletion. Furthermore we have proposed a theoretical explanation for the observance of poor SBS phase conjugation when the pump beam is astigmatic. Our explanation rests on the presence of a (spatially) rapidly changing phase angle in the region of high Brillouin gain to enhance discrimination against nonconjugate modes for beams without astigmatism. This rapid change in the Guoy phase angle occurs at different points in the medium for each of the two transverse dimensions when the pump beam is astigmatic; therefore there exists a region of high gain with no rapid phase change for each of the two transverse dimensions.

Our simulations have shown that the inclusion of the Kerr-type nonlinearity is essential in predicting the behavior of the SBS process when the pump beam is astigmatic, but has little effect in the case of a beam without aberration. Furthermore, simulations have shown that the value of the ratio $\chi_{Kerr}^{(3)} / \chi_{SBS}^{(3)}$ as obtained from the literature is not sufficient to predict the threshold for instability of the Stokes wave seen in experiment. We have proposed three means that may account for this inconsistency: incorrect evaluation of the ratio $\chi_{Kerr}^{(3)} / \chi_{SBS}^{(3)}$, the introduction of high spatial frequencies on the pump beam due to thermal nonlinearities in the Brillouin

medium, and the presence of a spatio-temporal instability similar to the one shown to exist with frequency-degenerate counterpropagating beams.

The theory and experiments presented here may be used to determine the optimal conditions for the SBS phase conjugation of astigmatic beams. The necessity to incorporate the effects of $\chi_{Kerr}^{(3)}$ into the simulation indicates that a reduction in the ratio of $\chi_{Kerr}^{(3)} / \chi_{SBS}^{(3)}$ may assist in reducing the nonconjugate Stokes component. For example the use of acetone instead of other more popular Brillouin media may be preferred. Also, the use of very pure Brillouin media to enhance the value of the Brillouin gain may help.

Finally, the most effective method of ensuring good phase-conjugation of astigmatic beams is to ensure that the SBS process occurs in the regime of the undepleted pump. Theoretical, numerical and experimental investigations all demonstrate that pump depletion is required for the spatial instability observed during SBS of astigmatic beams to develop. One method to ensure that the SBS process occurs in the undepleted pump regime is through the use of a Brillouin oscillator/amplifier arrangement.^{74,111-114} Specifically, a Brillouin oscillator/amplifier arrangement designed such that the leading edge of a temporally smooth pulse is passed through to the oscillator portion, but the maximum energy extraction occurs in the amplifier portion, would ensure that the focal region is always near the SBS threshold value. This type of arrangement has been studied extensively in recent published research.¹¹⁴

Chapter 5

Amplitude and Phase Fluctuations in Stimulated Brillouin Scattering

All of the phenomena associated with stimulated Brillouin scattering discussed thus far have been adequately described by a steady-state theory. As long as the pulse length of the laser is significantly longer than the phonon lifetime, and the rise time of the pulse is not shorter than a phonon lifetime, the approximation of steady-state is generally valid. However, SBS is the amplification of noise and will therefore have some of the characteristics of the initiating noise. The stochastic initiation of the SBS process manifests itself as phase and amplitude fluctuations on the Stokes beam.

The study of the stochastic initiation of SBS is interesting in its own right and several authors have investigated the physics behind the process.⁶⁵⁻⁷² Besides the interesting physics of the process, the study of amplitude and phase fluctuations in SBS is of practical interest. If SBS phase conjugation is to be used in the design of solid-state lasers, random phase jumps and amplitude fluctuations are unacceptable for most applications. In this chapter I will discuss the physics behind the transient phenomena of phase and amplitude fluctuations in SBS, and demonstrate that these effects can be minimized by a judicious choice of focusing geometry.

5.1 Effects of amplitude fluctuations of the initiating radiation

In the derivation of the equations applicable to SBS in Chapter 2, time was conspicuously absent. The time derivatives of the envelopes in the optical and acoustic wave equations were dropped, and the entire analysis was completed under the approximation of steady-state. While this approximation was adequate for the analysis we have presented so far, it is important to remember that in the absence of noise, the process of SBS does not exist.

The noise responsible for the initiation of stimulated Brillouin scattering is due to the scattering of the pump light off of thermal fluctuations in the medium.

These fluctuations change stochastically in both amplitude and phase on a time scale that is on the order of the phonon lifetime of the medium. Therefore, one would expect the Stokes light to exhibit amplitude and phase fluctuations on a similar time scale.

Indeed, in the regime of the undepleted pump, the process of SBS may be considered simply the linear amplification of the stochastic noise in the medium and these stochastic fluctuations are observed. When the Brillouin gain parameter becomes on the order of the SBS threshold value (i.e. when pump depletion becomes important), the intensity fluctuations of the Stokes wave take on a different character than the stochastic noise in the medium.

In the regime of the depleted pump, the stochastic amplitude fluctuations are suppressed and the Stokes wave does not exhibit all of the features of its random initiation. In fact, the intensity fluctuations in the Stokes wave due to the inherent amplitude fluctuations in the noise seed can be almost entirely suppressed, just as intensity fluctuations can be suppressed by any saturated amplifier. Boyd, et al.⁷⁰ and Gaeta, et al.⁷¹ have shown theoretically and experimentally that when the pump beam is significantly below threshold, such that the Brillouin gain parameter $G \ll 25$, the fluctuations in the Stokes intensity are completely stochastic in nature and occur on a time scale on the order of a phonon lifetime. Likewise, they have shown that when the pump is at or above SBS threshold, these amplitude fluctuations are suppressed.

When viewing SBS in the pump depletion limit in the context of amplifier theory, the suppression of the amplitude fluctuations is easily understood; what is not so intuitive however, is the prediction that the amplitude noise on the Stokes wave is dependent upon the length of the interaction region. This dependence has been predicted by numerical simulations^{70,71} but never verified experimentally.

The explanation for the dependence of the amplitude fluctuations on the length of the interaction region is based on the fact that during the SBS process, the pump laser is depleted in a region of length approximately given by

$$L = \frac{l}{GI_{xh}}, \quad (5.1)$$

where as before l is the length of the medium, G is the Brillouin gain parameter (~ 25 at or above SBS threshold) and I_{xh} is the intensity of the pump beam normalized to

the threshold intensity (e.g. $I_{xth} = 2$ when the pump beam is two times above SBS threshold).

Any given amplitude fluctuation will be amplified without saturating the SBS process (thus producing an amplitude fluctuation in the Stokes beam) if the energy in the noise spike is considerably less than the energy contained in the laser field within the region of strong amplification. For the case of large pump depletion, most of the energy in the pump beam can be found in the region of length L near the front of the medium. Assuming that any given noise spike has an intensity on the order of the pump beam, upon entering the region defined by the length L from the front of the medium, the noise will see unsaturated amplification if the length of the noise feature is less than L . That is, if there is a sufficiently small amount of energy in the noise spike, the amplification of the noise will be linear. Since we may assume that the amplitude noise features are on the order of a phonon lifetime (τ_{phonon}) in length, the condition for a noise feature in the medium to produce a noise feature in the Stokes output is given approximately by

$$\frac{c}{n} \tau_{phonon} < L \quad (5.2)$$

where n is the index of refraction of the medium and c is the speed of light.

Defining the spontaneous Brillouin linewidth Γ as the inverse of the phonon lifetime and the product nl/c as the transit time of light through the medium $T_{transit}$, the condition for amplitude noise suppression is given by

$$GI_{xth} > \Gamma T_{transit} \quad (5.3)$$

For the case of focused SBS beams the analysis above must be altered. As is demonstrated by Figures 3.1 and 3.2, equation (5.1) is not a valid assumption in the case of focused beams. A better approximation of the length of the pump depletion region is the distance from the focal point of the focusing lens to the front of the SBS medium, regardless of the intensity of the pump beam (provided it is over SBS threshold). If the focusing lens is in contact with the front of the medium, the pump depletion distance is the focal length of the focusing lens. For a short medium this approximation is particularly accurate, as can be seen from Figure 3.2. Replacing the

focal length of the lens for L in equation (5.2) leads to the condition for suppression of amplitude fluctuations for focused beams. Thus one expects that amplitude fluctuations will be suppressed for the case when

$$\Gamma T_f \leq 1, \quad (5.4)$$

where T_f is the transit time of light over the focal length of the lens in the medium.

The functional response of the rms intensity fluctuation of the Stokes beam to a change in T_f is not immediately obvious. However, up to some limiting point where the fluctuations in amplitude are similar to those of the initiating radiation, one may assume that there is a monotonic increase in the rms intensity fluctuations with increasing T_f .

In all cases considered in this section there has been an implicit assumption that the transit time of light through the medium is significantly shorter than the duration of the pump pulse. Although in all of our experiments this is the case, should the transit time through the medium be longer than the pump pulse duration the important time scale becomes the pump pulse duration rather than the transit time through the medium.

5.2 Effects of phase fluctuations of the initiating radiation

There are of course two aspects to the initiating noise of the SBS process: amplitude and phase. The discussion in section 5.1 above in no way indicates that the phase fluctuations of the Stokes radiation that are attributable to the stochastic initiation of SBS are suppressed by reducing the interaction length. A close analysis of the SBS process however reveals that there is a mechanism that may be exploited to reduce the noise on the Stokes beam attributable to phase fluctuations in the initiating radiation.

The phase fluctuations of the initiating radiation lead to a broadening of the linewidth of the Stokes wave. In the limit of spontaneous Brillouin scattering the spectrum of the Stokes light is given by the inverse of the phonon lifetime of the medium, which is the spontaneous Brillouin linewidth Γ . However in the case of stimulated Brillouin scattering, the spectrum is gain-narrowed so that the linewidth is given by^{2,70}

$$\Delta\omega = \Gamma\sqrt{\ln 2/G}, \quad (5.5)$$

where again G is the Brillouin gain parameter. Since it was shown in Chapter 2 that above SBS threshold G can be considered constant at ~ 27 , the ratio of the narrowed linewidth to the spontaneous linewidth is $\Delta\omega/\Gamma \approx 0.16$.

For a discussion of the phase fluctuations of SBS it is useful to define the coherence time τ_{coh} as the inverse of the linewidth. The coherence time is the time that one would expect the phase of the Stokes wave to become completely decorrelated. This decorrelation time is approximately given by $\tau_{coh} \approx 6\tau_{phonon}$.

The decorrelation of the phase of the Stokes wave is due directly to the change in phase of the initiating noise. This change in the phase of the noise field can be due to either a gradual change in phase or an abrupt phase "jump". The effects of these phase changes on the SBS process have been observed experimentally,⁶⁵⁻⁶⁷ and recently Mangir et al. have directly observed the phase drift as well as the phase jumps.⁷² These phase effects lead to amplitude noise as well as phase noise.

To understand the coupling between the phase and amplitude fluctuations in the Stokes beam consider the case when, after the onset of SBS, the phase of the initiating radiation changes by π . Upon the change of phase of the initiating radiation the existing acoustic field will not provide the coupling between the Stokes wave and the pump wave that had ensured the amplification of the Stokes wave. The time it takes for the acoustic field to adjust to the new Stokes field is on the order of a phonon lifetime. Therefore there will be a drop in the energy in the Stokes beam for a period of time approximately equal to a phonon lifetime. Upon readjustment of the phonon field, there will be a transient energy spike in the Stokes wave, since the lack of a Stokes wave for a short period of time has allowed the pump beam to transit the medium undepleted; there will of course be a similar but inverted noise feature in the transmitted pump beam. Eventually the SBS process reaches a steady-state again. Thus the random phase shifts in the initiating radiation result in amplitude fluctuations in the Stokes wave, with a shape that may be described as similar to an inverse dispersive profile, as well as the phase fluctuations. The abrupt change in phase of the Stokes wave, with the accompanying amplitude fluctuation has been termed a phase jump,⁷² although the same phenomenon has been termed a phase

wave in superfluorescence¹¹⁵ and the amplitude fluctuation alone has been called a Raman soliton in stimulated Raman scattering.^{116,117}

The condition for the suppression of the amplitude noise attributable to phase fluctuations may be derived by noting that the energy in the intensity spike of the Stokes wave is given by

$$\Delta E = I_p A T_{transit}, \quad (5.6)$$

where I_p is the pump intensity and A is the cross-sectional area of the beam. From equation (5.6) we may estimate the intensity of the noise spike by

$$I_{noise} = \frac{\Delta E}{A \tau_{phonon}}. \quad (5.7)$$

Assuming that the Stokes beam's intensity is on the order of the pump beam's intensity, the ratio of the intensity of the noise spike to the mean Stokes intensity is

$$\frac{I_{noise}}{I_s} \sim \frac{T_{transit}}{\tau_{phonon}} = \Gamma T_{transit}. \quad (5.8)$$

Therefore, to minimize the amplitude effects attributable to phase jumps in the Stokes seed one must minimize the product $\Gamma T_{transit}$. This is a more restrictive condition than was found for minimizing the effects of amplitude noise, in that equation (5.8) implies that to minimize the amplitude effects due to phase jumps one must meet the condition

$$\Gamma T_{transit} \ll 1. \quad (5.9)$$

The argument presented above that led to an expected dependence of the noise properties of the Stokes amplitude on the physical interaction length cannot be applied to the stochastic change in the phase of the initiating radiation. However, one may make an intuitive argument that phase fluctuations will be suppressed if the transit time of light through the interaction region is less than or on the order of a phonon lifetime. That is, if there is virtually instantaneous communication (on the

time scale of the acoustic wave) between the front and back of the interaction region, there will be discrimination against initiating radiation that is out of phase with the existing acoustic wave. This discrimination will reduce the number of phase fluctuations (and accompanying amplitude fluctuations) in the Stokes wave.

From the arguments presented in these two sections we may make some predictions about the behavior of amplitude and phase fluctuations present on the Stokes wave that are attributable to the stochastic initiation of the SBS process. First, we may predict that the rms intensity fluctuation of the Stokes beam due to amplitude and phase fluctuations in the initiating noise is proportional to the product of the Brillouin linewidth and transit time of light through the Brillouin medium. In the case of a focused pump beam, the transit time through the medium is replaced with the focal length of the lens. Thus we expect that the rms intensity fluctuation of the Stokes beam will be monotonically increasing with increasing T_f .

Predictions about the phase characteristics of the Stokes wave are slightly more tenuous. The analysis above indicates that the phase fluctuations on the Stokes beam will be reduced for cases where the product $\Gamma T_{transit}$ is on the order of unity. For cases where the product $\Gamma T_{transit}$ is much larger than unity, it is not clear that the phase fluctuations are dependent upon the length of the interaction region at all.

Our analysis leads us to believe that there are three mechanisms by which amplitude fluctuations on the Stokes wave may be suppressed, and there is one mechanism by which phase fluctuations may be suppressed. All of these suppression mechanisms depend on reducing the length of the interaction region. We have experimentally verified these predictions by examining the intensity and phase of Stokes beams produced in the focused geometry using lenses of several focal lengths.

5.3 Experimental verification

To experimentally verify the prediction that amplitude fluctuations are suppressed under the conditions of equation (5.4), light from a single longitudinal mode, frequency-doubled, Q-switched Nd:YAG laser operating in a TEM₀₀ mode with a 20 ns pulse duration (FWHM) was used to produce SBS Stokes light using lenses of varying focal length to focus the beam into the Brillouin medium. To ensure that the pulse was many phonon lifetimes in length CCl₄ was chosen as the Brillouin medium ($\tau_{phonon} = 180$ ps). The energy of the pump beam was kept constant at approximately twice the SBS threshold, although we found no systematic

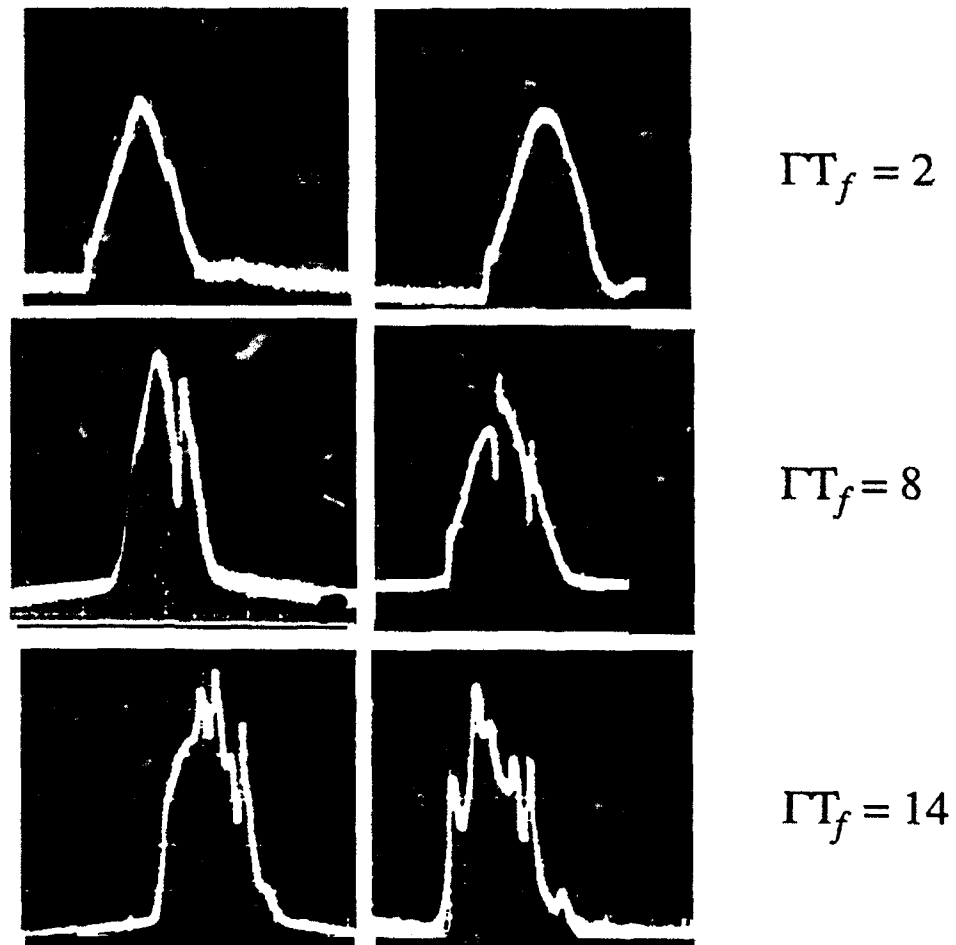


Figure 5.1. Typical Stokes pulse profiles for varying interaction lengths.

dependence upon the pump intensity, as predicted. Temporal profiles of the Stokes pulses produced using different focal lengths of lenses were recorded on film and compared. Typical Stokes temporal profiles for three different values of ΓT_f are

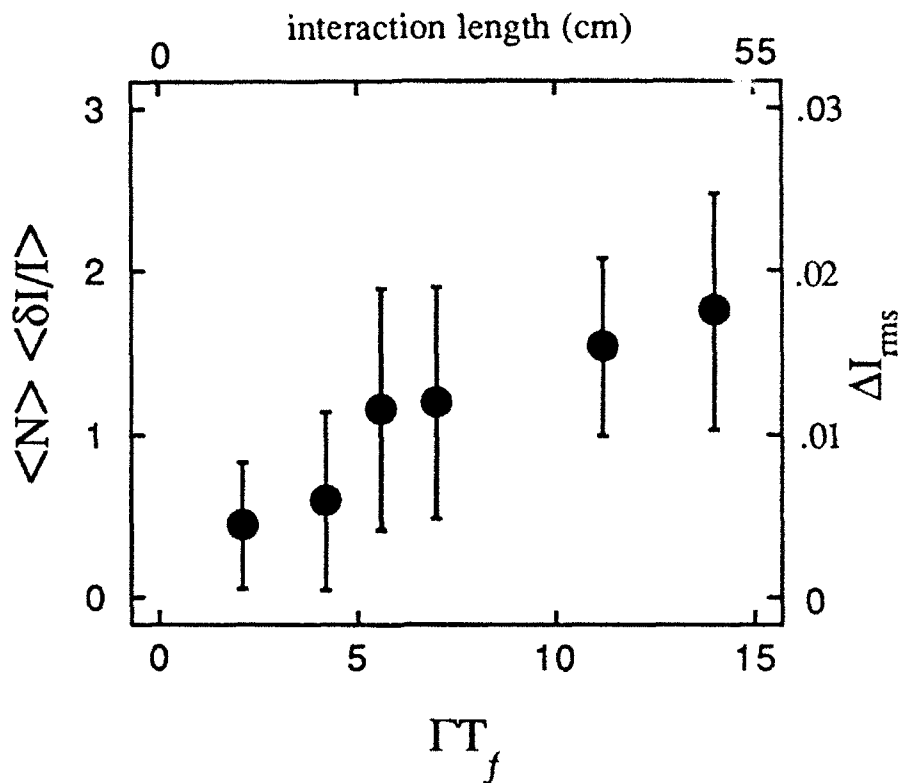


Figure 5.2. Experimental verification of the dependence of intensity fluctuations of the Stokes beam on the length of the SBS interaction region.

shown in Figure 5.1. Note the increase in amplitude and frequency of the intensity fluctuations as the interaction length becomes longer.

To quantify the increase in amplitude fluctuation of the Stokes beam with the increase in interaction length we recorded many Stokes pulse profiles for each experimental geometry. The number of intensity fluctuations on each Stokes beam was counted and the normalized amplitude of the intensity fluctuation was determined in each case. The mean number of intensity fluctuations $\langle N \rangle$, multiplied by the mean normalized amplitude of the fluctuation $\langle \delta I / I \rangle$, was then converted into an estimate of the rms intensity variation. This conversion is accomplished by multiplying the product $\langle N \rangle \langle \delta I / I \rangle$ by the ratio of the characteristic time scale of the intensity fluctuation to the Stokes pulse length. In our experiment the conversion factor is

$$\tau_{\text{phonon}} / \tau_{\text{Stokes}} \approx .01.$$

Figure 5.2 shows the results of these experiments. The tendency toward more intensity variation for larger ΓT_f is obvious. Besides the monotonic increase in the mean rms intensity variation, it is important to note the evidence of the stochastic initiation that can be seen in the increased variance of the data.

To investigate the behavior of the Stokes phase to a variation in interaction length we used the apparatus shown in Figure 5.3. Light from a single longitudinal mode, frequency-doubled, Q-switched Nd:YAG laser operating in a TEM_{00} mode was split into two beams of nominally equal energy. Each beam was focused into a separate cell containing carbon tetrachloride. The Stokes beams from the two cells were then combined on a beamsplitter, and the resulting interference pattern was imaged onto an optical multichannel analyzer (OMA). The integration time of the OMA was very much longer than the pulse length of the laser, and thus the OMA produced a time-integrated record of the interference pattern.

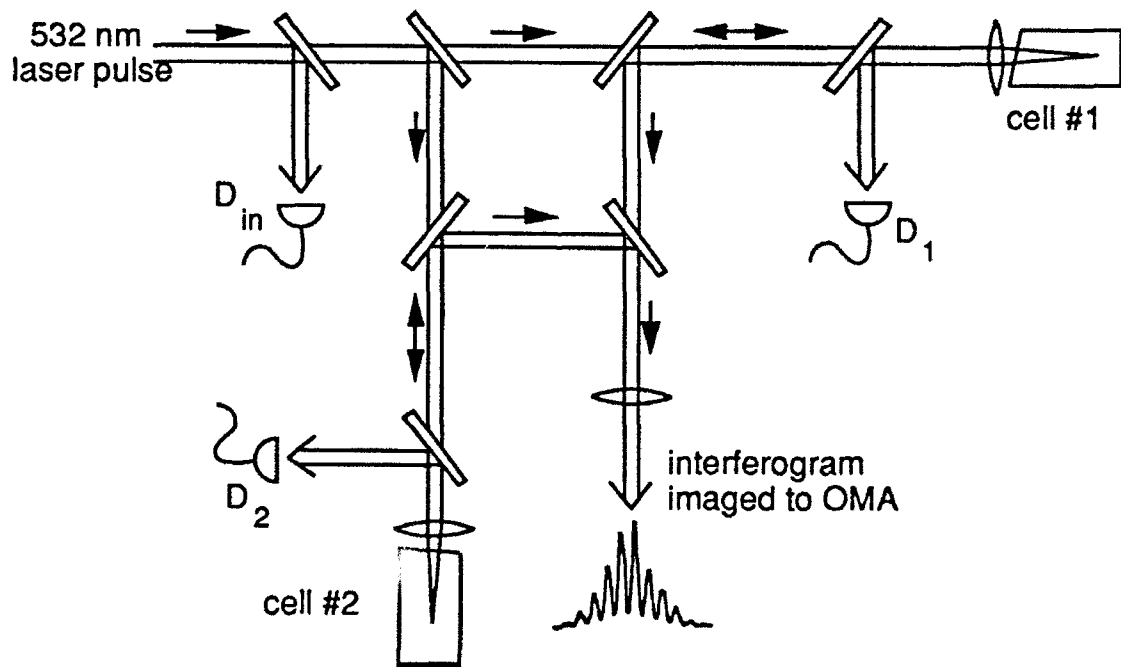


Figure 5.3. Experimental arrangement for the investigation of phase fluctuations.

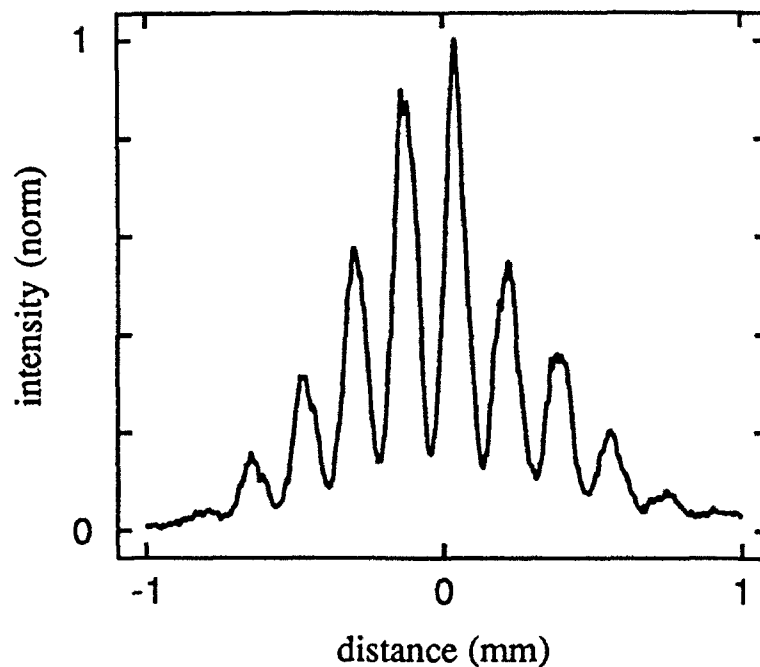


Figure 5.4. Interference pattern produced by two Stokes beams, each having a duration in excess of 100 phonon lifetimes.

A typical example of such a pattern, obtained using a small value of ΓT_f , is shown in Figure 5.4. Note that the fringe visibility of this pattern is nearly 100%, even though the 20 ns duration of the Stokes pulses (FWHM) was more than 100 times longer than the phonon lifetime and was 16 times longer than the inverse of the gain narrowed linewidth as predicted by equation (5.5).

The results presented in Figure 5.4 demonstrates qualitatively the suppression of phase fluctuations through use of a small value of ΓT_f . In order to analyze these results more quantitatively, the digitized interference pattern was used to determine the fringe visibility V . Since the initiation of SBS is stochastic in nature, the fringe visibility varied from shot-to-shot, and in our data analysis we use the mean fringe visibility $\langle V \rangle$, which was obtained by averaging the visibility for many laser shots. The coherence time τ_{coh} of the Stokes light can then be estimated through use of the relation¹¹⁸

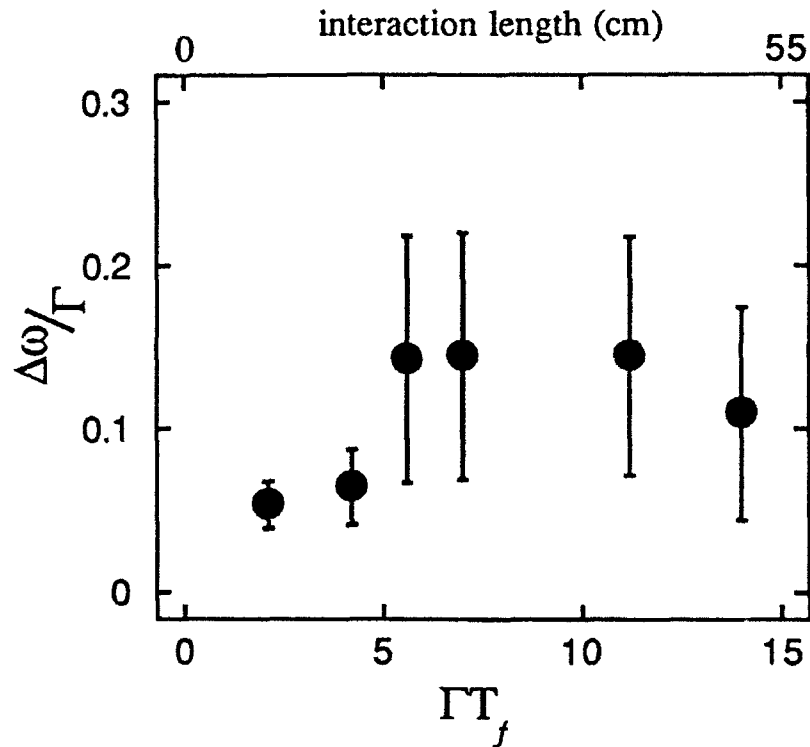


Figure 5.5. Variation of the linewidth of the Stokes emission with increasing interaction length.

$$\langle V \rangle \approx \frac{1}{\sqrt{T_{Stokes}/\tau_{coh}}}, \quad (5.10)$$

where T_{Stokes} is the duration of the Stokes pulse and we assume $T_{Stokes}/\tau_{coh} \geq 1$. In performing the measurements great care was taken to prevent feedback between the Brillouin cells: the entrance windows of the cells were tipped at an angle to the incident beam, the back of the cells were rendered opaque and nonreflecting, and all lenses were slightly tilted to avoid back reflections. The results of these experiments are shown in Figure 5.5.

The data of Figure 5.5 demonstrates that, as in the case of the intensity fluctuations, not only do the phase fluctuations diminish with a shorter interaction region, but the statistical fluctuations are also reduced. That is, the phase noise associated with stochastic initiation of the SBS process is reduced by limiting the interaction region such that $\Gamma T_f \sim 1$. The suppression of the phase fluctuations,

unlike the intensity fluctuations, appears to saturate for values of $\Gamma T_f \geq 5$. Thus the linewidth of stimulated Brillouin scattering can be narrowed by reducing the length of the interaction region, but only if the interaction length is reduced to a value such that $\Gamma T_f \leq 5$. This is consistent with our understanding of the method suppression of the phase fluctuations, since once the transit time of light through the interaction region is significantly longer than a phonon lifetime, we expect little dependence of the phase noise on the product ΓT_f .

5.4 Conclusions

The inherent noise in both the phase and amplitude of the Stokes wave due to the stochastic initiation of the SBS process can reduce the effectiveness of SBS in solid-state laser applications. The reduction or elimination of this noise is of paramount importance if optical phase conjugation by SBS is to be used in any practical manner in the design of solid-state lasers.

The results presented in this chapter demonstrate that both the amplitude and phase noise inherent in the SBS process can be significantly reduced by the judicious choice of focusing optics used to create the Stokes wave. In the past other researches had proposed that the amplitude noise could be reduced by limiting the SBS interaction region, and a plausible theory had been put forward to explain this reduction.

Our work here has demonstrated the virtual elimination of the amplitude fluctuations due to the stochastic initiation process when using a short Brillouin interaction region. Furthermore, we have demonstrated that this same geometry reduces the phase fluctuations attributable to the initiation process. In the following chapter, we will report how this new information was applied, with all of the other available information on SBS phase conjugation, to construct an inexpensive, robust phase-conjugate solid-state laser.

Chapter 6

Design and Construction of a Solid-State Phase-Conjugate Laser

Besides the interesting physics, the motivation for the research presented thus far has been in the context of the applicability of SBS to solid-state phase-conjugate lasers. Therefore it is appropriate to conclude this work with a chapter devoted to the design and construction of a solid-state phase conjugate laser system.

In the previous chapters we have implicitly assumed that it has been the SBS process itself that has limited the wide spread construction and use of phase-conjugate lasers, and we have concentrated on the study of SBS in this context. However in addition to the scientific issues of the SBS process, there are other issues that must be considered in the design of a working phase-conjugate laser. Some of these issues are purely engineering issues, such as the disruption of the pulse due to phase-conjugate feedback into the oscillator. Other issues are practicality issues, such as cost, safety and robustness of the system.

In designing a solid-state phase-conjugate laser we considered the scientific, engineering and practicality issues. The research presented in the previous chapters, and that reported in the literature, was used to ensure the best phase conjugation available by the SBS process. Having decided on the best design for a phase-conjugator, we then considered engineering and practicality issues in the design of the laser itself. The result is a solid-state phase-conjugate laser design that is versatile, robust and relatively inexpensive.

6.1 Issues in the design of solid-state phase-conjugate lasers

Besides the practical issues of overall cost and durability there are two issues that must be addressed from a scientific viewpoint: extraction of the energy from the laser and feedback of radiation into the oscillator. To investigate the impact of these issues consider the block diagram of a phase-conjugate laser shown in Figure 6.1. Upon leaving the oscillator the pulse must first pass through the extraction

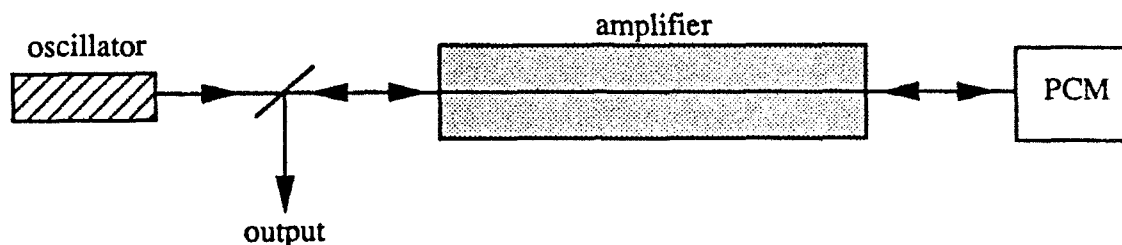


Figure 6.1. Block diagram of a phase-conjugate laser.

mechanism and into the amplifier. If the method of extraction is active, such as with the use of a Pockels cell, then the pulse length is limited by the length of the amplifier segment of the laser. That is, the pulse must be shorter than twice the transit time through the amplifier portion or else the back of the pulse will still be entering the Pockels cell when the leading edge is arriving in the opposite direction. The use of a Pockels cell then limits the pulse length of the laser or requires a large area on the optical table. Additionally, Pockels cells are expensive and extensive timing and power issues must be addressed when they are in use. For these reasons it is not common to use a Pockels cell for extraction of the laser energy except when the amplifier is used in a regenerative configuration.

An alternative method for the extraction of the energy from the laser is based on the fact that a phase-conjugate mirror made by SBS is not a vector phase-conjugate mirror. Since the polarization properties of the pump beam are not conjugated, light entering the SBS cell with left-hand polarization will emerge with the same handedness, just as with normal specular reflection. Therefore the insertion of an appropriately oriented quarter-wave plate and a polarizer prior to the SBS cell can be used to extract all of the energy from the phase-conjugate mirror, even if the incident pulse is longer than twice the length of the amplifier. This method of energy extraction is shown schematically in Figure 6.2. For use in high energy lasers a thin-film polarizer (TFP) is used rather than a polarizing beamsplitter to reduce the possibility of damage.

A significant drawback to using the method just described for extraction of the beam from the amplifier is that any depolarization in the amplifiers results in some of the energy being fed back into the oscillator. Depolarization in solid-state laser amplifiers is known to be a problem.⁸² In practice, it is not unusual to find that the

depolarization upon double passing a Nd:YAG to be on the order of 10-20%. The amplifiers in our laboratory typically depolarize the beam on the order of 5% when used in the double-pass configuration at maximum pump power. Thus for a pulse amplified to approximately one Joule in energy, as much as 50 mJ may be injected back into the oscillator.

Usually isolation of the oscillator is accomplished by the use of a Faraday rotator. Besides being expensive, the typical large-area permanent magnet Faraday rotator designed for use at $1.06\mu\text{m}$ has an isolation ratio on the order of $\sim 100:1$. This means that even with a Faraday rotator between the point of extraction and the oscillator, hundreds of microjoules may be fed back into the oscillator. This fed-back radiation will seed the oscillator at a frequency different than that at which it is lasing, and the effect will be an amplitude jump with a frequency and phase shift in the pulse. Therefore, unless multiple Faraday rotators are used, the maximum pulse length of a single longitudinal mode phase-conjugate laser is usually determined by the length of the amplifier section of the laser when a passive extraction method is used as well as when an active system used.

As noted above, the problems beyond the phase-conjugate mirror are not scientifically challenging. With enough money and space the problems noted here can be easily corrected. The challenge is in designing a phase-conjugate laser that has a small footprint, high energy, variable pulse length and good beam quality and is still low in cost. In the next section we will describe such a laser.

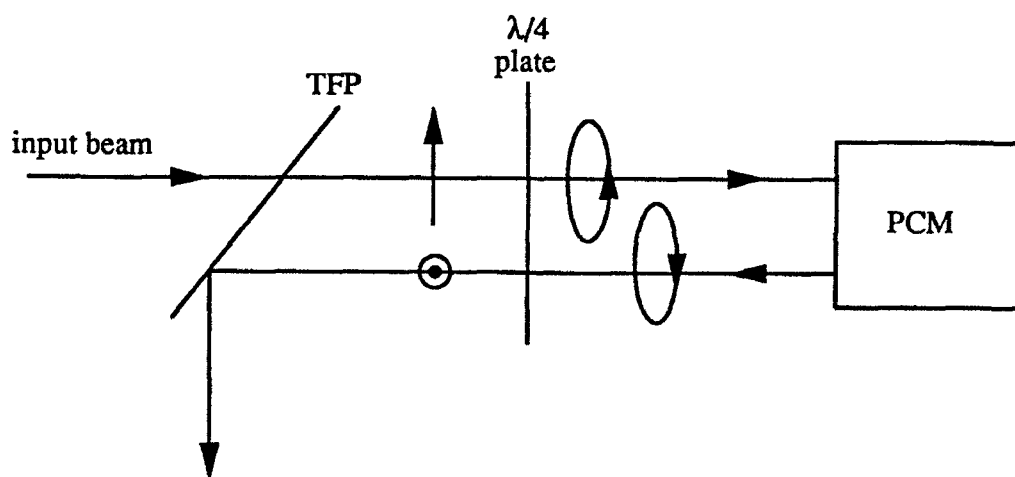


Figure 6.2. Method for passive extraction of phase-conjugate radiation. TFP is an abbreviation for thin-film polarizer.

6.2 Design for a phase-conjugate laser

The key to building a phase-conjugate laser meeting all of the design criteria, including cost, is in the choice of the phase-conjugate mirror and the design of the oscillator. We have chosen the general design shown in Figure 6.1, with the extraction method described above and shown in Figure 6.2.

The laser itself consists of an oscillator with a 7 mm, flashlamp pumped rod and two amplifiers (7 and 9 mm Nd:YAG flashlamp pumped rods) used in a double pass configuration. The electronics and gain media are taken from a commercially available system and can operate at a one, five or 10 Hz repetition rate.

Since the gain media are flashlamp pumped Nd:YAG rods, the aberration impressed on the beam upon passing through the amplifiers is nominally cylindrically symmetric. Therefore, many of the issues raised in Chapter 4 are not a consideration in this system as they might be in a system with state-of-the-art gain media (i.e. slab lasers). In particular, a focused beam from the amplifiers produces only one intensity maxima along the beam path when focused into a medium. This being the case, the issues raised in Chapter 4 relating to the ratio of $\chi_{SBS}^{(3)} / \chi_{Kerr}^{(3)}$ are minimal, and it is possible to use many of the SBS media that are unsuitable for beams with astigmatic distortions.

The phase-conjugate mirror is shown schematically in Figure 6.3. It consists of a high pressure vessel with $\frac{3}{4}$ inch thick AR coated windows on each end. The cell is filled with 1800 psi of nitrogen at room temperature. The beam enters the front of the SBS cell, traverses the entire length of the cell, and exits the rear window where it is reflected by a high reflectivity mirror with a radius of curvature of 25 cm. The mirror focuses the beam back into the cell slightly off-axis to avoid the possibility of counter-propagating beams that may lead to temporal instabilities in the Stokes wave.¹⁰⁷⁻¹¹⁰ The slight astigmatism induced by off-axis focusing of the beam is not sufficient to produce multiple intensity maxima along the beam path and therefore the Stokes beam does not exhibit the spatial instability discussed in Chapter 4. The short focal length of the focusing mirror virtually eliminates all phase and amplitude fluctuations due to the stochastic initiation as described in Chapter 5. As shown in Figure 6.3, a neutral density filter is placed between the SBS cell and the focusing mirror. Typically, this filter has an optical density of 0.1 and its purpose is to reduce

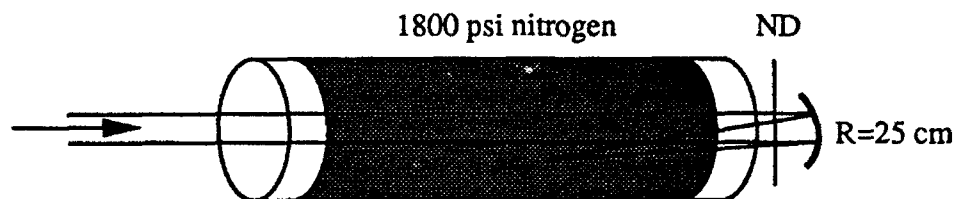


Figure 6.3. High pressure nitrogen cell in a folded oscillator/amplifier design.

the intensity at the focal point in the cell and reduce the instance of optical breakdown.

The phase-conjugate mirror is a folded oscillator-amplifier design that has all of the advantages of the SBS oscillator-amplifier designs discussed in the literature,^{74,111-114} but only takes up half of the space. The choice of high pressure nitrogen as the SBS medium has several advantages over other media. Besides being inexpensive, gaseous nitrogen is self-repairing after breakdown, shows no evidence of thermally induced aberrations at repetition rates to 10 Hz, is readily available and has no health risks associated with its use. Additionally, should it become necessary to address thermal problems in the medium due to the use of higher repetition rates or power levels, the nitrogen can be flowed through the cell and vented into the atmosphere.

The entire phase-conjugate laser is shown schematically in Figure 6.4. Note from figure 6.4 that there is no isolation of the oscillator other than that provided by the quarter-wave plate and polarizer. This is because we have addressed the problem of feedback by eliminating its effect on the oscillator, not by eliminating the feedback.

Besides the SBS cell, the most important key to a high quality, robust and inexpensive phase-conjugate laser is the oscillator design. Our oscillator is an all solid-state, Q-switched ring oscillator. We have demonstrated TEM₀₀ mode operation with transform limited pulses of duration from 40 to 400 ns, with no noticeable degradation in performance after almost a year of use.

The ring oscillator consists of a flashlamp pumped, 7 mm Nd:YAG rod. Both triangular and rectangular ring designs have been used, with slightly better beam

quality in the triangular configuration and slightly higher energy in the rectangular configuration. The color-center Q-switch¹¹⁹ consists of a piece of polished LiF crystal 10 cm in length that has been irradiated with 10^8 rad (water) of 22 Mev γ -rays from a Co^{60} source. The pulse length is determined by the length of the cavity, with the minimum pulse length of ~ 40 ns (FWHM) determined by the minimum necessary length to fit in all of the components.

The use of the ring design has several advantages over a linear oscillator design, chiefly the lack of influence of the fed-back radiation and the ease of single longitudinal mode operation. The only necessary condition to ensure that the oscillator is not affected by phase-conjugate feedback, provided the feedback is not too large, is that the loss in one direction exceeds the gain. Therefore, the Faraday rotator in the oscillator that ensures unidirectional operation also eliminates the effects of feedback. Since the Faraday rotator need only produce enough rotation so that the loss exceeds the gain, it is not necessary that the rotator produce a full 45° rotation of the polarization vector. Our Faraday rotator produces a rotation of approximately 23° , and is built on the compact design of Gauthier et al.¹²⁰ Using the minimum rotation necessary and the compact design reduces the cost and the space requirements significantly.

The laser shown in Figure 6.4 produces pulses up to one Joule in energy with pulse lengths of 40 ns. The output is limited by the damage threshold of the components and is not a fundamental limitation of the design. Spectral analysis of the beam via a Fabrey-Perot interferometer with a free spectral range of 0.2 cm^{-1} revealed consistent single longitudinal mode operation.

6.3 Conclusions

In this chapter I have reported on the design and construction of a low cost, compact phase-conjugate laser. The use of a novel Q-switched ring oscillator eliminates the effects of phase-conjugate feedback, one of the major limiting factors in phase-conjugate lasers. Our design employs a high pressure nitrogen cell for a phase conjugate mirror, and produces a near diffraction-limited beam with energy up to one Joule. The single longitudinal mode pulse can have a length from 40 ns upward, and operation with pulses as long as 400 ns has been demonstrated. As of this writing the laser described here has been in operation for a period in excess of a year with no obvious degradation in performance.

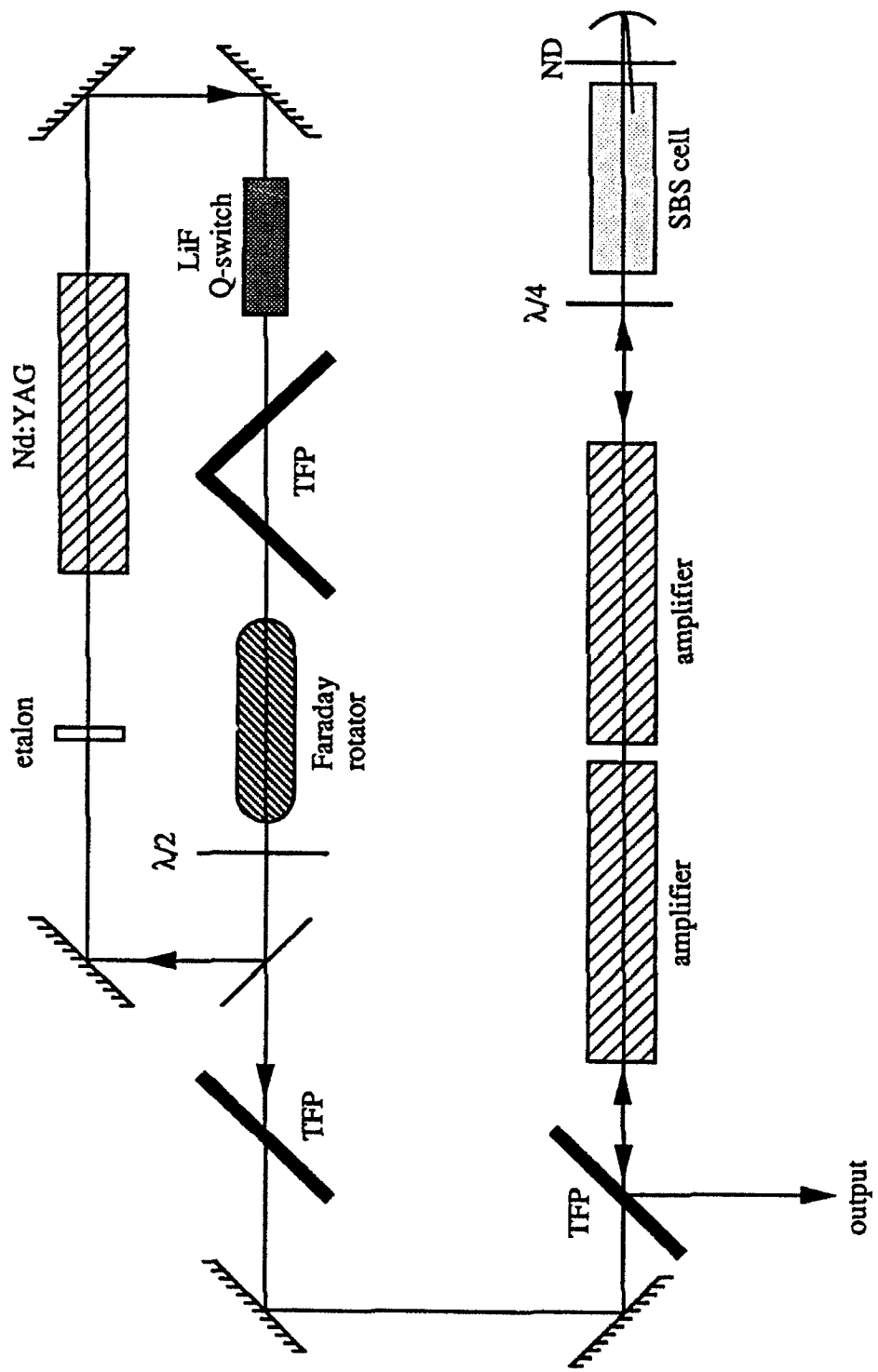


Figure 6.4. Detailed schematic of the phase-conjugate laser.

Chapter 7 Conclusions

In this work I have investigated some of the fundamental theoretical and experimental aspects of stimulated Brillouin scattering. While the investigations were within the context of using SBS in phase-conjugate solid-state lasers, the goal has been a fundamental understanding of the physics of the SBS process. Once the physics of SBS is understood, the engineering becomes straightforward.

The investigations presented here have centered on understanding the importance of the nonlinear interaction between the pump and the Stokes wave in the focused geometry and in the regime of strong pump depletion. To accomplish this study a modal decomposition technique was applied to the SBS process and new insight resulted. Approaching SBS from this new direction allowed a detailed examination of the SBS process that included nonlinear transverse effects. Additionally, the modal decomposition made possible the three dimensional simulation of the SBS process with focused beams.

Reports of three dimensional numerical simulations of SBS with focused beams having energy that ensures the process is well into the pump depletion regime are nonexistent in the literature. Our simulations have allowed us to investigate several important aspects of the SBS process and to understand many heretofore unknown aspects of SBS with focused beams. Some of these interesting aspects are: the spatial effects of distributed noise, the presence of phase shifts in the Stokes modes, nonlinear behavior of the Brillouin gain parameter and a universal dependence of the energy in the pump beam at any point in the Brillouin medium.

One of the more interesting results from the simulation concerned the distribution of energy within the Brillouin interaction region. Contrary to popular thought, the depletion of the pump energy during the SBS process using focused beams is not confined to the focal region. Instead, under circumstances normally found in the laboratory, most of the energy is extracted from the pump beam well

away from the focal region. An experimental study of the energy distribution within the Brillouin interaction region confirmed the results of the simulation.

One of the primary focuses of this research has been to understand the process of optical phase conjugation by SBS and its inherent limitations. Of particular interest is the case of pump beams that are smoothly aberrant. In our work, the phase conjugation of astigmatic beams was studied in depth. An attempt was made to sort out the conflicting reports in the literature, and then original theoretical and experimental work was presented that determined the etiology of poor SBS phase conjugation of astigmatic beams.

It was shown that the reason astigmatic beams are not well conjugated is because stimulated Brillouin scattering with pump beams that are not undergoing a rapid phase shift in a region of high gain are spatially unstable. This instability is only present when the process takes place in the regime of the depleted pump. Thus through our work we have understood the process of SBS well enough to propose an engineering solution. To ensure the accurate phase-conjugation of astigmatic beams by SBS, one need only ensure that the process takes place in the context of the undepleted pump. On a more fundamental level, the study of the spatial instability is of interest in and of itself.

Another aspect of SBS that we have investigated is the presence of phase and amplitude fluctuations on the Stokes beam due to the stochastic initiation. A dependence of the number of amplitude fluctuations caused by a change in the initiating radiation during SBS on the length of the interaction region had been proposed in the past. We experimentally verified this conjecture and then went on to show that the phase fluctuations are also reduced by a reduction of the interaction length.

Finally, I have reported on the design and construction of a solid-state phase-conjugate laser. The phase-conjugate mirror design is based on all of the information presented in previous chapters. However, in the design of a phase-conjugate laser it is often not the phase-conjugate mirror that limits the usefulness, but rather the engineering problems of cost, space and complexity. We have presented a simple, robust and inexpensive design for a phase-conjugate solid-state laser. Our laser produces single longitudinal TEM_{00} pulses of variable pulse lengths, with pulse energy of up to one Joule.

Thus the research presented here has provided new insight into the physics of the process of optical phase conjugation by stimulated Brillouin scattering. In particular, some of the limitations of the SBS process in producing a phase-conjugate wave have been determined and methods to enhance the phase-conjugating ability have been found.

In conclusion, it is encouraging that a field of research as established as the study of SBS still holds the potential for new discovery. I look forward to the time when the richness of the nonlinear process can be fully realized by simultaneously addressing the spatial and temporal aspects of optical phase conjugation by SBS.

Appendix A

Derivation of the Dependence of Beam Parameters on SBS Threshold for Focused Gaussian Beams

Consider a Gaussian beam focused into the center of a Brillouin medium of length l by a lens of focal length f . To determine the effect of the physical parameters of the beam on the SBS threshold we will assume that SBS threshold is reached when

$$\int_{-l/2}^{l/2} gI(z)dz = 25, \quad (\text{a.1})$$

where g is the Brillouin gain of the medium, $I(z)$ is the on-axis intensity of the beam and dz is the differential length element.

For a focused Gaussian beam⁹⁴

$$I(z) = \frac{2P}{\pi w(z)^2}, \quad (\text{a.2})$$

where P is the total power in the beam and the spot size $w(z)$ is defined in the usual manner by

$$w(z) = w_0 \sqrt{1 + \left(\frac{z}{z_R}\right)^2}. \quad (\text{a.3})$$

Here w_0 is the spot size at the beam waist and z_R is the Rayleigh range defined by

$$z_R = \frac{\pi w_0^2}{\lambda}, \quad (\text{a.4})$$

where λ is the wavelength of the light and

$$w_0 = \frac{f\lambda}{\pi w(f)}. \quad (\text{a.5})$$

Assuming that $l \gg z_R$, substituting equations (a.2)-(a.5) into equation (a.1) yields

$$\int_{-l/2}^{l/2} gI(z)dz = \frac{2\pi gP}{\lambda} \quad (\text{a.6})$$

Equation (a.6) may be rearranged to show the dependence of beam parameters on the power necessary to reach threshold:

$$P_{th} = \frac{\lambda}{50\pi g}. \quad (\text{a.7})$$

Since g is wavelength independent, equation (a.7) shows that for focused beams the threshold for SBS is proportional to the wavelength of the light, and independent of the focal length of the lens and the length of the Brillouin medium.

Appendix B

Derivation of the Relationship Between Astigmatism on a Laser Beam and the Separation of Foci

In order to quantify the astigmatism on a nominally collimated beam, one may focus the beam and measure the separation between the foci. The wavefront aberration may then be calculated once the beam radius has been defined. The equations that relate the wavefront aberration to the separation between the foci are derived below.

From the standard equations of geometrical optics the separation between the foci of a focused astigmatic beam is given by¹²¹

$$\Delta f = \frac{2R^2}{n} b_3 \eta^2, \quad (\text{b.1})$$

where Δf is the separation between the foci, η is the field coordinate, R is the radius of the reference sphere and b_3 is the Seidel coefficient for the astigmatism. In terms of the coordinate at the lens (y), the transverse ray aberration is given by

$$\delta\eta = \frac{-2R}{n} b_3 \eta^2 y, \quad (\text{b.2})$$

and the relation between the transverse ray aberration component and the wavefront aberration is given by

$$\delta\eta = \frac{-R}{n} \frac{\partial W_\lambda}{\partial y}. \quad (\text{b.3})$$

Taking the radius of the reference sphere to be the focal length of the lens used to focus the beam, and defining the transverse extent of the beam to be the beam

radius r , the relationship between the separation between foci and the aberration present on the beam is given by

$$W_\lambda = \frac{\Delta f n r^2}{2 f^2}. \quad (\text{b.4})$$

If, as in the case presented in the text, the beam under consideration is Gaussian in intensity, one may wish to define the radius of the beam at the focusing lens as the spot size. The wavefront aberration may then be written in terms of the Rayleigh range of the focused beam (z_R), where the spot size at the focal point of the lens is given by

$$w_o = \frac{f \lambda}{\pi w(f)}. \quad (\text{b.5})$$

Using these criteria the separation between the foci is related to the wavefront aberration by

$$\Delta f = \frac{2\pi}{n} z_R W_\lambda, \quad (\text{b.6})$$

where W_λ is in terms of the wavelength of the light.

Appendix C

Overlap Integrals for the First Three Hermite-Gaussian Modes

As given by equation (2.29) the overlap integral is defined as

$$\xi_{jkl_n} = \left(\frac{2}{\pi}\right) (2^{j+k+l+n} j! k! l! n!)^{-1/2} \times \int_{-\infty}^{\infty} dx' H_j(\sqrt{2}x') H_k(\sqrt{2}x') H_l(\sqrt{2}x') H_n(\sqrt{2}x') \exp(-4x'^2), \quad (\text{c.1})$$

where

$$x' = \frac{x}{w(z)}. \quad (\text{c.2})$$

The following table lists the values of the overlap integrals for the case of three Hermite-Gaussian modes. All odd-numbered modes are identically zero due to parity considerations and the values of the overlap integrals are invariant to a permutation of the indices. Therefore, the 81 overlap integrals reduce to only nine non-trivial values.

j,k,l,n	ξ_{jkl_n}
0,0,0,0	0.5642
2,0,0,0	-0.1995
1,1,0,0	0.2821
2,2,0,0	0.2116
1,1,2,0	0.0997
2,2,2,0	0.0249
1,1,1,1	0.4231
2,2,1,1	0.2468
2,2,2,2	0.3614

Table c.1. Values of the overlap integrals for the first three Hermite-Gaussian modes.

Bibliography

1. I. L. Fabelinskii, *Molecular Scattering of Light*, Plenum Press, New York, 1968.
2. B. Ya. Zel'dovich, N. F. Pilipetsky and V. V. Shkunov, *Principles of Phase Conjugation*, Springer-Verlag, Berlin, 1985.
3. R. W. Boyd, *Nonlinear Optics*, Academic Press, San Diego, 1992.
4. V. S. Starunov and I. L. Fabelinskii, "Stimulated Mandel'shtam-Brillouin scattering and stimulated entropy (temperature) scattering of light," *Sov. Phys. USPEKHI* **12**, 463 (1970).
5. B. Ya. Zel'dovich, private communication.
6. B. Ya. Zel'dovich, V. I. Popovichev, V.V. Ragul'skii and F. S. Faizullof, "Connection between the wavefronts of the reflected and exciting light in stimulated Mandel'shtam-Brillouin scattering," *JETP Lett.* **15**, 109 (1972).
7. V. V. Ragul'skii, "Stimulated Mandel'shtam-Brillouin scattering lasers," *Trudy Fian* **85**, 1 (1976).
8. N. Basov and I. Zubarev, "Powerful laser systems with phase conjugation by SMBS mirror," *Appl. Phys.* **20**, 261 (1979).
9. A. A. Kalinina, V. V. Lyubimov, L. V. Nosova and I. B. Orlova, "Telescopic small-signal amplifier with a Brillouin mirror," *Sov. J. Quant. Elect.* **9**, 1336 (1979).
10. N. G. Basov, A. P. Vasin, V. F. Efimkov, I. G. Zubarev, M. G. Smirnov and V. B. Sobolev, "Investigation of a hypersonic wavefront-reversing mirror operating in a master-oscillator-amplifier configuration," *Sov. J. Quant. Elec.* **16**, 788 (1986).
11. V.I. Kryzhanovskii, V. A. Serebryakov and V. E. Yashin, "Experimental study of a two-pass neodymium glass laser amplifier with quarter-wave decoupling and a stimulated Mandel'shtam-Brillouin scattering mirror," *Sov. Phys. Tech. Phys.* **27**, 825 (1982).
12. N. G. Basov, *Phase Conjugation of Laser Emission*, Nova Science, Commack, (1988).

13. T. R. O'Meara, "Compensation of laser amplifier trains with nonlinear conjugation techniques," *Opt. Eng.* **21**, 243 (1983).
14. B. N. Borisov, O. S. Borodulina, Yu. I. Kruzhilin, S. Yu. Maslakov and A. V. Mel'nikov, "Pulse-periodic neodymium laser with wavefront reversal in a stimulated-Brillouin-scattering mirror and with frequency doubling," *Sov. J. Quant. Elect.* **13**, 1411 (1983).
15. S. Yu. Natarov and E. I. Shklovskii, "Specific configuration of a four-pass laser amplifier with a stimulated Brillouin scattering mirror," *Sov. J. Quant. Elect.* **14**, 871 (1984).
16. N. F. Andreev, G. A. Pasmanik, P. P. Pashinin, S. N. Sergeev, R. V. Serov, E. I. Shklovskii and V. P. Yanovskii, "Multipass amplifier with full utilization of the active element aperture," *Sov. J. Quant. Elect.* **13**, 641 (1983).
17. Yu. P. Vasil'ev, P. P. Pashinin, R. V. Serov and E. I. Shklovskii, "Multipass neodymium glass laser amplifier with a stimulated Brillouin scattering mirror," *Sov. J. Quant. Elec.* **14**, 1562 (1984).
18. I. D. Carr and D. C. Hanna, "Performance of a Nd:YAG oscillator/amplifier with phase-conjugation via stimulated Brillouin scattering," *Appl. Phys. B* **36**, 83 (1985).
19. S. Chandra, R. C. Fukuda and R. Utano, "Sidearm stimulated scattering phase-conjugated laser resonator," *Opt. Lett.* **10**, 356 (1985).
20. W. R. Rapoport and S. Strauch, "Nd:YAG slab oscillators, amplifiers and optical phase conjugation," in *Proc. of the SPIE Vol. 736, New Slab and Solid-State Laser Technologies and Applications*, J. Guch and J. Eggleston, eds., (SPIE, Bellingham, Washington, 1985) p. 65.
21. I. M. Bel'dyugin, B. Ya. Zel'dovich, M. V. Zolotarev and V.V. Shkunov, "Lasers with wavefront-reversing mirrors (review)," *Sov. J. Quant. Elec.* **15**, 1583 (1986).
22. V. Kh. Bagdasarov, N. N. Denisov, P. P. Pashinin and I. I. Shk.ovskii, "Single-frequency pulse-periodic YAG:Nd laser with a high peak power and a low divergence of radiation," *Sov. J. Quant. Elect.* **17**, 862 (1987).
23. M. E. Brodov, O. N. Gilyarov, A. V. Ivanov, B. N. Kulikovskii and P. P. Pashinin, "Eight-pass neodymium glass slab amplifier with a waveguide and with phase conjugation," *Sov. J. Quant. Elect.* **17**, 1265 (1987).
24. V. M. Leont'ev, V. G. Novoselov, Yu. P. Rudnitskii and L. V. Chernysheva, "Solid-state laser with a composite active element and diffraction-limit divergence," *Sov. J. Quant. Elec.* **17**, 220 (1987).
25. V. N. Alekseev, V. V. Golubev, D. I. Dmitriev, A. N. Zhilin, V. V. Lyubimov, A. A. Mak, V. I. Reshetnikov, V. S. Sirazetdinov and A. D. Starikov,

- "Investigation of wavefront reversal in a phosphate glass amplifier with a 12-cm output aperture," *Sov. J. Quant. Elect.* **17**, 455 (1987).
26. P. P. Pashinin and E. J. Shklovsky, "Solid-state lasers with stimulated-Brillouin-scattering mirrors operating in the repetitive-pulse mode," *J. Opt. Soc. Am. B* **5**, 1957 (1988).
 27. D. A. Rockwell, "A review of phase-conjugate solid-state lasers," *J. Quant. Elec.* **24**, 1124 (1988).
 28. M. S. Barashkov, I. M. Bel'dyugin, M. V. Zolotarev, M. I. Krymskii, S. P. Oshkin, A. F. Umnov and M. A. Kharchenko, "Stimulated emission in a solid-state ring laser with a stimulated Brillouin scattering mirror," *Sov. J. Quant. Elect.* **20**, 631 (1990).
 29. J-L. Ayrat, J. Montel, J-P. Huignard, "Master oscillator-amplifier Nd:YAG laser with a SBS phase-conjugate mirror," in *Proc. SPIE Vol. 1500, Innovative Optics and Phase Conjugate Optics*, R-J. Ahlers and T. T. Tschudi, eds., (SPIE, Bellingham, Washington, 1991) p. 81.
 30. N. F. Andreev, N. G. Bondarenko, I. V. Eremina, S. V. Kuznetsov, O. V. Palashov, G. A. Pasmanik and E. A. Khazanov, "Single-mode YAG:Nd laser with a stimulated Brillouin scattering mirror and conversion of radiation to the second and fourth harmonics," *Sov. J. Quant. Elect.* **21**, 1045 (1991).
 31. H. Meng and H. J. Eichler, "Nd:YAG laser with a phase-conjugating mirror based on stimulated Brillouin scattering in SF₆ gas," *Opt. Lett.* **16**, 569 (1991).
 32. R. J. St. Pierre, H. Injeyan, R. C. Hilyard, M. E. Weber, J. G. Berg, M. G. Wickham, C. S. Hoefler and J. P. Machan, "One Joule Per Pulse, 100 Watt, Diode-Pumped, Near Diffraction Limited, Phase Conjugated, Nd:YAG Master Oscillator Power Amplifier," in *Advanced Solid-State Lasers and Compact Blue-Green Lasers Technical Digest, 1993*, (Optical Society of America, Washington, D. C., 1993), Vol. 2, pp. 2-4.
 33. M. S. Mangir and D. A. Rockwell, "A 4.5-J SBS phase-conjugate mirror producing an excellent near- and far-field fidelity," in *Proceedings of the Conference on Lasers and Electro-optics 1992*, Optical Society of America, Washington, D. C., p. 178 (1992).
 34. R. St. Pierre, H. Injeyan and J. Berg, "Investigations of SBS phase-conjugate fidelity fluctuations in Freon 113," in *Proceedings of the Conference on Lasers and Electro-optics 1992*, Optical Society of America, Washington, D. C., p. 180 (1992).
 35. E. Gregor, S. Matthews, R. Muir, O. Kahan, T. Chen, J. Source, M. Polumbo, C. Kalina, K. Nielson and J. Ortize, "A conductively cooled diode pumped phase conjugate Nd:YLF laser with 0.5 Joule, 100 Hz at 547nm output," in *Advanced Solid-State Lasers and Compact Blue-Green Lasers Technical*

- Digest, 1993*, (Optical Society of America, Washington, D. C., 1993), Vol. 2, pp. 5-7.
36. N. G. Basov, V. F. Efimkov, I. G. Zubarev, A. V. Kotov, A. B. Mironov, S. I. Mikhailov and M. G. Smirnov, "Influence of certain radiation parameters on wavefront reversal of a pump wave in a Brillouin mirror," *Sov. J. Quant. Elect.* **9**, 455 (1979).
 37. V. V. Lyubimov, A. A. Mak and V. E. Yashin, "Some problems in using wavefront reversal in laser systems," *Academy of Sciences USSR Bulletin, Phys. Sci.* **51**, 114 (1987).
 38. J. C. Bellum, T. G. Crow and E. L. Camp, "Experimental investigation of phase conjugation in stimulated Brillouin scattering of beams with mild cylindrical aberration," *Opt. Lett.* **13**, 36 (1988).
 39. C. L. Vercimak, C. Marshall, T. R. Moore and D. Milam, "Near field modulation induced by SBS phase conjugation of astigmatic beams," in *Proceedings of the Conference on Lasers and Electro-optics 1989*, Optical Society of America, Washington, D. C., p. 26 (1989).
 40. A. Yariv and R. A. Fisher in *Optical Phase Conjugation*, R. A. Fisher, editor, Academic Press, New York, 1983.
 41. N. C. Griffen and C. V. Heer, "Focusing and phase conjugation of photon echoes in Na vapor," *Appl Phys. Lett.* **33**, 865 (1978).
 42. E. I. Shtyrkov and V. V. Samartsev, "Dynamic holograms on the superposition by interference of atomic states," *JETP Lett.* **27**, 648 (1978).
 43. M. Fujita, H. Nakatsuka, H. Nakanishi and M. Matsuoka, "Backward echo in two-level systems," *Phys. Rev. Lett.* **42**, 974 (1979).
 44. J. C. AuYeung, in *Optical Phase Conjugation*, R. A. Fisher, editor, Academic Press, New York, 1983.
 45. A. V. Mamaev and A. A. Zozulya, "Conjugation of mutually incoherent light beams in the geometry of two interconnected ring mirrors," *J. Opt. Soc. Am. B* **8**, 1447 (1991).
 46. D. A. Glazkov, A. A. Gordeev, I. G. Zubarev and S. I. Mikhailov, "Brillouin loop oscillator pumped by incoherent beams," *Sov. J. Quant. Elect.* **21**, 545 (1991).
 47. N. V. Bogodaev, V. V. Eliseev, L. I. Ivleva, A. S. Korshunov, S. S. Orlov, N. M. Plozkov and A. A. Zozulya, "Double phase-conjugate mirror: experimental investigation and comparison with theory," *J. Opt. Soc. Am. B* **9**, 1493 (1992).
 48. R. K. Tyson, *Principles of Adaptive Optics*, Academic Press, San Diego, (1991).

49. C. R. Giuliano, "Applications of optical phase conjugation," *Phys. Today* **34**, 27 (1981).
50. A. A. Ilyukhin, G. V. Peregudov, M. E. Plotkin, E. N. Ragozin and V. A. Chirkov, "Focusing of a laser beam on a target using the effect of wave-front inversion (WFI) produced as a result of stimulated Mandel'shtam-Brillouin scattering (SMBS)," *JETP Lett.* **29**, 328 (1979).
51. M. D. Levenson, K. M. Johnson, V. C. Hanchett and K. Chaing, "Projection photolithography by wave-front conjugation," *J. Opt. Soc. Am.* **71**, 737 (1981).
52. P. P. Pashinin and E. I. Shklovskii, "Laser with a stimulated Brillouin scattering mirror switched on by its own priming radiation," *Sov. J. Quant. Elect.* **18**, 1190 (1988).
53. V. S. Arakelyan and G. E. Rylov, "Laser with a wavefront-reversing mirror and Q switching by stimulated Brillouin backscattering," *Sov. J. Quant. Elect.* **15**, 433 (1985).
54. B. Fischer, S. Sternklar and S. Weiss, "Photorefractive Oscillators," *J. Quant. Elec.* **25**, 550 (1989).
55. C. Cho, I. Young and E. Kim, "Linear phase-conjugate oscillator employing a photorefractive crystal," *Opt. Lett.* **14**, 569 (1989).
56. W. Lee, S. Chi, P. Yeh and R. Saxena, "Theory of phase conjugate oscillators. I," *J. Opt. Soc. Am. B* **7**, 1411 (1990).
57. C. Gu and P. Yeh, "Theory of photorefractive phase-conjugate ring oscillators," *J. Opt. Soc. Am. B* **8**, 1428 (1991).
58. W. Lee, S. Chi, P. Yeh and R. Saxena, "Theory of phase-conjugate oscillators. II," *J. Opt. Soc. Am. B* **8**, 1421 (1991).
59. N. G. Basov, V. F. Efimkov, I. G. Zubarev, A. V. Kotov, S. I. Mikhailov and M. G. Smirnov, "Inversion of wavefront in SMBS of a depolarized pump," *JETP Lett.* **28**, 197 (1978).
60. M. R. Summers, J. B. Trenholme, R. J. Gelinas, S. E. Stokowski and J. E. Marion, "Progress in high-average-power solid-state laser development at Lawrence Livermore National Laboratory 1987," in *Proceedings of the Conference on Lasers and Electro-optics 1987*, Optical Society of America, Washington, D. C., p. (1987).
61. N. F. Andreev, V. I. Bespalov, M. A. Dvoret'skii and G. A. Pasmanik, "Nonstationary stimulated Mandel'shtam-Brillouin scattering of focused light beams under saturation conditions," *Sov. Phys. JETP* **58**, 688 (1983).

62. A. A. Betin, A. F. Vasil'ev, O. V. Kulagin, V. G. Manishin and V. E. Yashin, "Phase conjugation in nonstationary stimulated Brillouin scattering of focused beams," *Sov. Phys. JETP* **62**, 468 (1985).
63. D. Milam, C. L. Vercimak and T. R. Moore, "Calculation of intensity modulation imposed on the input beam by self-focusing at the SBS threshold," in *Proceedings of the Conference on Lasers and Electro-optics 1989*, Optical Society of America, Washington, D. C., p. 26 (1989).
64. C. B. Dane, W. A. Neuman and L. A. Hackel, "Pulse-shape dependence of stimulated-Brillouin-scattering phase-conjugation fidelity for high input energies," *Opt. Lett.* **17**, 1271 (1992).
65. V. I. Bespalov, A. A. Betin, G. A. Pasmanik and A. A. Shilov, "Observation of transient field oscillations in the radiation of stimulated Mandel'shtam-Brillouin scattering," *JETP Lett.* **31**, 631 (1980).
66. M. V. Vasil'ev, A. L. Gyulameryan, A. V. Mamaev, V. V. Ragul'skii, P. M. Semenov and V. G. Sidorovich, "Recording of phase fluctuations of stimulated scattered light," *JETP Lett.* **31**, 634 (1980).
67. N. G. Basov, I. G. Zubarev, A. B. Mironov, S. I. Mikhailov and A. Yu. Olulov, "Phase fluctuations of the Stokes wave produced as a result of stimulated scattering of light," *JETP Lett.* **31**, 645 (1980).
68. S. M. Wandzura, "Stimulated scattering does not have a steady state," in *Proceedings of the Conference on Lasers and Electro-optics 1988*, Optical Society of America, Washington, D. C., p. 8 (1988).
69. E. M. Dianov, A. Ya. Karasic, A. V. Lutchnikov and A. N. Pilipetskii, "Saturation effects at backward stimulated scattering in the single-mode interaction," *Opt. Quant. Electron.* **21**, 381 (1989).
70. R. W. Boyd and K. Rzazewski, "Noise initiation of stimulated Brillouin scattering," *Phys. Rev. A* **42**, 5514 (1990).
71. A. L. Gaeta and R. W. Boyd, "Stochastic dynamics of stimulated Brillouin scattering in an optical fiber," *Phys. Rev. A* **44**, 3205 (1991).
72. M. S. Mangir, J. J. Ottusch, D. C. Jones and D. A. Rockwell, "Time-resolved measurements of stimulated-Brillouin-scattering phase jumps," *Phys. Rev. Lett.* **68**, 1702 (1992).
73. M. V. Vasilev, V. G. Sidorovich and N. S. Shlyapochnikova, "Quality of phase conjugation during stimulated Brillouin scattering," *Opt. Spectr. (USSR)* **54**, 393 (1983).
74. A. F. Vasil'ev and V. E. Yashin, "Stimulated Brillouin scattering at high values of the excess of the pump energy above the threshold," *Sov. J. Quant. Elect.* **17**, 644 (1987).

75. R. H. Lehmberg and K. A. Holder, "Numerical study of optical ray retracing in laser-plasma backscatter," *Phys. Rev. A* **22**, 2156 (1980).
76. R. H. Lehmberg, "Numerical study of phase conjugation in stimulated backscatter with pump depletion," *Opt. Comm.* **43**, 369 (1982).
77. N. B. Baranova, B. Ya. Zel'dovich and V. V. Shkunov, "Wavefront reversal in stimulated light scattering in a focused spatially inhomogeneous pump beam," *Sov. J. Quant. Elect.* **8**, 559 (1978).
78. N. B. Baranova and B. Ya. Zel'dovich, "Transverse enhancement of coherence of the scattered field in wavefront reversal," *Sov. J. Quant. Elect.* **10**, 172 (1980).
79. B. Ya. Zel'dovich and T. V. Yakovleva, "Small-scale distortions in wavefront reversal of a beam with incomplete spatial modulation (stimulated Brillouin backscattering, theory)," *Sov. J. Quant. Elect.* **10**, 181 (1980).
80. N. B. Baranova and B. Ya. Zel'dovich, "Wavefront reversal of focused beams (theory of stimulated Brillouin backscattering)," *Sov. J. Quant. Elect.* **10**, 555 (1980).
81. B. Ya. Zel'dovich and T. V. Yakovleva, "Calculations of the accuracy of wavefront reversal utilizing pump radiation with one-dimensional transverse modulation," *Sov. J. Quant. Elect.* **11**, 186 (1981).
82. W. Koechner, *Solid-State Laser Engineering*, 2nd ed. Springer-Verlag, Berlin, 1988.
83. M. A. Summers, J. B. Trenholme, R. J. Gelinas, S. K. Doss, R. D. Boyd and C. D. Swift, "Optical distortions in zigsag slab amplifiers," *Conference on Lasers and Electro-Optics, 1989 Technical Digest Series*, Vol. 11 (Optical Society of America, Washington, D. C. 1989) p. 240.
84. S. T. Bobrov, K. V. Gratsianov, A. F. Kornev, V. V. Lyubimov, V. G. Pankov, A. I. Stepanov and Yu. G. Turkevich, "Improving the quality of phase conjugation of SBS mirrors with smooth aberrations," *Opt. Spectr. (USSR)* **62**, 241 (1987).
85. M. V. Vasilev, V. G. Sidorovich and N. S. Shlyapochnikova, "Quality of phase conjugation during stimulated Brillouin scattering," *Opt. Spectr. (USSR)* **54**, 393 (1983).
86. V. V. Golubev, V. S. Sirazetdinov and A. D. Starikov, "Conditions for the correction of astigmatic distortions in laser beams by the SBS mirror," *Opt. Spectr. (USSR)* **62**, 526 (1987).
87. L. P. Schelonka, "The fidelity of stimulated Brillouin scattering with weak aberrations," *Opt. Comm.* **64**, 293 (1987).

88. A. F. Vasil'ev, V. M. Mit'kin, A. N. Shatsev and V. E. Yashin, "Precision of correction of smooth phase distortions by the method of optical phase conjugation as a result of stimulated Brillouin scattering of focused beams," *Sov. J. Quant. Elect.* **18**, 493 (1988).
89. L. P. Schelonka and C. M. Clayton, "Effect on focal intensity on stimulated-Brillouin-scattering reflectivity and fidelity," *Opt. Lett.* **13**, 42 (1988).
90. C. Hoefler, H. Injeyan, B. Zukowski and M. Nguyen-vo, "Phase conjugation of astigmatic aberrations by stimulated Brillouin scattering," in *Proceedings of the Conference on Lasers and Electro-optics 1989*, Optical Society of America, Washington, D. C., p. 24. (1989).
91. M. Lefebvre, S. Pfeifer and R. Johnson, "Dependence of stimulated-Brillouin-scattering phase-conjugation correction on the far-field intensity distribution of the pump light," *J. Opt. Soc. Am. B* **9**, 121 (1992).
92. J. Brock, M. Caponi, L. Frantz, G. Harpole, C. Hoefler, H. Injeyan, F. Patterson, D. Shemwell and J. Tyminski, *Nonlinear Optics Technology Phase II Final Report*, Defense Advanced Research Projects Agency contract #N00014-85-C-0257, (1988).
93. J. W. Goodman, *Statistical Optics*, Wiley, New York (1985).
94. see for example A. E. Siegman, *Lasers*, University Science, Mill Valley, (1976).
95. A. L. Gaeta and R. W. Boyd, "Stochastic dynamics of stimulated Brillouin scattering in an optical fiber," *Phys. Rev. A.* **44**, 3205 (1991).
96. see for example W. H. Press, S. A. Teukolsky, W. T. Vetterling and B. P. Flannery, *Numerical Recipes*, Cambridge University Press, New York (1992).
97. N. V. Okladnikov, G. L. Brekhovskikh, A. I. Sokolovskaya and A. A. Garmonov, "Wavefront reconstruction (phase conjugation) and diffraction efficiency of dynamic holograms in stimulated light scattering," *Sov. Tech. Phys. Lett.* **7**, 159 (1981).
98. A. I. Sokolovskaia, G. L. Brekhovskikh and A. D. Kudriavtseva, "Real-time holography and wave-front conjugation by stimulated scattering," *J. Opt. Soc. Am.* **73**, 554 (1983).
99. K. V. Gratsianov, V. V. Lyubimov, V. G. Pankov and A. I. Stepanov, "Effect of the overpumping zone on formation of the phase-conjugate wave on phase conjugation by SBS," *Opt. Spect. (USSR)* **64**, 414 (1988).
100. J. Munch, R. F. Wuerker and M. J. LeFebvre, "Interaction length for optical phase conjugation by stimulated Brillouin scattering: an experimental investigation," *Appl. Opt.* **28**, 3099 (1989).

101. V. M. Rysakov, Yu. V. Aristov and V. I. Kortokov, "Three-dimensional stimulated Mandelshtam-Brillouin scattering," *Opt. Spect. (USSR)* **47**, 412 (1979).
102. M. A. Osborne, "Stimulated Brillouin scattering using cylindrical focusing optics," *J. Opt. Soc. Am. B* **7**, 2106 (1990).
103. M. Maier, G. Wendl and W. Kaiser, "Self-focusing of laser light and interaction with stimulated scattering processes," *Phys. Rev. Lett.* **24**, 352 (1970).
104. D. Milam, T. R. Moore and C. L. Vercimak, unpublished.
105. W. L. Smith, "Nonlinear Refractive Index," in *Handbook of Laser Science and Technology, Volume III: Optical Materials Part A*, M. J. Webber, ed., CRC Press, Boca Raton (1986).
106. H. J. Eichler, R. Menzel, R. Sander and B. Smandek, "Reflectivity enhancement of stimulated Brillouin scattering liquids by purification," *Opt. Comm.* **89**, 260 (1992).
107. P. Narum, A. L. Gaeta, M. D. Skeldon and R. W. Boyd, "Instabilities of laser beams counterpropagating through a Brillouin-active medium," *J. Opt. Soc. B.* **5**, 623 (1988).
108. A. L. Gaeta, M. D. Skeldon, R. W. Boyd and P. Narum, "Observation of instabilities of laser beams counterpropagating through a Brillouin medium," *J. Opt. Soc. Am. B* **6**, 1709 (1989).
109. O. Kulagin, G. A. Pasmanik, A. L. Gaeta, T. R. Moore, G. J. Benecke and R. W. Boyd, "Observation of Brillouin chaos with counterpropagating laser beams," *J. Opt. Soc. Am. B* **8**, 2155 (1991).
110. W. J. Firth, A. Fitzgerald and C. Pare', "Transverse instabilities due to counterpropagation in Kerr media," *J. Opt. Soc. Am. B* **7**, 1087 (1990).
111. D.A. Glazkov, V.F. Efimkov, I. G. Zubarev, S. A. Pastukhov and V. B. Sobolev, "Competition between Stokes waves in a phase-conjugating hypersonic mirror based on an oscillator-amplifier system operating under saturation conditions," *Sov. J. Quant. Elec.* **18**, 974 (1988).
112. I. A. Varlamova, V. V. Golubev and V. S. Sirazetdinov, "Investigation of oscillator amplifier phase-conjugating mirrors based on stimulated Brillouin scattering," *Sov. J. Quant. Elec.* **19**, 1631 (1989).
113. D. R. Hull, R. A. Lamb and J. R. Digman, "Efficient phase conjugation at high energies using two cells," *Opt. Comm.* **72**, 104 (1989).

114. G. J. Crofts, M. J. Damzen and R. A. Lamb, "Experimental and theoretical investigation of two-cell stimulated-Brillouin-scattering systems," *J. Opt. Soc. Am. B* **8**, 2282 (1991).
115. F. A. Hopf, "Phase-wave fluctuations in superfluorescence," *Phys. Rev. A* **20**, 2064 (1979).
116. K. Druhl, R. G. Wenzel and J. L. Carlsten, "Observation of solitons in stimulated Raman scattering," *Phys. Rev. Lett.* **51**, 1171 (1983).
117. J. C. Englund and C. M. Bowden, "Spontaneous generation of Raman solitons from quantum noise," *Phys. Rev. Lett.* **57**, 2661 (1986).
118. A. L. Gaeta, unpublished.
119. D. S. Sumida, S. C. Rand, D. A. Rockwell, "Room-temperature Q-switching of Nd:YAG by F_2^- color centers in LiF," in *Proceedings of the Conference on Lasers and Electro-optics 1986*, Optical Society of America, Washington, D. C., p. 214. (1986).
120. D. J. Gauthier, P. Narum and R. W. Boyd, "Simple, compact, high-performance permanent-magnet Faraday isolator," *Opt. Lett.* **11**, 623 (1986).
121. see for example, W. T. Welford, *Aberrations of Optical Systems*, Adam Hilger, Bristol (1986).